Excitatory drive onto dopaminergic neurons in the rostral linear nucleus is enhanced by norepinephrine in an α_1 adrenergic receptor-dependent manner

By

Megan Ann Williams

Dissertation

Submitted to the Faculty of the

Graduate School of Vanderbilt University

in partial fulfillment of the requirements

for the degree of

DOCTOR OF PHILOSOPHY

in

Neuroscience

August, 2015

Nashville, Tennessee

Approved:

Aurelio Galli, Ph.D.

David Bader, Ph.D.

Ariel Deutch, Ph.D.

Danny Winder, Ph.D.

“Life isn't a destination -- it's a journey. We all come upon unexpected curves and turning points, mountain tops and valleys. Everything that happens to us shapes who we are becoming. And in the adventure of each day, we discover the best in ourselves.”
--Unknown

To Mom & Dad, my first and biggest supporters

To Jonathan, my best friend, my love, my source of unwavering support

To all the supporters of my journey, both old and new, near and far

ACKNOWLEDGEMENTS

First, I would like to thank my family and friends, both old and new, near and far. I thank my parents, Steve and Carla, for taking me to the library and taking me fishing, for instilling in me a love of learning and exploration. My parents have always encouraged me in my education and been supportive of my dreams and goals, even when I moved across the country to pursue a path that they don't always understand. I would also like to thank the many members of my extended family and the new friends and family members I've gained for always being curious and supportive about what I do. Finally, I would like to thank my wonderful husband Jon whom I met in graduate school. He has supported me through many stressful times and has proven to be an excellent voice of reason time and again. Jon reminds me to smile and to laugh, to love and to remember what's most important.

I would like to acknowledge the financial support I received while working on my dissertation research. From 2010-2011, I received support from the Ion Channel and Transporter Biology training grant (T32-NS07491) awarded to Al George. From 2013-present, this work was supported by an NIH Ruth L. Kirschstein National Research Service Award (NRSA) fellowship from the National Institute on Drug Abuse (DA034429) awarded to Megan (Fettig) Williams. The imaging and data analysis in Chapter II and III were performed in part through the use of the VUMC Cell Imaging Shared Resource. I would also like to thank the continued support of the Vanderbilt Brain Institute, Neuroscience Program in Substance Abuse, Neuroscience Graduate

Program, and Interdisciplinary Graduate Program for providing assistance, training, and educational resources throughout my graduate career.

Next, I would like to thank the many people who have been provided monumental scientific support throughout my graduate training. I am grateful to the members of my thesis committee Dr. David Bader, Dr. Ariel Deutch, Dr. Aurelio Galli (chair), and Dr. Danny Winder (advisor) for providing me with valuable scientific direction and supporting my professional goals. In addition, I would like to thank Dr. Robert T. Matthews for generating the data in Chapter II, which were originally included in a manuscript with the data in Chapter III. I would especially like to thank Dr. Danny Winder for being the best mentor I could have asked for. Over the years, Danny has worn many hats and he wears them all well. Lastly, but certainly not least, I would like to thank my Winder lab mates, for I truly could not have done this without them. Thank you for making the lab a great place to work every day. The many conversations we've shared about science and life have made me into a better scientist, but most of all, a better person.

TABLE OF CONTENTS

Appendix

LIST OF TABLES

LIST OF FIGURES

LIST OF ABBREVIATIONS

NE..... Norepinephrine

DA..... Dopamine

GPCR..... G protein-coupled receptor

ADHD..... Attention deficit hyperactivity disorder

SN..... Substantia nigra

VTA..... Ventral tegmental area

NAc..... Nucleus accumbens

PFC..... Prefrontal cortex

PBP..... Parabrachial pigmented nucleus

RLi..... Rostral linear nucleus

TH..... Tyrosine hydroxylase

DR..... Dorsal raphe

PAG..... Periaqueductal gray

I_h..... Hyperpolarization current

D_2R..... Dopamine receptor D_2

DAT..... Dopamine transporter

VMAT2..... Vesicular monoamine transporter 2

VGLUT2..... Vesicular glutamate transporter 2

CeA..... Central nucleus of the amygdala

BNST..... Bed nucleus of the stria terminalis

PTSD..... Post-traumatic stress disorder

LC ..... Locus coeruleus

DBH ..... Dopamine beta hydroxylase

AR ..... Adrenergic receptor

EPSCs ..... Excitatory postsynaptic currents

LTD ..... Long term depression

FG ..... Fluorogold

PBS ..... Phosphate-buffered saline

CRF ..... Corticotropin releasing factor

CLi ..... Caudal linear nucleus

sEPSCs ..... Spontaneous excitatory postsynaptic currents

ACSF ..... Artificial cerebrospinal fluid

mEPSCs ..... Miniature excitatory postsynaptic currents

TTX ..... Tetrodotoxin

DMSO ..... Dimethylsulfoxide

CPA ..... Conditioned place aversion

ChR2 ..... Channelrhodopsin-2

NIH ..... Novelty induced hypophasia

CPP ..... Conditioned place preference

HCN ..... Hyperpolarization-activated cyclic nucleotide- gated channel

CHAPTER I

Introduction

The catecholamines, dopamine and norepinephrine, are modulatory neurotransmitters that influence synaptic transmission widely in the brain. Norepinephrine (NE) is involved in stress, arousal, cognitive performance, and the maintenance of homeostasis (Abercrombie et al., 1988; Aston-Jones and Cohen, 2005; Blessing and Willoughby, 1985; Clayton et al., 2004; Hilaire et al., 2004; Korf et al., 1973; Rinaman, 2003). The dopamine (DA) system plays a role in a variety of functions including controlling motor functions, motivated behavior, natural or drug related reward, associative learning, and mood (Bromberg-Martin et al., 2010; Fields et al., 2007; Grace et al., 2007; Ikemoto and Bonci, 2014; Meye and Adan, 2014; Nestler and Carlezon, 2006; Nikulina et al., 2014; Walsh and Han, 2014). The catecholamines exert a modulatory role on neurotransmission and signal through G protein-coupled receptors (GPCRs). They can act either pre-synaptically to influence synthesis and release of neurotransmitter at the terminal and firing of the neuron at the somatodendritic level or post-synaptically to influence the action of the neurotransmitter. NE is known to innervate DA neurons and may work to fine tune the actions of DA, a process termed metamodulation (Katz and Edwards, 1999). The dysfunction of the midbrain DA system can contribute to many diseases such as Parkinson's disease, schizophrenia, attention deficit hyperactivity disorder (ADHD), mood disorders, and drug abuse (Barrot, 2014). Understanding the complicated midbrain DA system, and its interactions with NE, is

critical to understanding the development of these disorders and gain insights into novel therapeutics for the treatment of these diseases. The mesotelencephalic DA system arises from neurons located in midbrain areas that have a wide range of projection targets. Dopamine acts through five distinct GPCR subtypes. The five subtypes are divided into two classes. The D_1 receptor family contains subtypes D_1 and D_5 that are coupled to G_s and the D_2 receptor family contains subtypes D_2, D_3, and D_4 which are coupled to $G_{i/o}$ (Missale et al., 1998). The D_2 receptors often act as autoreceptors to inhibit synthesis and release of DA and regulate the firing of the neuron (Deutch and Roth, 1990). The dynamics of dopamine release are critically tied to the behavioral actions of DA. In order to understand how DA is released we must first examine the DA neurons controlling the release. This introduction will discuss the heterogeneity and function of DA neurons, the role of DA in stress, and NE modulation of DA neurons.

History and organization of the catecholamine systems

The catecholamine neurons were first visualized in the early 1960s. Prior to the widespread use of selective antibody immunohistochemistry techniques, Bengt Falck and Nils-Åke Hillarp developed a novel histofluorescence method that allowed visualization of the monoamines, which include serotonin, dopamine, norepinephrine, and epinephrine, within the central and peripheral nervous system (Falck et al., 1962). The Falck-Hillarp fluorescence method is based on the exposure of freeze dried tissue to formaldehyde vapor which converts dopamine and norepinephrine to iso-quinoline molecules that emit a yellow-green fluorescence under the microscope. This is the first

method that allowed visualization of monoamines within neurons and gave the first conclusive evidence of monoamines as neurotransmitters.

Following the development of the Falck-Hillarp fluorescence method, investigations of the catecholamine systems flourished. The catecholamine cell groups were first mapped by Annica Dahlström and Kjell Fuxe in 1964. Dahlström and Fuxe assigned the groups labels starting with the letter A for “aminergic.” A1-A7 are groups of noradrenergic neurons while groups A8-A12 contain dopamine (Dahlström and Fuxe, 1964). The basic organization of the catecholamine cell groups by Dahlstöm and Fuxe stands up today, however, later modifications on the Falck-Hillarp method and the use of immunohistochemical methods have allowed for greater sensitivity and precision in the identification of catecholamine cell groups. Five additional DA cell groups, A13-A17 and three epinephrine cell groups C1-C3 were added (Hokfelt et al., 1984). A summary of the anatomical location of the NE and DA cell groups are in Table 1. Norepinephrine arises from the locus coeruleus (A4 and A6 areas) and ventral medulla (A1, A5 and A7 areas) or dorsomedial medulla (A2 area). The majority of DA neurons arise from midbrain (A8-A10) and hypothalamic groups (A11-A15). The A9 group contains the DA neurons of the substantia nigra (SN) which heavily project to the striatum and play a large role in motor control.

The A10 group consists of the DA neurons of the ventral tegmental area (VTA) which heavily project to the nucleus accumbens (NAc) and prefrontal cortex (PFC) and are involved in motivated behavior and reward. The original “A” nomenclature has retained well because many of the catecholamine cell groups are not defined to one anatomical region, and there are species variations among the distributions of the cell

groups (Bjorklund and Dunnett, 2007; Hokfelt et al., 1984). As well as the discovery of additional groups, further refinements in nomenclature have occurred. In 1979, the A10 group (VTA) was subdivided into four distinct nuclei based on cytoarchitecture (Phillipson, 1979a). The four nuclei of the A10 group are the parabrachial pigmented (PBP), paranigral, interfascicular, and caudal linear nuclei. The rostral linear nucleus (RLi) is composed of small and round neurons, and Phillipson suggested the RLi was likely a caudal extension of the A11 cell group and considered it independent to the VTA (Phillipson, 1979a). In contrast to the A11 cell group, few RLi fibers enter the periventricular path to innervate diencephalic areas and none innervate the spinal cord (Del-Fava et al., 2007). In 1987, it was suggested by Oades and Halliday that the rostral linear nucleus (RLi) be incorporated into the A10 group based on anatomical connections and more recent anatomical data support this idea (Del-Fava et al., 2007; Oades and Halliday, 1987). The VTA is usually thought of as an anatomical entity because its outputs do not reflect VTA cytoarchitectural nuclear divisions (Oades and Halliday, 1987; Phillipson, 1979a), but are instead organized topographically (Beckstead et al., 1979; Fallon and Moore, 1978). For this reason, it is useful in this dissertation to refer to lateral and medial VTA areas, with “lateral” generally referring to lateral areas of the PBP and paranigral nuclei and “medial” referring to medial areas of the PBP and paranigral nuclei, as well as the RLi and CLi. A caveat to the distinction between medial and lateral VTA areas is that although this terminology is a useful means of discussing a broad trend, these separations are not absolute.

In 1984, Hökfelt et al. proposed that the tyrosine hydroxylase (TH) positive neurons of the dorsal raphe (DR) and periaqueductal gray (PAG) should be considered

a dorso-caudal extent of the A10 group and termed them the A10dc group (Hokfelt et al., 1984). The dopaminergic network of the PAG is composed of small and large neurons, and there are no clear borders separating the small DA neurons of the PAG and RLi (Flores et al., 2006; Hasue and Shammah-Lagnado, 2002). In addition, the TH positive cells anterior to the VTA in the supramammillary nucleus were termed the A10 ventrorostral (A10vr) group (Hokfelt et al., 1984). See Figure 1 for a schematic of the midbrain DA neuron groups.

Table 1: Description of the catecholamine cell groups

Noradrenergic cell groups		Dopaminergic cell groups	
A1	near the nucleus ambiguus in the ventrolateral medulla	A8	retrorubral field
A2	nucleus of the solitary tract in the dorsal medulla	A9	substantia nigra
A3	dorsal to the inferior olivary complex (only observed in rodents)	A10	ventral tegmental area nuclei: parabrachial pigmented, paranigral, interfascicular, rostral linear, and caudal linear nuclei
A4	along the superior cerebellar peduncle and merges with A6	A10vr	anterior to the VTA in the supramammillary region
A5	along the ventrolateral margin of the pontine tegmentum	A10dc	periaqueductal gray and dorsal raphe
A6	locus coeruleus	A11	rostral periaqueductal gray to the posterior hypothalamus adjacent to the mammillothalamic tract
A7	in pontine reticular formation in ventrolateral pons	A12	arcuate nucleus of the hypothalamus
		A13	zona incerta region
		A14	along the third ventricle in the rostral hypothalamus including the posterior part of the paraventricular hypothalamamic nucleus
		A15	anterior hypothalamus region above the optic chiasm/suproptic nucleus and ventral to the anterior commissure
		A16	olfactory bulb
		A17	retina

Sources: (Bjorklund and Dunnett, 2007; Hokfelt et al., 1984; Kandel, 2013; Li et al., 2014)

Figure 1: Schematic of the organization of the midbrain dopamine cell groups in the rat brain.
(Left) Coronal sections from the Paxinos and Watson atlas showing midbrain nuclei containing dopaminergic neurons. The distance from Bregma is indicated below each plate. (Right) The subdivisions of the VTA, as described by Phillipson, are shown on coronal plates of the rat modified from rat brain atlases. The distance from Bregma is indicated above each plate.
Abbreviations: aopt, accessory optic tract; CLi, caudal linear nucleus; cp: cerebral peduncle; fr, fasciculus retroflexus; IF, interfascicular nucleus; IP, interpeduncular nucleus; ml, medial lemniscus; MM, medial mammillary nucleus; mp, mammillary peduncle; PAG, periaqueductal gray; PBP, parabrachial pigmented nucleus; pn, pontine nuclei; PN, paranigral nucleus; R, red nucleus; RLi, rostral linear nucleus; RRF, retrorubral field; scp, superior cerebellar peduncle; SNC, substantia nigra pars compacta; SNL, substantia nigra, lateral part; SNR, substantia nigra, reticular part; SuMM, supramammillary nucleus, medial part; tVTA, tail of the VTA; VTA, ventral tegmental area.
**Adapted from Flores et al 2006 and Sanchez-Catalan et al 2014.*

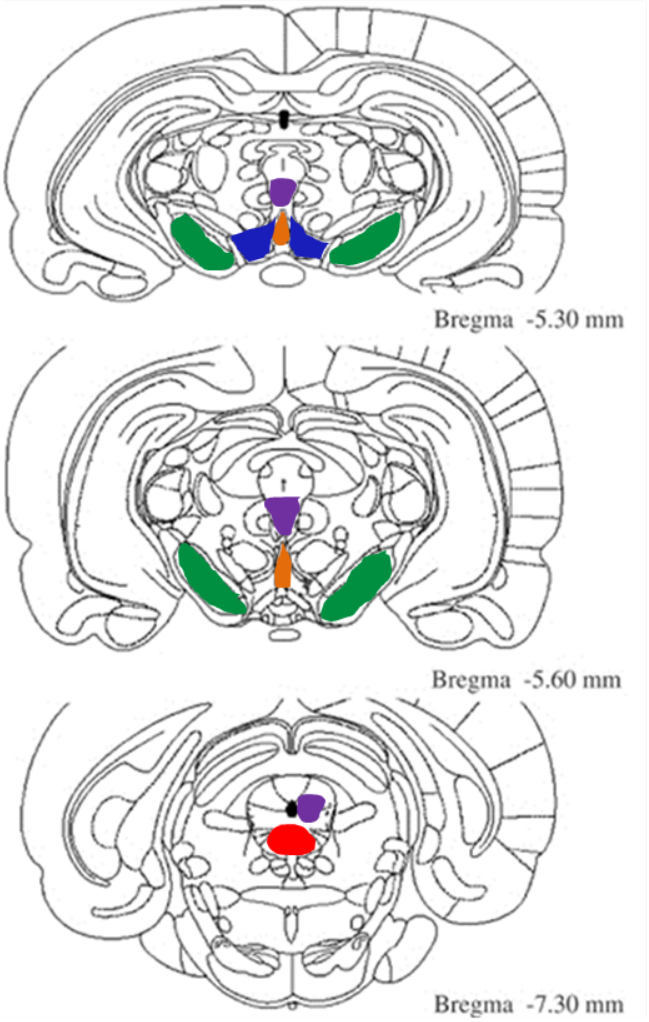
Bregma -5.30 mm
Bregma -5.60 mm
Bregma -7.30 mm
periaqueductal gray – A10dc
rostral linear n.
ventral tegmental area
substantia nigra
dorsal raphe – A10dc

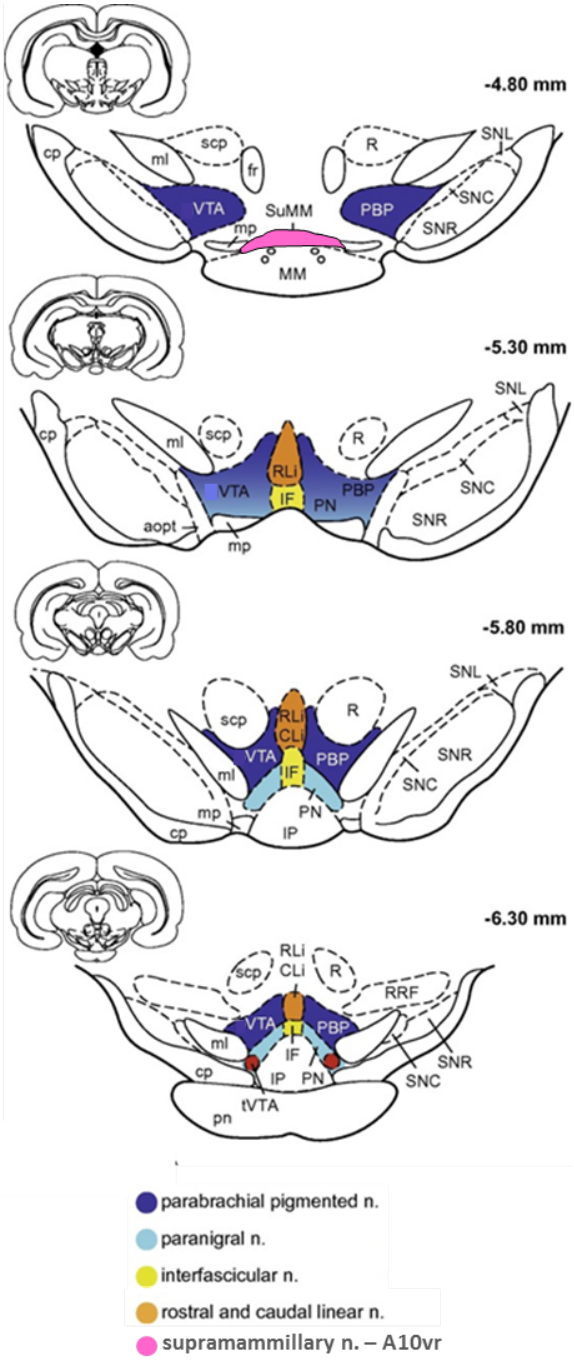
-4.80 mm
scp
cp
ml
fr
R
SNL
VTA
SuMM
PBP
SNC
mp
SNR
MM
-5.30 mm
RLi
IF
PN
aopt
-5.80 mm
CLi
IP
-6.30 mm
RRF
tVTA
pn
parabrachial pigmented n.
paranigral n.
interfascicular n.
rostral and caudal linear n.
supramammillary n. – A10vr

Heterogeneity amongst ventral tegmental area (A10) dopamine neurons

Electrophysiological properties

Original electrophysiology studies of midbrain DA neurons focused on *in vivo* recordings in the rat SN. It was determined that long duration action potentials, D_2 autoreceptor mediated inhibition of firing, and the presence of I_h, a hyperpolarization activated inward cation current, were properties that could be used to accurately identify SN DA neurons *in vivo* (Grace and Bunney, 1980; Grace and Bunney, 1983; Grace and Onn, 1989). These properties were then used to identify VTA DA neurons for *in vitro* electrophysiology studies in brain slices. However, the validity of this identification method has come into question (Margolis et al., 2006). In the SN approximately 85-95% of neurons are thought to be dopaminergic while in the VTA, only 55-60% of the neurons are dopaminergic (Lacey et al., 1989; Margolis et al., 2006; Swanson, 1982). Therefore, it is particularly important to establish accurate criteria to identify VTA DA neurons. Margolis et al. tried to find an accurate electrophysiological marker for VTA DA neurons *in vitro* and found that DA neurons cannot be distinguished from other VTA neurons by size, shape, input resistance, I_h size, or spontaneous firing rate (Margolis et al., 2006). In addition, some non-dopaminergic neurons of the VTA have I_h, while some TH positive neurons in the VTA lack I_h, and some VTA DA neurons are insensitive to D_2 agonists, while some non-DA neurons do show inhibition due to D_2 receptor (D_2R) activation (Margolis et al., 2006).

It has been shown that the DA neurons of the A10 group are not a homogenous group, but have distinct molecular and physiological properties based on their projection

targets and anatomical location. Recent studies have shown that some TH positive neurons located in the medial aspects of the VTA, specifically the medial PBP and medial paranigral VTA nuclei, and A10dc areas lack I_h (Hnasko et al., 2012; Lammel et al., 2011; Li et al., 2013a). The DA neurons of the A10 group that lack I_h primarily project to the medial prefrontal cortex (mPFC) and the nucleus accumbens medial shell, while those with I_h primarily project to the nucleus accumbens lateral shell or belong to the nigrostriatal pathway (Lammel et al., 2011). Action potential width and D_2R mediated inhibition of VTA DA neurons differ based on projection target. NAc projecting DA neurons have both of these characteristics, amygdala projecting VTA DA neurons show neither, and PFC projecting DA neurons do show D_2R autoinhibition, but have short duration action potentials (Margolis et al., 2008). In contrast, Lammel et al found that PFC projecting DA neurons lack D_2R autoinhibition, while amygdala, NAc, and striatal projecting DA neurons are sensitive to D_2R autoinhibition (Lammel et al., 2008). There are some methodological differences between these two studies that might underlie this discrepancy. The Margolis study was in young (20-36 days) rats and the electrophysiology recordings were done in horizontal brain slices, while Lammel and colleagues used slightly older mice (12 weeks) and coronal brain slices. Taken together, these data suggest that the classical method of identifying VTA DA neurons by long duration action potentials, D_2R autoinhibition, and the presence of I_h leads to an overrepresentation of NAc projecting DA neurons and an exclusion of amygdala and PFC projecting DA neurons.

Genetic reporter lines for identification of dopamine neurons

Due to the concerns discussed above, the use of genetic reporter animal lines has arisen as a popular way to identify DA neurons for electrophysiology studies. Reporter mouse lines allow for selection of DA neurons based on expression of a fluorescent reporter. This is a useful strategy for the selection of VTA DA neurons and is necessary in regions where the distribution of DA neurons is sparse, such as regions of the A10dc. For example, Li et al. used a TH-eGFP BAC transgenic mouse line to identify DA neurons of the vPAG for electrophysiological studies (Li et al., 2013a). In addition to direct reporter lines, there are Cre-driver mouse lines that can be crossed to reporter lines such as a ROSA-*tomato* line or combined with Cre-dependent optogenetic tools. For the specific selection of midbrain DA neurons, TH-cre and DAT-cre (dopamine transporter) lines are commonly used. However, one large caveat to the use of reporter mouse lines is the fidelity of the reporter. For example, Li et al. found that the proportion of eGFP positive neurons in the vPAG that colocalize with TH is approximately 70% (Li et al., 2013a). In addition, the TH-cre lines have been found to exhibit non-DA cell expression patterns around VTA nuclei, particularly in midline areas (Lammel et al., 2015). DAT-cre driver lines seem to exhibit less ectopic expression, but these lines may lead to exclusion of some midline DA neurons that lack or have low levels of DAT expression (Lammel et al., 2015; Stuber et al., 2015). In summary, reporter and cre-driver mouse lines are valuable tools for the identification of midbrain DA neurons, but must be used with caution and the fidelity of the reporter line must be confirmed in the specific brain region studied.

Molecular expression profiles

In addition to differences in electrophysiological properties, there are differences in molecular expression profiles among the A10 group. Levels of dopamine transporter (DAT) and vesicular monoamine transporter 2 (VMAT2), which are responsible for reuptake of DA and packaging of DA into vesicles, respectively, are lower in some DA neurons of the medial VTA than those in the lateral VTA and SN (Lammel et al., 2008; Lammel et al., 2015; Li et al., 2013b). Levels of D_2 autoreceptors are also low or lacking in some medial VTA DA neurons (Hnasko et al., 2012; Lammel et al., 2008; Li et al., 2013b). Some of these medial VTA DA neurons with low DAT or D_2 autoreceptor expression have been shown to project to the PFC (Hnasko et al., 2012; Lammel et al., 2008; Li et al., 2013b; Sesack et al., 1998). Specifically, PFC projecting DA neurons lack synthesis- and impulse-modulating D_2 autoreceptors, but have release-modulating D_2 autoreceptors (Bannon et al., 1981; Chiodo et al., 1984; Deutch and Roth, 1990; Galloway et al., 1986). The absence or low levels of D_2R mRNA in PFC projecting DA neurons contrasts with data from Margolis et al. discussed above that indicates PFC projecting DA neurons are sensitive to D_2R mediated autoinhibition. These electrophysiology studies were performed in rats, while the mRNA expression data is in both rats and mice. Therefore, species differences may account for the discrepancy. An alternative explanation is that the two studies represent different populations of PFC projecting DA neurons, with one population sensitive to D_2R mediated autoinhibition while another population lacks this property. In addition, these expression levels are all studies of mRNA expression which does not necessarily correlate to differences in expression or function of proteins. An area of interest in recent years is that a subset of DA neurons, which are primarily located in medial VTA areas, express the vesicular

glutamate transporter 2 (VGLUT2) and have the ability to corelease glutamate (Hnasko et al., 2010; Li et al., 2013b; Stuber et al., 2010; Yamaguchi et al., 2011). Taken together, these differences in molecular expression profiles and electrophysiology properties indicate a potential functional heterogeneity among the subsets of VTA DA neurons.

Firing patterns of dopamine neurons

The firing of DA neurons is characterized by a low frequency (1-8 Hz) tonic or pacemaker activity that is interspersed with either transient (<500 ms) phasic sequences of high-frequency firing (>15 Hz), called “bursts”, or transient pauses of activity, where DA neurons fire no action potentials (Paladini and Roeper, 2014). Spontaneous pacemaker firing is independent of afferent input, while bursting activity is activated by glutamatergic afferents, specifically stimulation of the NMDA receptor (Cooper, 2002; Deister et al., 2009; Grace, 1991; Overton and Clark, 1992; Seutin et al., 1993). Increases in GABAergic inhibition are thought to underlie the pauses in DA neuron activity (Matsui and Williams, 2011; Paladini et al., 1999). Bursting activity leads to a larger increase in synaptic DA than regular firing at the same rate (Gonon, 1988) and is classically thought to primarily occur during presentation of reward or salient cues (Cooper, 2002; Schultz et al., 1993). The majority of DA neurons are strongly activated by reward and reward-predicting stimuli (75-90%), while a subset of DA neurons (10-20%) are activated by punishers and conditioned aversive stimuli such as air puffs, hypertonic saline or electric shock (Schultz, 2010). The DA neurons that respond to aversive stimuli may be more frequently encountered in more medial regions of the

VTA, where a high concentration of DA neurons project to the PFC (Brischoux et al., 2009; Lammel et al., 2011). In the PFC and amydgala there is a more sustained DA release pattern than in the striatum (Garris and Wightman, 1994). Lammel et al found that the VTA DA neurons that project to the PFC, basolateral amygdala, and NAc are able to fire action potentials at a higher frequency (20-30 Hz) than those that project to the striatum (<10 Hz) (Lammel et al., 2008). In addition, some PFC projecting DA neurons lack D_2R autoinhibition and have low levels of DAT expression. These factors likely contribute to the sustained pattern of DA release seen in the PFC.

Functional implications of dopamine neuron heterogeneity

Prior to the last five years many studies of VTA DA neurons focused on DA neurons in lateral VTA areas while DA neurons in the medial VTA and A10dc areas were largely ignored. The few studies that have focused on medial DA neurons have shown interesting results. Lammel et al. show that only an aversive stimulus increases the AMPA/NMDA ratio of medial PBP and paranigral DA neurons projecting to the PFC, while the AMPA/NMDA ratio of traditional NAc projecting lateral VTA DA neurons is increased only by rewarding stimuli (Lammel et al., 2011). DA neurons of the A10dc areas, specifically those located in the PAG, are regulated by a variety of actions including acute ethanol, heroin reward, and the sleep-wake cycle (Flores et al., 2006; Li et al., 2013a; Lu et al., 2006). The A10dc and medial DA neurons of the RLi and CLi primarily project to the PFC, central nucleus of the amygdala (CeA), and the bed nucleus of the stria terminalis (BNST) (Deutch et al., 1991; Hasue and Shammah-Lagnado, 2002; Lammel et al., 2008; Lammel et al., 2011). These downstream regions

are heavily involved in addiction and reward, as well as stress and anxiety related behaviors. There is some evidence that the DA neurons of the PAG play roles in alcohol and heroin reward. For example, depletion of RLi and PAG DA abolishes heroin conditioned place preference behavior in rats, and acute alcohol induces an enhancement of glutamatergic transmission and increases firing rate of vPAG DA neurons (Flores et al., 2006; Li et al., 2013a). However, there have been very few studies examining the roles of midline DA neurons in stress and anxiety.

Sensitivity of the dopamine system to stress

Stress may lead to pathological conditions such as anxiety disorders, depression, post-traumatic stress disorder (PTSD), and addiction, and stress is commonly stated as a cause of relapse for those suffering from drug addiction (Sareen et al., 2006; Sinha et al., 2011). There is evidence that DA plays a role in the stress response; therefore, further examination of DA's involvement in stress may lead to novel treatment pathways for stress-induced pathological conditions.

Acute stress increases c-fos expression in a subset of dopamine neurons

Stress may alter the activity of DA neurons, and one way of looking at this is through the expression of immediate early genes such as *c-fos*. Activation of immediate early genes represents metabolic activation or increases in the activity of a neuron. Following acute immobilization stress there is an increase in Fos immunoreactivity in areas positive for TH terminals in the rat CeA (Honkaniemi, 1992; Honkaniemi et al., 1992). Other acute stressors, such as exposure to TMT, mild foot shock, and restraint,

lead to an increase in Fos immunoreactivity among DA neurons of the VTA, but not SN in rats (Deutch et al., 1991; Redmond et al., 2002). Deutch and colleagues determined that this stress-induced *c-fos* increase varies by VTA subregions, with the highest increases in the PBP and CLi, and that the majority of double labeled Fos and TH neurons project to the mPFC with few projecting to the NAc (Deutch et al., 1991). The CLi DA neurons heavily project to the BNST and CeA (Hasue and Shammah-Lagnado, 2002), but this study did not determine whether the Fos labeled cells project to these regions of the extended amygdala.

Alterations in dopamine concentration and metabolism

Stress may also lead to changes in the DA levels and metabolism. For example, intermittent tail shock and foot shock stress increase extracellular DA levels in the striatum, NAc, and mPFC (Abercrombie et al., 1989; Kalivas and Duffy, 1995; Sutoo and Akiyama, 2002). Several acute stressors including immobilization, restraint, exposure to the predator odor TMT, and foot shock increase DA metabolism in downstream regions such as the mPFC, NAc shell, CeA, and BNST (Coco et al., 1992; Deutch et al., 1991; Morrow et al., 1997; Morrow et al., 2000). In contrast, chronic stress paradigms such as six days restraint stress or three weeks of restraint combined with unavoidable tail shock decrease the levels of DA and its metabolites in the NAc shell (Imperato et al., 1993; Mangiavacchi et al., 2001). Based upon the increase in *c-fos* expression and changes in DA levels in target regions, alterations in firing of DA neurons after acute stress exposure might be expected.

Alterations in the firing of dopamine neurons

There is some evidence that the firing of DA neurons is inhibited by aversive stimuli, such as foot shock, in anesthetized rats (Ungless et al., 2004). However, there are studies in which firing of putative DA neurons is enhanced with stress. *In vivo* electrophysiology recordings indicate that noxious tail pinch of the anesthetized rat selectively increases the firing rate of A10 DA neurons that innervate the PFC, but not DA neurons that project to the NAc (Mantz et al., 1989). One session of restraint stress in awake rats increases the number of spikes within a burst in VTA DA neurons that have a high level of basal bursting activity (Anstrom and Woodward, 2005). A single exposure to social defeat stress in rats also increases burst firing in VTA DA neurons and increases DA release in the NAc core (Anstrom et al., 2009). An increase in DA firing rate after acute stress correlates with previous data discussed highlighting increases in DA concentration and metabolism after acute stress.

In contrast, rats that are subjected to chronic cold stress undergo a decrease in the number of spontaneously active DA cells compared to control animals (Moore et al., 2001). The firing rate and percentage of spikes fired in bursts are not significantly altered from that of control animals. However, the distribution of bursting across VTA and SN DA neurons differs between the two groups. There is a population of DA neurons in the stressed animals that exhibit an extremely high bursting rate. The decrease in active DA cells with a chronic stressor correlates with data showing decreased levels of DA in target regions after chronic stress (Imperato et al., 1993; Mangiavacchi et al., 2001). These data suggest that chronic stress may inactivate one population of DA neurons while increasing burst activity in another. There is evidence

that populations of DA neurons possess the ability to switch from single spiking mode to burst firing mode (Cooper, 2002). These populations may represent DA neurons that project to different target regions, such as PFC, NAc, BNST or CeA. Different populations of DA neurons and their projection targets may mediate unique responses to stress, perhaps differing in sensitivity to stress or mediating the switch in response from acute to chronic stress. Since stress modifies the firing properties of some DA neurons and norepinephrine is a major stress neurotransmitter, it can be postulated that the actions of norepinephrine inputs may be partially responsible for the stress effects of DA.

Norepinephrine

One system by which stress could regulate DA is the neurotransmitter norepinephrine (NE). Interactions of the NE and DA system contribute to the pathophysiology of schizophrenia, major depressive disorder, and ADHD, which is often comorbid with major depressive and anxiety disorders (El Mansari et al., 2010; Hensler et al., 2013; Sharma and Couture, 2014). First I will provide background on the anatomy and signaling of NE and then discuss known interactions of NE and DA. The NE system was first visualized and characterized in the early 1960s along with the dopamine system. The noradrenergic cell groups (A1-A7) are defined in Table 1. The ascending axons of A1 and A2 combine to form the ventral noradrenergic bundle, while the locus coeruleus (LC) forms the dorsal noradrenergic bundle. The LC has a broad projection field, and NE arising from the LC has been shown to play roles in arousal and cognitive performance (Aston-Jones and Cohen, 2005; Clayton et al., 2004). The non-LC NE

neurons are located in brainstem homeostatic centers and have been shown to be involved in a variety of processes. For example, A1 neurons control the release of vasopressin, A2 neurons are involved in regulation of food intake, and A5 neurons regulate the respiratory rhythm generator of the rostral ventrolateral medulla (Blessing and Willoughby, 1985; Hilaire et al., 2004; Rinaman, 2003). The role of NE in stress has been widely studied (Abercrombie et al., 1988; Cecchi et al., 2002a; Korf et al., 1973; Smagin et al., 1995; Valentino et al., 1993). Many stressors increase the firing of NE neurons and increase NE turnover in target regions (Abercrombie et al., 1988; Cecchi et al., 2002a; Cecchi et al., 2002b; Korf et al., 1973).

Noradrenergic innervation of the dopamine system

It has long been known that the LC projects to the VTA (Geisler and Zahm, 2005; Jones and Moore, 1977; Phillipson, 1979b; Simon et al., 1979). More recently, it was determined that there is a large non-LC noradrenergic innervation to DA regions. Through dopamine beta hydroxylase (DBH) immunohistochemistry and anatomical tracing studies, Mejías-Aponte found that the VTA DA nuclei receive noradrenergic innervation from A1, A2, A5 and LC (Mejias-Aponte et al., 2009). Out of the nuclei investigated, the medial aspects of the PBP and paranigral VTA nuclei receive the smallest proportions of noradrenergic efferents. The RLi and CLi have a larger overall NE input and a larger percentage of NE arising from non-LC sources, while the medial PBP and paranigral nuclei have a large proportion of NE input arising from LC (Mejias-Aponte et al., 2009). There is also a noradrenergic input from the LC to the PAG, near the A10dc DA population (Lu et al., 2006). Electron microscopy studies have shown that

NE afferents have extrasynaptic and synaptic connections onto VTA DA neurons (Liprando et al., 2004). The abundant NE innervation makes the midbrain DA neurons prime candidates to undergo modulation by NE after stress. Furthermore, the varying noradrenergic input combined with differing outputs for distinct DA neuron populations indicates a possible differential sensitivity to stress among DA neuron populations.

Noradrenergic receptors

Norepinephrine can act through nine different adrenergic receptors (ARs). These nine ARs are divided into three classes: α_1-, α_2-, and β-ARs. Each class is further divided into the following subtypes: α_1-ARs consist of α_{1A}, $\alpha_{1B,}$ and α_{1D}; the α_2-ARs are α_{2A}, α_{2B}, and α_{2C}; and the β-ARs are β_1, β_2, and β_3 (Bylund et al., 1994). Adrenergic receptors are GPCRs that can act to modulate synaptic transmission at either pre- or post-synaptic sites. α_1-ARs signal through G_q mediated pathways, the α_2-ARs are linked to $G_{i/o}$ signaling, and the β-ARs signal through G_s mechanisms (Hein, 2006). There is some evidence of expression of the following ARs in the VTA: α_1-ARs, α_{2C}-ARs, and β_1- and β_2-ARs (Day et al., 1997; Greene et al., 2005; Jones et al., 1985; Lee et al., 1998; Rainbow et al., 1984).

Noradrenergic modulation of dopamine neurons

Alterations in the excitability of dopamine neurons

NE has been shown to bidirectionally modulate the firing of DA neurons. A series of *in vivo* studies done by Grenhoff and colleagues show that electrical stimulation of

the LC and administration of drugs acting on adrenergic receptors can alter DA neuron firing within the SN and VTA of rats (Grenhoff and Svensson, 1988; Grenhoff and Svensson, 1989; Grenhoff et al., 1993; Grenhoff and Svensson, 1993). These studies show that activation of the α_1-AR leads to increased burst firing of VTA DA neurons, and burst firing can be increased or decreased with blockade or activation of α_2-ARs, respectively. *Ex vivo* recordings in rat brain slices show that transient activation of α_1-ARs via iontophoresis leads to an outward current that would likely inhibit firing of VTA DA neurons while prolonged activation leads to an inward current that may make VTA DA neurons more excitable (Guiard et al., 2008a; Paladini and Williams, 2004). An LC selective lesion enhances the *in vivo* firing of VTA DA neurons, suggesting a net inhibitory role of LC-NE on VTA DA neurons (Guiard et al., 2008b). There is also evidence of adrenergic modulation of I_h, the hyperpolarization activated cation current, in putative VTA DA neurons in rat brain slices. The activation of α_2-ARs leads to an inhibition of I_h and inhibition of spontaneous firing in DA neurons that can be blocked by selective α_2-AR antagonists (Inyushin et al., 2010). These results are in concordance with the Grenhoff studies, in which activation of α_2-ARs lead to a decrease in firing rate *in vivo*. The role of NE on excitability of DA neurons may vary depending on the specific receptors activated and their site(s) of action, the length of agonist application, and the source of NE input. In general, activation of α_1-ARs and α_2-ARs leads to an increase and decrease, respectively, in the excitability of midbrain DA neurons. Further work needs to be done in this area to determine the mechanisms underlying NE modulation of DA neuron firing. One possibility is that NE may modulate synaptic transmission which then influences the firing of DA neurons.

Noradrenergic modulation of synaptic transmission onto dopamine neurons

Norepinephrine is a powerful modulator of synaptic transmission in many brain regions, including the VTA. Since there are NE inputs in the VTA and evidence of multiple AR subtypes, it is possible that NE may modulate synaptic transmission onto DA neurons. Indeed, activation of α_1-ARs decreases GABAergic transmission onto VTA DA neurons via a presynaptic mechanism (Velasquez-Martinez et al., 2015). Changes in GABAergic input on VTA DA neurons can control their firing patterns, and decreased GABAergic inhibition contributes to the generation of bursts in DA neurons (Lobb et al., 2010; Morikawa and Paladini, 2011; Paladini et al., 1999; Paladini and Tepper, 1999). Stimulation of glutamate afferents facilitates the switch from pacemaker firing to burst firing in midbrain DA neurons (Harnett et al., 2009; Overton and Clark, 1992; Seutin et al., 1993). Therefore, modulation of glutamatergic transmission onto DA neurons by NE could have profound effects on firing of DA neurons and subsequently, the amount of DA released in target regions.

The α_1-AR is involved in many different physiological processes

The α_1-AR is involved in the development of stress and anxiety responses, as well as addiction-related behaviors (Cecchi et al., 2002b; Greenwell et al., 2009; Jimenez-Rivera et al., 2006). In addition, stimulation of the α_1-AR has numerous effects in the periphery and central nervous system. There are many examples of α_1-ARs influencing GABAergic transmission. For example, in the piriform cortex and the CA1 region of the hippocampus α_1-AR activation leads to an excitation of interneurons

(Bergles et al., 1996; Hillman et al., 2009; Marek and Aghajanian, 1996). α_1-AR mediated increases in inhibitory drive have been shown to occur in many brain regions such as the frontal, entorhinal and cerebellar cortices, basolateral amygdala, BNST, and medial septum (Alreja and Liu, 1996; Braga et al., 2004; Dumont and Williams, 2004; Herold et al., 2005; Kawaguchi and Shindou, 1998; Lei et al., 2007). In addition to the effects of α_1-AR activation on GABAergic transmission, there are many examples of α_1-AR activation modulating glutamatergic transmission. In layer V of pyramidal cells of rat cortex, α_1-AR activation causes a decrease in excitatory postsynaptic currents (EPSCs) through postsynaptic mechanisms (Kobayashi et al., 2009). Numerous studies indicate that α_1-AR activation leads to long term depression (LTD) of excitatory transmission in several brain regions such as visual cortex, hippocampus, and BNST (Kirkwood et al., 1999; McElligott and Winder, 2008; McElligott et al., 2010; Scheiderer et al., 2004; Scheiderer et al., 2008). In contrast, there are also many studies indicating that α_1-AR stimulation increases spontaneous EPSCs and/or miniature EPSCs in many brain regions including cultured hippocampal neurons, hypothalamus, mPFC, and prelimbic cortex (Aubert et al., 2001; Dong et al., 2005; Gordon and Bains, 2003; Gordon and Bains, 2005; Marek and Aghajanian, 1999).

In addition to their actions in the CNS, there are also many actions of α_1-ARs in the periphery. α_1-ARs mediate smooth muscle contraction which can result in vasoconstriction and hypertension (Piascik and Perez, 2001). In contrast, α_1-ARs underlie relaxation of the smooth muscle in the gut. The α_1-AR has a positive inotropic effect on the heart and can induce glycogenolysis and gluconeogenesis from adipose tissue (Purves, 2012). α_1-AR agonists are commonly used to treat nasal congestion,

while α_1-AR antagonists can be used to treat hypertension or benign prostrate hyperplasia (Lepor et al., 2012).

Summary

In recent years, it has become apparent that dopamine neurons of the A10 group do not belong to one homogenous group. They differ in their basic electrophysiological properties and molecular expression profiles. For example, some DA neurons located in the medial VTA and other midline areas such as the PAG lack a robust I_h and have lower levels of D_2R, DAT, VMAT2, and TH mRNA expression. Even though these unique populations of DA neurons have received attention in recent years, classical studies of VTA neurons largely ignore midline DA neurons. In this dissertation, we will focus on the unique, understudied DA neurons of the RLi and A10dc regions. These midline DA neurons are activated by stress, receive a dense noradrenergic input, and comprise a large portion of the DA input to the extended amygdala, an area heavily involved in stress and anxiety related behaviors (Deutch et al., 1991; Hasue and Shammah-Lagnado, 2002; Mejias-Aponte et al., 2009; Meloni et al., 2006). The circuitry of these DA neurons makes them prime candidates for NE neuromodulation. In the second chapter of this dissertation, I report retrograde tracing studies that identify sub-regions of DA neurons that project to the dorsal BNST in a TH-eGFP reporter mouse line. Then in the third chapter, the effects of NE on excitatory transmission onto DA neurons of the RLi in the TH-eGFP mouse are examined.

CHAPTER II

A10dc dopamine neurons innervate the dorsal lateral bed nucleus of the stria terminalis

Dopamine signaling is critically important in both acute and chronic responses to drugs of abuse. To date, most work has focused on the impact of drugs of abuse on dopamine neurons in the ventral tegmental area. However, an additional population of midline dopamine neurons in the periaqueductal grey and dorsal raphe, the A10dc, may play a critical role in addiction. These neurons are particularly interesting, as they project to several regions of the brain that regulate anxiety like behavior and stress responsivity. Since stress is the most frequent cause of relapse in previously addicted humans, we have begun to explore the anatomy of A10dc DA neurons in a mouse model, with the long term goal of understanding the role of these neurons in anxiety and addiction related behaviors. We used a transgenic mouse line that expresses eGFP under the control of the tyrosine hydroxylase promoter to visually identify DA neurons within the ventral tegmental area, rostral linear and caudal linear nuclei, ventral lateral periaqueductal grey, and dorsal raphe. Retrograde tracer was injected into the bed nucleus of the stria terminals, a region of the extended amygdala shown to be important in stress-induced reinstatement of drug-seeking. As shown previously in rats, both A10dc and ventral tegmental area DA neurons project to the dorsal BNST. The largest numbers of eGFP-expressing neurons labeled with tracer were found in the ventral tegmental area, rostral linear nucleus, and A10dc group, located in the caudal portion of the dorsal raphe and adjacent ventral periaqueductal grey.

Introduction

In human drug abusers, a major hurdle for successful long-term rehabilitation has been relapse of drug use even after a drug-free period of many years. Of the many reasons for relapse, stress has been cited as a primary cause (Erb, 2010; Sinha et al., 2011). Brain networks that are active during stress responses include interconnected parts of the prefrontal cortex, extended amygdala, ventral tegmental area (VTA), hypothalamus, and brainstem areas such as the periaqueductal grey and norepinephrine containing nuclei. In particular, the bed nucleus of the stria terminalis (BNST) within the extended amygdala and the VTA, have been shown to be critical for relapse of drug-seeking behavior (Briand et al., 2010; Erb, 2010). Therefore investigations of the BNST and its immediate network partners may lead to therapeutic targets for breaking the cycle of drug addiction that rules the lives of susceptible individuals.

In order to design rational therapies for prevention to relapse, a clearer understanding of the cellular and molecular events that underlie changes in how network partners communicate at each stage of the addiction cycle is needed. VTA DA (A10) neuron activity patterns have been shown to encode reward error information (Tobler et al., 2005) and a single cocaine injection is sufficient to cause a long-term increase in the AMPA/NMDA receptor ratio at glutamatergic synapses onto VTA DA neurons (Borgland et al., 2004; Kauer and Malenka, 2007). The DA released at synapses in several brain areas controls synaptic plasticity that plays important roles in the behavioral effects of drugs of abuse (Thomas et al., 2001). For example, in the BNST DA enhances spontaneous glutamatergic transmission (Kash et al., 2008) and

decreases evoked glutamatergic and inhibitory transmission (Krawczyk et al., 2011a; Krawczyk et al., 2011b). In addition, DA mediates a form of long term potentiation at BNST GABA synapses (Krawczyk et al., 2013), decreases BNST NMDA currents in cocaine self-administering rats (Krawczyk et al., 2014), and regulates long-term intrinsic excitability of BNST neurons (Francesconi et al., 2009). The BNST receives some of its DA afferents from the VTA. However, anatomical studies in rats show that about half of the DA neurons that project to the BNST are in the dorsal-caudal extension of the A10 DA neurons, called the A10dc cell group, which is located in the dorsal, rostral linear and central linear raphe nuclei (Hasue and Shammah-Lagnado, 2002; Zahm et al., 2001). Importantly, these brainstem nuclei have been shown to be involved in the relay of visceral stress information as well as anxiety and pain (Meloni et al., 2006; Walker and Davis, 2008). Also, a small but potentially significant DA input to the BNST has been shown to originate from the ventral lateral periaqueductal grey (vlPAG) in rats (Meloni et al., 2006). The DA neurons of the RLi and vlPAG are involved in the rewarding properties of heroin (Flores et al., 2006).

In recent years, an appreciation of the heterogeneity of DA neurons has arisen. It has been shown that DA neurons have different molecular expression profiles and electrophysiology properties based on their projection targets (Lammel et al., 2008; Margolis et al., 2008). Modulation of AMPA/NMDA ratios of A10 DA neurons in response to rewarding or aversive stimuli varies by their projection target (Lammel et al., 2011). In fact, DA neurons that project to the nucleus accumbens medial shell are modified by a cocaine injection while those that project to the PFC only respond to an

aversive stimulus (Lammel et al., 2011). While there has been much recent work in this area, none of these studies examine DA neurons that project specifically to the BNST.

In this study, we sought to identify sub-regions of DA neurons that project to the mouse dorsal BNST. In addition we utilized a TH-eGFP transgenic reporter mouse to confirm the fidelity of eGFP in populations that project to the BNST. These studies will be crucial for guiding future electrophysiology studies investigating subpopulations of DA neurons that project to the BNST, as in Chapter III.

Methods

Animals

Male mice ages 7-10 weeks were used in these experiments in accordance with animal use protocol approved by the Institutional Animal Care and Use Committee of Vanderbilt University. All experiments were carried out in strict accordance with the recommendations in the Guide for the Care and Use of Laboratory Animals (NIH, Publications 864-23). Mice were group housed in the Vanderbilt vivarium with free access to food and water under a 12/12 hour light/dark cycle. C57BL/6J mice were used for the initial identification of brain areas with TH+ neurons that project to the BNST. Subsequent retrograde tracer and neuron count data were obtained from a TH-eGFP BAC transgenic mouse line (Strain Name: STOCK Tg(Th-EGFP)DJ76Gsat/Mmnc). Mating pairs of mice were from the Mutant Mouse Regional Resource Center in North Carolina. In this mouse line, the genome was modified to contain multiple copies of a modified BAC in which an eGFP reporter gene was inserted immediately upstream of

the coding sequence of the gene for tyrosine hydroxylase. Data presented here were obtained from a lineage of transgenic mice maintained in-house derived by cross-breeding with Swiss Webster mice (Taconic).

Stereotaxic surgeries and tracer injections

7-10 week old mice were anesthetized with Isoflurane and secured in a stereotaxic apparatus (MyNeuroLab, Angle 2). The skull above the BNST was exposed and a small hole drilled through the bone. A glass micropipette with a tip diameter of approximately 30 μm was back-filled with a 3% solution of the retrograde tracer, fluorogold (FG), dissolved in cacodylate buffer (0.1 M, pH 7.0), and then inserted into the BNST. FG was microiontophoresed into the BNST with +1.5 μA in a 7 sec on/7 sec off cycle that lasted for 8 minutes. Ten minutes later, the pipette was withdrawn and the scalp wound was sutured closed. After recovery from the anesthesia, mice were returned to their home cage and given buprenorphin analgesic at 0.1 mg/kg, sc., every 12 hours for 4 days. At 8 days post injection, mice were overdosed with Nembutal (100 mg/kg, i.p.) for harvesting of brain tissue.

Immunohistochemistry and microscopy

Mice were transcardially perfused with ice–cold phosphate-buffered saline (PBS), followed by ice-cold 4% paraformaldehyde in PBS. Brains were removed from the skull and post-fixed in the same fixative overnight at 4°C and were then transferred to 30% sucrose in PBS. Two to five days later, 50 μm thick coronal or 100 μm sagittal sections of brain were sliced on a cryostat (Leica CM3050S). Free-floating sections were washed

in PBS (4x10 minutes), permeabilized with 0.5% Triton-X 100 in PBS, and then blocked with 10% normal donkey serum in PBS containing 0.1% Triton-X-100. Sections were then incubated with primary antibody in blocking solution for 48 hours at 4°C, followed by PBS washes (4x10 minutes) and incubation with cyanine dye-conjugated secondary antibodies for 24 hours at 4°C in PBS with 0.1% Triton-X-100. Finally, sections were washed (4x10 minutes), mounted on slides, sealed with PolyAquamount, and left overnight to dry. Stained sections were examined with a Zeiss 510 scanning confocal microscope. Z stacks of images were taken of every other sagittal section through the medial/lateral extent of the PAG or every 3rd coronal section through the rostral/caudal extent of the PAG and dorsal raphe nucleus (Franklin and Paxinos, 1997). Some FG injection site sections were imaged without immunohistochemistry, using intrinsic fluorescence induced by a 405 nm laser on a FV1000 Olympus confocal scanning microscope. Other injection site sections and all brainstem sections examined for retrograde labeled neurons were processed for immuno-staining for FG. Stained and unstained injection site sections gave similar results as to location and spread of FG. Control sections from wild type mice injected with FG and immuno-stained for FG showed only background fluorescence when imaged with eGFP channel settings, suggesting that after immuno-staining, native fluorescence of FG did not contribute to the eGFP signal.

Reagents

Fluorogold was obtained from Fluorochrome, mouse monoclonal anti-TH antibody from ImmunoStar (used at 1:2000 dilution), and rabbit polyclonal anti-

fluorogold antibody from Chemicon (used at 1:3000 dilution). Secondary antibodies were purchased from Jackson ImmunoResearch and included Cy5-conjugated donkey anti-mouse (1:500), and Cy3-conjugated donkey anti-rabbit (1:500) FAB fragments.

Data analysis

TH-positive neurons in these brain areas have been previously shown to be dopamine beta hydroxylase negative and therefore dopaminergic (Flores et al., 2006; Lein et al., 2007). A10dc DA neurons are distributed within several areas including the dorsal, rostral linear and central linear raphe nuclei, the medial part of the vlPAG which contains small DA neurons, and in other parts of the PAG adjacent to the aqueduct. For counting single and multiple labeled neurons, z stacks of imaged brain sections were projected onto a single plane using Zeiss LSM software. Projected images were then opened in Metamorph and neurons counted with the help of a manual logger function. The signal intensity threshold for counting neurons as positive for a marker was set at twice that of the brightest neurons in no primary antibody control sections (TH and FG), or for eGFP, neurons in brainstem areas that did not express eGFP. In order to reduce bias, random groups of 3-5 sections from each animal were counted by 2 or 3 different investigators to be sure that the number of neurons in each category did not vary more than 10% between investigators. Although formal stereological methods were not employed in counting labeled neurons, we are satisfied that the level of precision obtained by our chosen method is sufficient to accurately detect the location of labeled neurons needed to direct targeted electrophysiological recordings from subpopulations

of DA neurons that likely project to the dBNST. Quantitative data are expressed as mean ± S.E.M. unless otherwise noted.

Results

Preliminary identification of TH-positive BNST afferents

Wild-type C57BL/6J adult male mice were used for initial unilateral injections of FG into the dBNST. Two mice with tracer confined to the target region were serial-sectioned in the sagittal plane and stained for FG and TH. The injection site of an example mouse is shown in Figure 2. The spread of FG was confined to the dBNST in the medial/lateral and rostral/caudal directions. In this example mouse and others in this study, FG also spread in the rostral direction to include the transition zone between the dBNST and the nucleus accumbens (Franklin and Paxinos, 1997; AP level 0.62 mm to Bregma). In mice where the injection site missed the BNST (with FG injections into the striatum only or the rostral globus pallidus lateral or dorsal to the dBNST, n=4) there were at most one or two FG positive/eGFP positive neurons in the A10dc. As expected, striatal injections labeled large numbers of A9 eGFP positive neurons (data not shown).

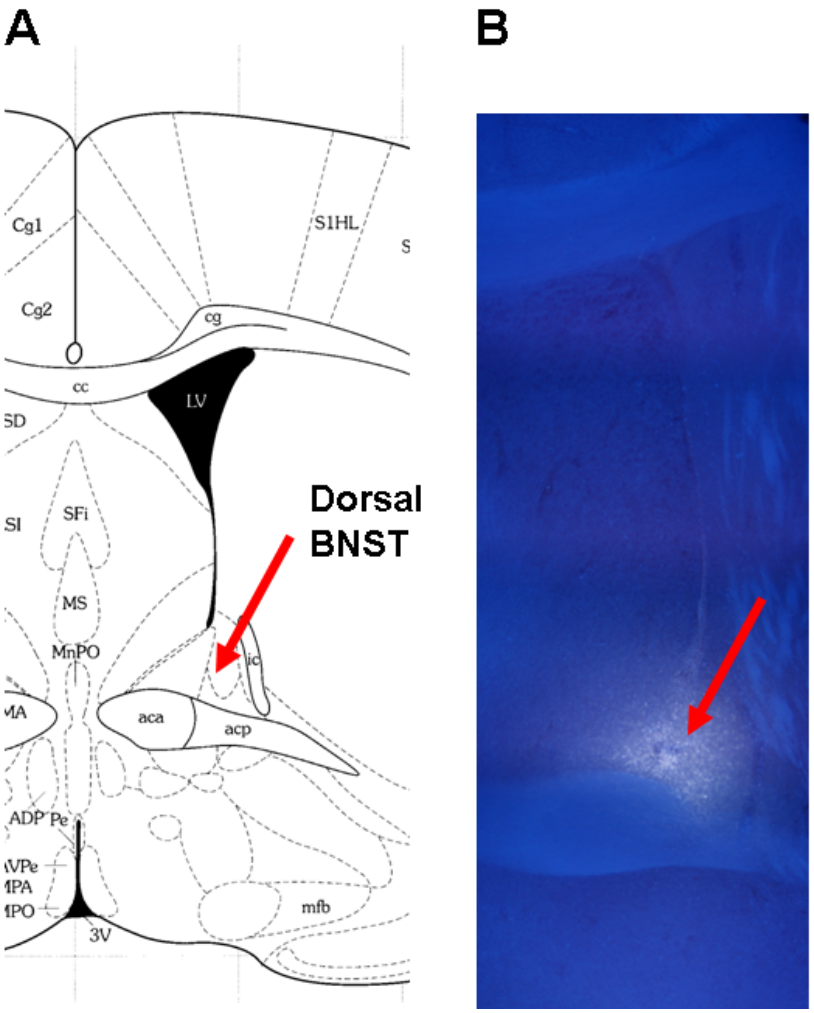

Figure 2: Example of a fluorogold injection into the dorsal BNST of a mouse. (A) Diagram of coronal brain section from Franklin & Paxinos mouse atlas showing location of the dorsal BNST. (B) results of an iontophoretic injection of fluorogold into the dorsal BNST. Fluorogold fluorescence is seen here without immunohistochemical staining. *Data obtained by Dr. Robert Matthews*

A brain atlas diagram of a parasagittal section that shows the nuclei of interest near the midline is shown in Figure 3A, and Figure 3B is a corresponding stained section from the same mouse as shown in Figure 2. The stained section shows the extent of the continuum of TH-positive neurons, including near midline A10, A10c, A10dc, and PAG neurons, plus neurons containing FG that project to the dBNST. In particular, single labeled and double labeled neurons were found throughout the extent of the DA neuron continuum. Three sub-regions appeared to be especially rich in double-labeled neurons, the VTA, the RLi and the caudal part of the DR (Figure 3B inset; see Figure 6 for cell counts).

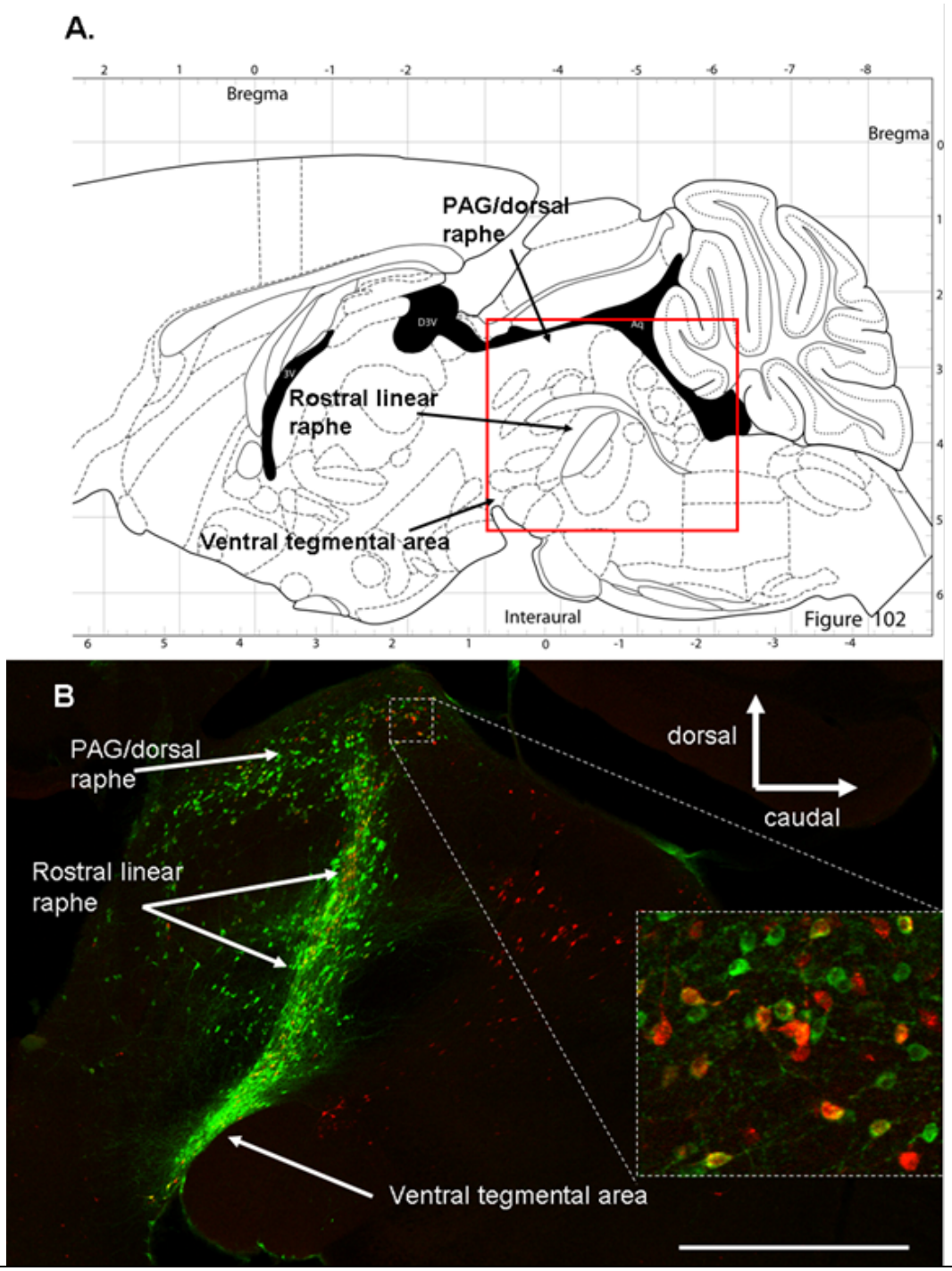

Figure 3: Retrograde tracer data showing that a subset of TH positive brainstem neurons project to the dorsal BNST.
(A) Diagram of a sagittal brain section from Franklin & Paxinos mouse atlas. (B) Example section of wild-type mouse brain injected with FG into the dBNST, taken from a medial/lateral coordinate closely matching the diagram in *A*. TH+ neurons are green and FG+ neurons are red. Inset: higher magnification view of the caudal part of the ventral PAG and dorsal raphe nucleus. Yellow/orange neurons are double labeled for FG and TH. Scale bar = 1 mm. *Data obtained by Dr. Robert Matthews*

Distribution of eGFP-expressing dopamine neurons that project to the dBNST

FG was injected into the dBNST of transgenic mice (n=6) expressing eGFP under control of the TH promoter. Using our preliminary experiments in wild type mice as a guide, serial coronal sections were cut throughout the rostral/caudal length of the DA neuron continuum of sub-nuclei where FG positive neurons were also observed. Every third section was processed for immuno-staining for FG and TH, and the numbers of eGFP+, TH+, FG+, double labeled and triple labeled neurons were counted in images captured from each section with a 20x lens. Figure 4 shows typical sections used for cell counting at the level of the caudal dorsal raphe (A,B) and about the middle of the RLi (C,D). For cell counts, multicolor images were examined as separate images of each fluorophore, and as overlapping pairs of fluorophores. Figure 5 shows a series of higher magnification images taken of the dorsal raphe nucleus of one mouse at AP=4.3 mm, centered approximately 100 μm ventral to the aqueduct. These images show the color of single, double or triple labeled neurons that were used in neuron counts. In order to address the questions of fidelity of eGFP expression within A10dc DA neurons, we counted TH+ neurons, eGFP+ neurons, and neurons with both markers from the RLi to the caudal end of the cerebral aqueduct. The percentage of TH+ neurons that were eGFP+ ranged from 41 to 82% and varied little along the rostral/caudal axis (62.9 ± 2.0 %, n=3 mice, 8 sections per animal), suggesting substantial but incomplete labeling of DA neurons by transgenic expression of eGFP in this mouse line. When fidelity of eGFP expression to catecholaminergic neurons only was assessed for the A10dc brain region, the number of eGFP neurons that were TH+ showed a gradient along the rostral/caudal axis. Fidelity was highest in rostral sections (93.1 ± 1.6% at AP= -3.5; n=3 mice), slightly

lower at the level of the PAG/DR enriched in cells that project to the BNST (Figure 6) (75.8 ± 2.1% at = -4.2; n=3 mice) and less than 50% at AP levels more caudal than AP= -4.6 (39.2 ± 2.7%). These data suggest that eGFP fluorescence in this mouse line is a good although imperfect marker for A10dc DA neurons throughout most of its rostral/caudal extent. Neurons that were triple labeled, that is TH positive, DA neurons expressing eGFP that project to the dBNST, were most abundant approximately 4.2 mm posterior to Bregma with a smaller peak of abundance at about 3.5 mm posterior to Bregma. At these coordinates, triple labeled neurons constituted 21.5% and 17.5% of all eGFP neurons, respectively. Most triple labeled neurons had relatively small soma, in agreement with findings in rats (Hasue and Shammah-Lagnado, 2002; Meloni et al., 2006). A summary graph of neuron counts for three mice whose injection sites had FG confined to the dBNST is shown in Figure 6. Three additional mice with spread of FG beyond the dBNST, laterally into the internal capsule, globus pallidus, and medial striatum had the same pattern and similar neuron counts in the A10dc/PAG areas but in addition had substantial numbers of double and triple labeled neurons in the substantia nigra (data not shown).

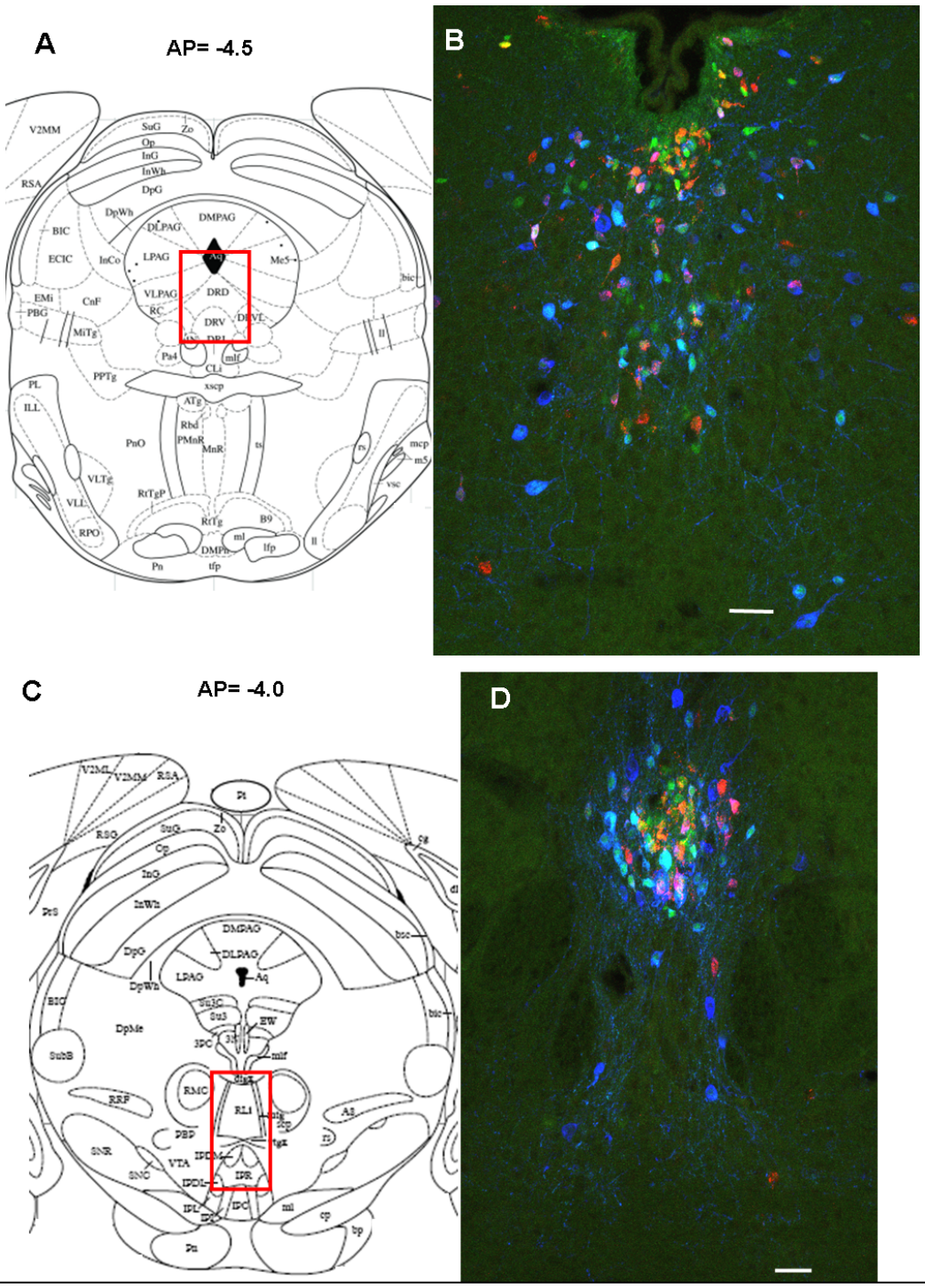

Figure 4: Examples of retrograde tracer data showing coronal sections from dorsal BNST-injected, TH-eGFP transgenic mice.
(A&C) Brain atlas diagrams showing structures of interest and the regions (red boxes) selected for imaging and counting labeled neurons. (B&D) Corresponding confocal images (projections of z-stacks from 50 µm thick brain sections) of the regions in A & B. Blue = TH: green = eGFP; red = FG; purple = TH & FG; orange = eGFP & FG; aqua = TH & eGFP; scale bar = 50 um, applies to C & D. See Figure 5 for high magnification images and Figure 6 for cell counts. *Data obtained by Dr. Robert Matthews*

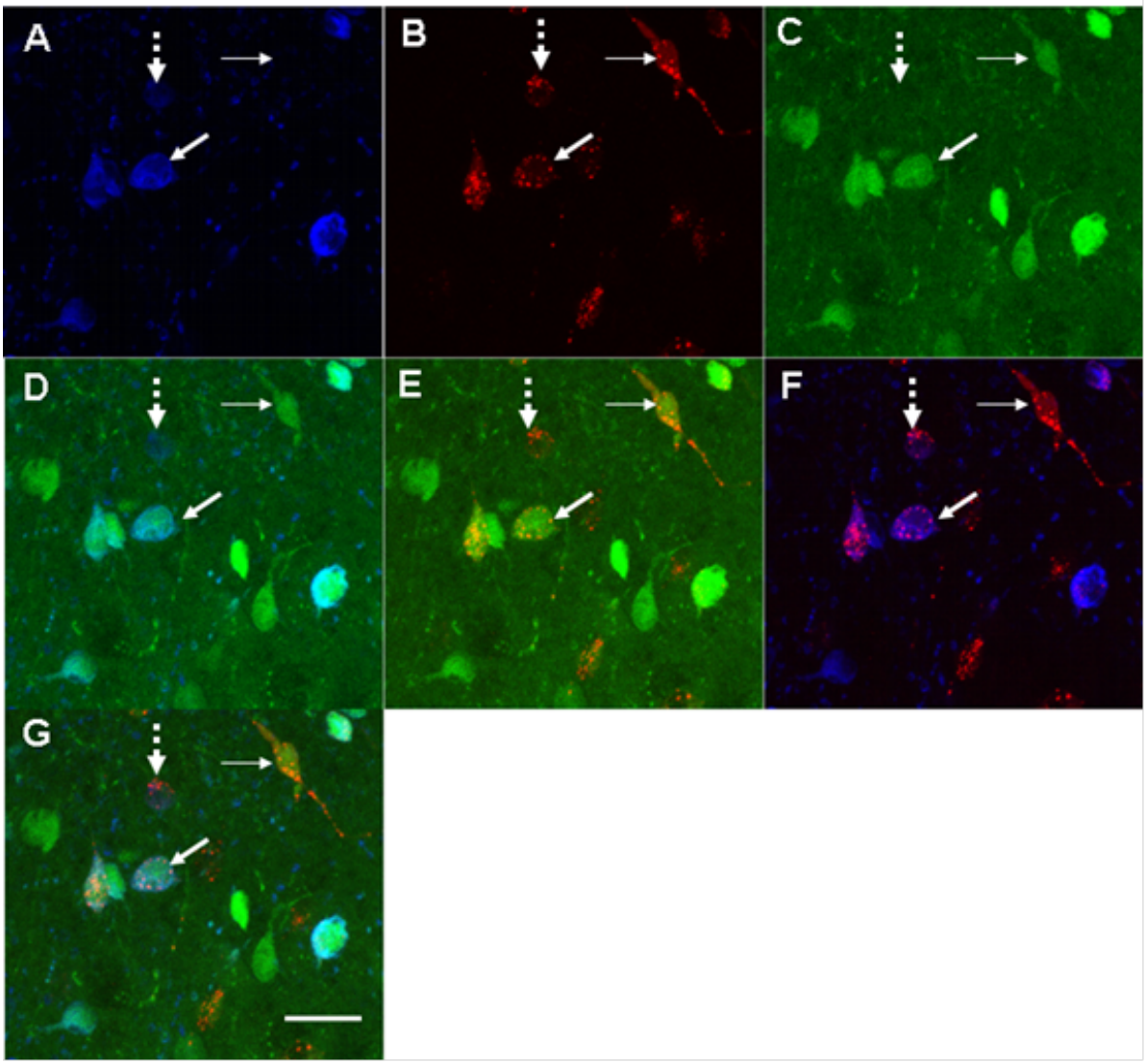

Figure 5: High magnification confocal images of dorsal raphe neurons from projections of a subset (20 µm thick) of confocal microscope images. (A-C). Examples of labeled neurons for TH (blue), FG (red) and eGFP (green). (D-F) Overlay images showing examples of double labeled neurons, TH & eGFP, FG & eGFP and FG & TH, respectively. (G) Overlay image showing all three markers. Dotted vertical arrows indicate a neuron showing TH and FG only. Horizontal thin arrows indicate a neuron showing FG and eGFP only. Diagonal thick arrows indicate a triple labeled neuron. This section also contains singly labeled neurons for each marker (not indicated). Scale bar equals 20 µm. *Data obtained by Dr. Robert Matthews*

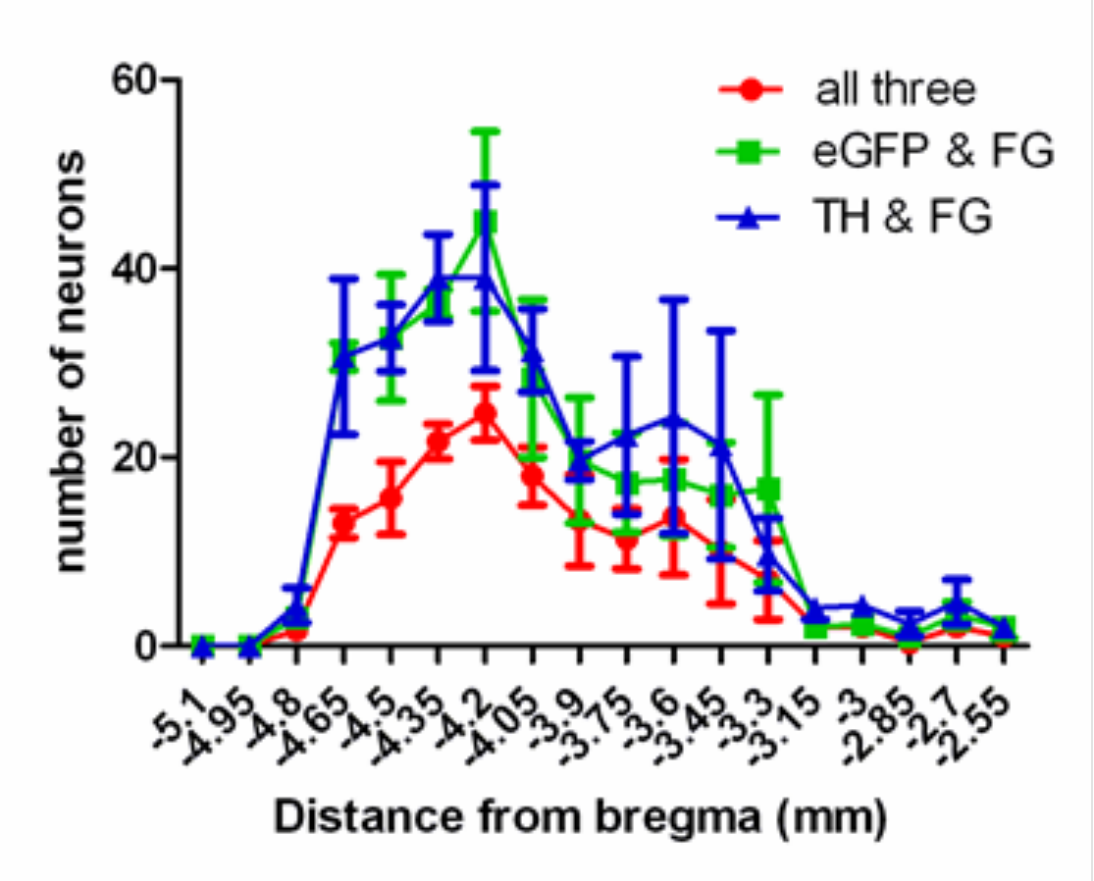

Figure 6: Plot of the number of labeled neurons counted in skip serial coronal sections from transgenic mice with unilateral injections of FG into the dBNST. Symbols represent the mean ± S.E.M., n=3. *Data obtained by Dr. Robert Matthews*

Discussion

The BNST has been subdivided into multiple regions along the anterior/posterior, medial/lateral and dorsal/ventral dimensions (Dong et al., 2000; Dong et al., 2001; Dong and Swanson, 2003). The anterior dorsal lateral region (dlBNST) is composed of several sub-nuclei (Ju and Swanson, 1989) that are involved in relapse of drug seeking behavior in response to stress in rodent models of drug addiction (Briand et al., 2010). The dBNST receives most of the DA innervation of the BNST with a gradation of fiber density that is highest in the medial dBNST (Alheid et al., 1998). We and others have shown that DA is involved in regulating corticotropin releasing factor (CRF) and glutamate dependent signaling in the BNST and therefore the DA afferents to the BNST likely encode information relevant to drug addiction related behaviors (Francesconi et al., 2009; Kash et al., 2008).

VTA DA neurons have been extensively studied, their electrophysiological properties, propensity for burst or pacemaker-like firing patterns, and the correlation of firing with reward and reward-related cues are known (Grace and Onn, 1989; Grace et al., 2007; Lammel et al., 2008; Margolis et al., 2006; Tobler et al., 2005). All drugs of abuse are known to increase dopaminergic neurotransmission and some have been shown to cause long-term changes in the VTA (Saal et al., 2003). In contrast to VTA DA neurons, A10dc and PAG DA neurons have not been extensively characterized, nor is it known if drugs of abuse have effects on glutamatergic synapses on identified DA neurons in these brain areas. Since the midline raphe/PAG areas are known to mediate reactions to stress, anxiety, and pain (Meloni et al., 2006), A10dc DA neurons are in a key position to report information to the dBNST that would combine with reward related

signals from VTA DA neurons and contribute to stress-induced relapse. Data presented here can be used as a guide for creating *ex vivo* brain slice preparations from TH-eGFP transgenic mice in order to record from DA neurons in sub-regions of the A10dc group that project to the dBNST. Questions can then be addressed as to how acute and chronic exposures to drugs of abuse affect synaptic transmission in these DA neuron nuclei as compared to the VTA.

In summary, we have shown that the A10dc neurons in mice contribute a large portion of the DA neurons that project to the dBNST and are easily identified in brain slice preparations from a transgenic mouse line that expresses eGFP in a subset of TH+ neurons. In particular, the caudal part of the dorsal raphe nucleus and the rostral linear raphe nucleus contain most of the DA afferent neurons that are found outside of the VTA and project to the BNST. These data agree with previously published data from rats. Selective recording from eGFP+ neurons from these mice will contribute to the understanding of their role in addiction related behaviors.

Anatomical Caveats

We would like to address the issue regarding the difficulty of delineating boundaries between the dopaminergic regions of the RLi, CLi, vPAG, and DR. The DA neurons in these regions are not delineated with clear boundaries and it is therefore difficult to distinguish regions for cell counts. This reason is the basis for our representation of cell counts in Figure 6 in terms of distance from Bregma rather than anatomical divisions. The anatomical descriptions of the data in this section were based on our interpretation of Hökfelt (Hokfelt et al., 1984) and the Paxinos and Watson

mouse brain atlas and we recognize that our interpretations are not without error . However, the results of these retrograde tracer studies coincide with published studies in the rat (Del-Fava et al., 2007; Hasue and Shammah-Lagnado, 2002; Meloni et al., 2006). The studies in Chapter II provide a guide for our electrophysiology studies in Chapter III in which we record from midline DA neurons in RLi areas that project to the BNST, have high stress-induced Zif268 expression (Figures 15-16), and have high fidelity in our TH-eGFP (Figure 7) BAC transgenic mouse.

CHAPTER III

Excitatory drive onto dopaminergic neurons in the rostral linear nucleus is enhanced by norepinephrine in an α_1 adrenergic receptor-dependent manner

Dopaminergic innervation of the extended amygdala regulates anxiety-like behavior and stress responsivity. A portion of this dopamine input arises from dopamine neurons located in the ventral lateral periaqueductal gray (vlPAG) and rostral (RLi) and caudal linear nuclei of the raphe (CLi). These regions receive substantial norepinephrine input, which may prime them for involvement in stress responses. Using a mouse line that expresses eGFP under control of the tyrosine hydroxylase promoter, we explored the physiology and responsiveness to norepinephrine of these neurons. We find that RLi dopamine neurons differ from other VTA dopamine neurons with respect to membrane resistance, capacitance and the hyperpolarization-activated current, I_h. Further, we found that norepinephrine increased the frequency of spontaneous excitatory postsynaptic currents (sEPSCs) on RLi dopamine neurons. This effect was mediated through the α_1 adrenergic receptor (AR), as the actions of norepinephrine were mimicked by the α_1-AR agonist methoxamine and blocked by the α_1-AR antagonist prazosin. This action of norepinephrine on sEPSCs was transient and not a form of synaptic plasticity, as it did not persist following the subsequent application of prazosin. Methoxamine also increased the frequency of miniature EPSCs, indicating that the α_1-AR action on glutamatergic transmission likely has a presynaptic mechanism. There was also a modest decrease in sEPSC frequency with the application of the α_2-AR agonist UK-14,304. These studies illustrate a potential

mechanism through which norepinephrine could recruit the activity of this population of dopaminergic neurons.

Introduction

Addiction exhibits significant comorbidity with mood and anxiety disorders, and stress is frequently stated as a cause for drug use relapse (Sareen et al., 2006; Sinha et al., 2011). The extended amygdala, which contains the bed nucleus of the stria terminalis (BNST) and the central nucleus of the amygdala (CeA), has been shown to play an important role in stress, anxiety, and addiction related behaviors (Davis et al., 2010; Erb, 2010; Koob, 2009). Dopaminergic afferents in the extended amygdala are thought to regulate anxiety-like behavior and stress responsivity (Meloni et al., 2006). While dopamine is classically regarded as a “reward” neurotransmitter, the firing of dopamine neurons increases following acute stress, and dopamine has also been proposed to encode aspects of aversive stimuli (Anstrom and Woodward, 2005; Anstrom et al., 2009; Brischoux et al., 2009; Coco et al., 1992; Deutch et al., 1991; Lammel et al., 2011; Matsumoto and Hikosaka, 2009). However, the impact of the midbrain dopamine system’s sensitivity to stress is not well understood and requires further investigation.

Dopamine release in the extended amygdala has several actions. For example, in the CeA and BNST dopamine enhances spontaneous glutamatergic transmission (Kash et al., 2008; Silberman and Winder, 2013). In the BNST, dopamine decreases evoked glutamatergic and inhibitory transmission (Krawczyk et al., 2011a; Krawczyk et al., 2011b), mediates a form of long term potentiation at GABA synapses (Krawczyk et

al., 2013), decreases NMDA currents in cocaine self-administering rats (Krawczyk et al., 2014), and regulates long-term intrinsic excitability of BNST neurons (Francesconi et al., 2009). The BNST receives a substantial proportion of its total dopaminergic input from the ventral lateral periaqueductal grey (vlPAG) and the dorsal-caudal extension of the A10 dopamine cell group of the ventral tegmental area (VTA), termed the A10dc cell group, which is located in the dorsal, rostral linear (RLi), and caudal linear raphe nuclei (CLi) (Hasue and Shammah-Lagnado, 2002; Meloni et al., 2006). The dopamine neurons of the lateral VTA have been extensively studied while those of the A10dc group have often been overlooked. While overall very little is known about A10dc roles and properties, evidence suggests that the RLi is particularly sensitive to stressors (Deutch et al., 1991).

There is an increasing appreciation regarding the functional heterogeneity of dopamine neurons. Electrophysiological properties of dopamine neurons, such as action potential width and the presence of a hyperpolarization-activated current (I_h), differ based on their projection targets and anatomical location (Lammel et al., 2011; Li et al., 2013a; Margolis et al., 2008). The modulation of excitatory synapses on dopamine neurons by aversive and rewarding stimuli also depend on their projection targets (Lammel et al., 2011). For example, the dopamine neurons located in the medial posterior VTA, near the RLi, have no I_h and their glutamatergic synapses are modified by aversive, but not rewarding stimuli (Lammel et al., 2011). Therefore, study of the basal electrophysiological properties of RLi dopamine neurons may give early insights into their actions.

The noradrenergic system is a key regulator of the stress response. Many stressors increase the firing of norepinephrine neurons and increase norepinephrine turnover in target regions (Abercrombie et al., 1988; Cecchi et al., 2002b; Korf et al., 1973). The locus coeruleus, A1, A2, and A5 norepinephrine groups send efferents to the RLi (Mejias-Aponte et al., 2009). Activation of α_1 or α_2 adrenergic receptors (ARs) induce changes in burst firing of VTA dopamine neurons, (Grenhoff and Svensson, 1989; Grenhoff et al., 1993; Grenhoff and Svensson, 1993; Guiard et al., 2008a) and glutamatergic transmission is crucial for burst firing of dopamine neurons (Overton and Clark, 1992; Seutin et al., 1993). Norepinephrine acts as a powerful modulator of excitatory neurotransmission in many limbic brain areas. Activation of β, α_1, and α_2-ARs have been shown to enhance or attenuate glutamatergic transmission in a variety of brain regions, including the hippocampus, CeA, BNST and VTA (Egli et al., 2005; Flavin and Winder, 2013; Gereau and Conn, 1994; Jimenez-Rivera et al., 2012; McElligott and Winder, 2008; McElligott et al., 2010; Nobis et al., 2011; Shields et al., 2009; Velasquez-Martinez et al., 2012). Therefore, norepinephrine might modulate glutamatergic transmission on RLi dopamine neurons.

Given the interconnections of the RLi with circuitry mediating stress and anxiety and the stress sensitivity of RLi dopamine neurons, it is important to investigate the actions of norepinephrine on RLi dopamine neurons. Using a tyrosine hydroxylase (TH)-eGFP reporter mouse line, we found differences in basal electrophysiological properties, such as I_h, membrane resistance and capacitance, of VTA and RLi dopamine neurons. We also investigated the actions of norepinephrine on spontaneous glutamatergic transmission and found an increase in the frequency of spontaneous

excitatory postsynaptic currents (sEPSCs) on RLi dopamine neurons. Through the application of specific AR agonists and antagonists, we determined that this enhancement of excitatory transmission is due to the activation of α_1-ARs. α_1-ARs also increased the frequency of miniature EPSCs indicating a potential presynaptic locus for this modulation. In addition to this large α_1-AR mediated enhancement of excitatory transmission, we also found a modest α_2-AR mediated depression of excitatory transmission in RLi dopamine neurons.

Methods

Animals

Male mice ages 3-5 weeks were used in these experiments in accordance with animal use protocol approved by the Institutional Animal Care and Use Committee of Vanderbilt University. All experiments were carried out in strict accordance with the recommendations in the Guide for the Care and Use of Laboratory Animals (NIH Publications No. 8023). Mice were group housed in the Vanderbilt vivarium under a 12 hour light/dark cycle with food and water *ad libitum*. All mice were obtained from a transgenic mouse line (Strain Name: STOCK Tg(Th-EGFP)DJ76Gsat/Mmnc). Mating pairs of mice were initially obtained from the Mutant Mouse Regional Resource Center in North Carolina. In this mouse line, the genome was modified to contain multiple copies of a modified BAC in which an eGFP reporter gene was inserted immediately upstream of the coding sequence of the gene for TH. Data presented here were obtained from two lineages of transgenic mice maintained in-house, one derived by cross-breeding with Swiss Webster mice (Taconic), and the other by cross-breeding

with C57/B6 mice (Jackson Laboratories). The characterization of basal electrophysiology properties was performed in mice with the Swiss Webster background. The remainder of the electrophysiology studies and the immunohistochemistry were performed in TH-eGFP mice that were backcrossed with C57/B6 mice for many generations.

Immunohistochemistry and microscopy

Mice were transcardially perfused with ice-cold phosphate-buffered saline (PBS), followed by ice-cold 4% paraformaldehyde in PBS. Brains were removed from the skull and post-fixed in the same fixative overnight at 4^{o}C, and were then transferred to 30% sucrose in PBS. Two to five days later, 40 µm thick coronal sections of brain were sliced on a cryostat (Leica CM3050S). Free-floating sections were washed in PBS (4x10 minutes), permeabilized with 0.5% Triton-X 100 in PBS, and then blocked with 10% normal donkey serum in PBS containing 0.1% Triton-X 100. Sections were then incubated with a mouse monoclonal anti-TH antibody (from ImmunoStar used at 1:2000 dilution) in blocking solution for 48 hours at 4^{o}C, followed by PBS washes (4x10 minutes) and incubated with a Cy3-conjugated donkey anti-mouse secondary antibody (from Jackson ImmunoResearch used at 1:500 dilution) for 24 hours at 4^{o}C in PBS with 0.1% Triton-X 100. Finally, sections were washed (4x10 minutes), mounted on slides, sealed with PolyAquamount, and left overnight to dry. Stained sections were examined with a Zeiss 510 scanning confocal microscope.

Electrophysiology recordings

3-5 week old TH-eGFP mice were decapitated under Isoflurane anesthesia. The brains were quickly removed and placed in oxygenated ice-cold sucrose artificial cerebrospinal fluid (ACSF): 194 mM sucrose, 20 mM NaCl, 4.4 mM KCl, 2 mM $CaCl_2$, 1 mM $MgCl_2$, 1.2 mM NaH_2PO_4, 10 mM glucose, and 26 mM $NaHCO_3$. Three-hundred μm coronal slices of the VTA or RLi were prepared using a vibrating microtome (Leica VT 1200). Two RLi slices per mouse were generated. Slices were incubated for 1 hour in oxygenated ACSF at 28^{o}C: 124 mM NaCl, 2.5 mM KCl, 2.5 mM $CaCl_2$, 2 mM Mg_2SO_4, 1.25 mM NaH_2PO_4, 11 mM glucose, 26 mM $NaHCO_3$, and 0.4mM ascorbic acid. Slices then rested in a submerged superfusion chamber (Warner Instruments) for 30 minutes prior to recordings.

The TH-eGFP positive neurons were identified via fluorescent microscopy, and directly visualized with infrared video microscopy (Olympus) for patching. Recording electrodes were fabricated with a Flaming-Brown Micropipette Puller (Sutter Instruments) using thin-walled borosilicate glass capillaries (World Precision Instruments). Recording electrodes of resistance 2.5-5.5 MΩ were filled with an internal solution of 290-295 mOsmol, pH = 7.2-7.3, consisting of: 125 mM K^+-gluconate, 5 mM NaCl, 4.4 mM KCl, 10 mM HEPES, 0.6 mM EGTA, 4 mM ATP, and 0.4 mM GTP for I_h current recordings and 117 mM Cs^+-gluconate, 20 mM HEPES, 0.4 mM EGTA, 5mM TEA, 2mM $MgCl_2$, 4 mM ATP, and 0.3 mM GTP for the remainder of the electrophysiology recordings. All electrophysiology recordings were made using Clampex 9.2 and analyzed using Clampfit 10.2 (Molecular Devices). I_h currents were measured in the voltage-clamp recording configuration by stepping the holding potential from -60mV to -120mV for 1 second and then measuring the difference between the

current immediately following the step to -120mV and the current at the end of the -120mV step. Whole-cell, voltage-clamp recordings were performed as described previously (Egli et al., 2005; Kash et al., 2008; Nobis et al., 2011; Silberman and Winder, 2013). Briefly, AMPA receptor-mediated sEPSCs were made at −70 mV and pharmacologically isolated by the addition of 25 μM picrotoxin to the ACSF. Cells were allowed to equilibrate to whole-cell configuration for 5 min before recordings began. sEPSC recordings were acquired and analyzed in 2 min gap-free blocks, and access resistance was monitored between blocks of sEPSC recordings. Those experiments in which the access resistance changed by >20% were not included in the data analyses. For the experiment in which the effect of prazosin was determined, the antagonist was pre-applied for at least 15 minutes before application of norepinephrine and then remained onboard for the duration of the experiment. To isolate miniature EPSCs (mEPSCs) 1 uM tetrodotoxin (TTX) was added in addition to sEPSC recording conditions.

Data analysis

For counting single and multiply labeled neurons, z stacks of imaged brain sections were projected onto a single plane using Zeiss LSM software. Projected images were then opened in Metamorph and neurons counted with the help of manual logger functions. The signal intensity threshold for counting neurons as positive for a marker was set at twice that to the brightest neurons in no primary antibody control sections (TH), or for eGFP, neurons in brainstem areas that did not express eGFP. Quantitative data are expressed as mean ± S.E.M. unless otherwise noted.

For electrophysiology studies, statistical analyses were performed using Microsoft Excel 2010 and GraphPad Prism 6. Specifically, when comparisons were made between RLi and VTA basal excitability properties, an unpaired Student's *t*-test was used. When determining whether a compound had a significant effect, a Student's paired *t*-test was used, comparing the baseline value to the peak experimental value. Paired comparisons were made between baseline (the average of the last three recording blocks before drug is added) and the three recording blocks immediately following removal of drug application unless otherwise noted. When comparing antagonist effects on the norepinephrine-induced increase in sEPSCs, a repeated measures one-way ANOVA was used, followed by a Tukey's post-test to determine the significance of specific comparisons. Degrees of freedom were corrected using Greenhouse-Geisser estimates of sphericity. For the electrophysiology studies, "n" refers to the number of cells. At least four animals were used in each electrophysiology experiment. All values given throughout the study are presented as mean ± S.E.M.

Pharmacology

Isoproterenol hydrochloride, tetrodotoxin citrate, and picrotoxin were purchased from Tocris Bioscience. Norepinephrine bitartrate salt monohydrate, methoxamine hydrochloride, and prazosin hydrochloride were purchased from Sigma-Aldrich. All experimental drugs were bath applied at their final concentrations as noted in the text. Dimethylsulfoxide (DMSO) was the solvent used for stock solution of picrotoxin where the maximum final concentration of DMSO in ACSF was 0.02% by volume. All other

drugs, with the exception of prazosin, were easily dissolved in water. Prazosin was dissolved in water with vigorous heating and stirring.

Results

Electrophysiological characteristics of RLi dopamine neurons

We first wanted to confirm that the TH-eGFP mouse line would adequately report dopamine neurons in the RLi. To examine this, sections were processed for immunostaining for anti-TH and the numbers of eGFP+, TH+, and double labeled neurons were counted in images captured from each section with a 20x lens. In the RLi, the percentage of eGFP+ cells that were co-localized with TH+ cells was 95 ± 1% (n = 3) (Figure 7*B-E*). These data suggest that eGFP fluorescence in this mouse line is a good marker for dopamine neurons located in the RLi.

It has been reported that dopamine neurons have distinct electrophysiological profiles based on their projection targets and anatomical location (Lammel et al., 2011; Margolis et al., 2008). Therefore, we examined the basic electrophysiological properties of eGFP positive neurons located in the RLi and lateral VTA, specifically the parabrachial pigmented nucleus. Using whole-cell voltage clamp, we measured membrane resistance, membrane capacitance, and hyperpolarization-activated (I_h) current of TH-eGFP neurons in the RLi and VTA. RLi eGFP+ neurons exhibited a significantly higher membrane resistance (745 ± 115 MΩ, n = 16) than eGFP+ neurons in the lateral VTA (195 ± 53 MΩ, n = 10, $p < 0.01$) (Figure 7*F*). Further, the RLi neurons also displayed a smaller membrane capacitance (25 ± 2 pF, n = 16) than eGFP+

neurons in the lateral VTA (56 ± 5 pF, n = 10, $p < 0.0001$) (Figure *7G*). Having established these differences in basic membrane properties, we next sought to determine if the eGFP+ neurons in the RLi exhibit an I_h current. The presence of I_h current has long been used as a marker for dopamine neurons in the VTA (Grace and Onn, 1989; Hopf et al., 2007; Lacey et al., 1989; Margolis et al., 2006; Stuber et al., 2008). Recently, it has been shown that a subset of dopamine neurons do not possess a robust I_h current (Lammel et al., 2011; Margolis et al., 2006; Margolis et al., 2008). Consistent with this, we found that lateral VTA eGFP+ neurons displayed an I_h current similar to those observed in previous studies (-173 ± 46 pA, n = 10 cells from 4 mice) (Ungless et al., 2003). However, the eGFP+ neurons in the RLi of the same mice had a significantly smaller I_h current (-14 ± 4 pA, $p < 0.001$, n = 16 cells from 4 mice) when compared to the lateral VTA (Figure *7H-J*), with most neurons lacking any measurable current.

Figure 7: RLi dopamine neurons have distinct basal excitability profiles. (A) Diagram of a coronal brain section image from Franklin & Paxinos mouse atlas showing region selected for VTA electrophysiology recordings. (B) Diagram of a coronal brain section image from Franklin & Paxinos mouse atlas showing region selected for RLi electrophysiology recordings. (C) Coronal section of the RLi corresponding to the black rectangle in B displaying eGFP fluorescence, (D) tyrosine hydroxylase immunohistochemistry, and (E) the merged image showing the co-localization of eGFP and tyrosine hydroxylase labeled neurons. The arrows highlight examples of double labeled cells. (F) Bar graph showing the membrane resistance of eGFP positive neurons in the RLi and VTA. The eGFP positive neurons in the RLi exhibited a significantly higher membrane resistance compared to those in the VTA (** denotes $p < 0.01$). (G) Bar graph showing the capacitance of eGFP positive neurons in the RLi and VTA. The eGFP positive neurons in the RLi exhibited a significantly reduced capacitance compared to those in the VTA (**** denotes $p < 0.0001$). (H) Bar graph comparing the average peak I_h current for each group of dopamine neurons. There was a significant difference in the I_h current in the VTA dopamine neurons compared to dopamine neurons in the RLi (*** denotes $p < 0.001$). (I) A hyperpolarization voltage step in an eGFP positive neuron in the VTA leads to a robust inward current. (J) A hyperpolarization voltage step in an eGFP positive neuron in the RLi leads to a small but measureable inward current.

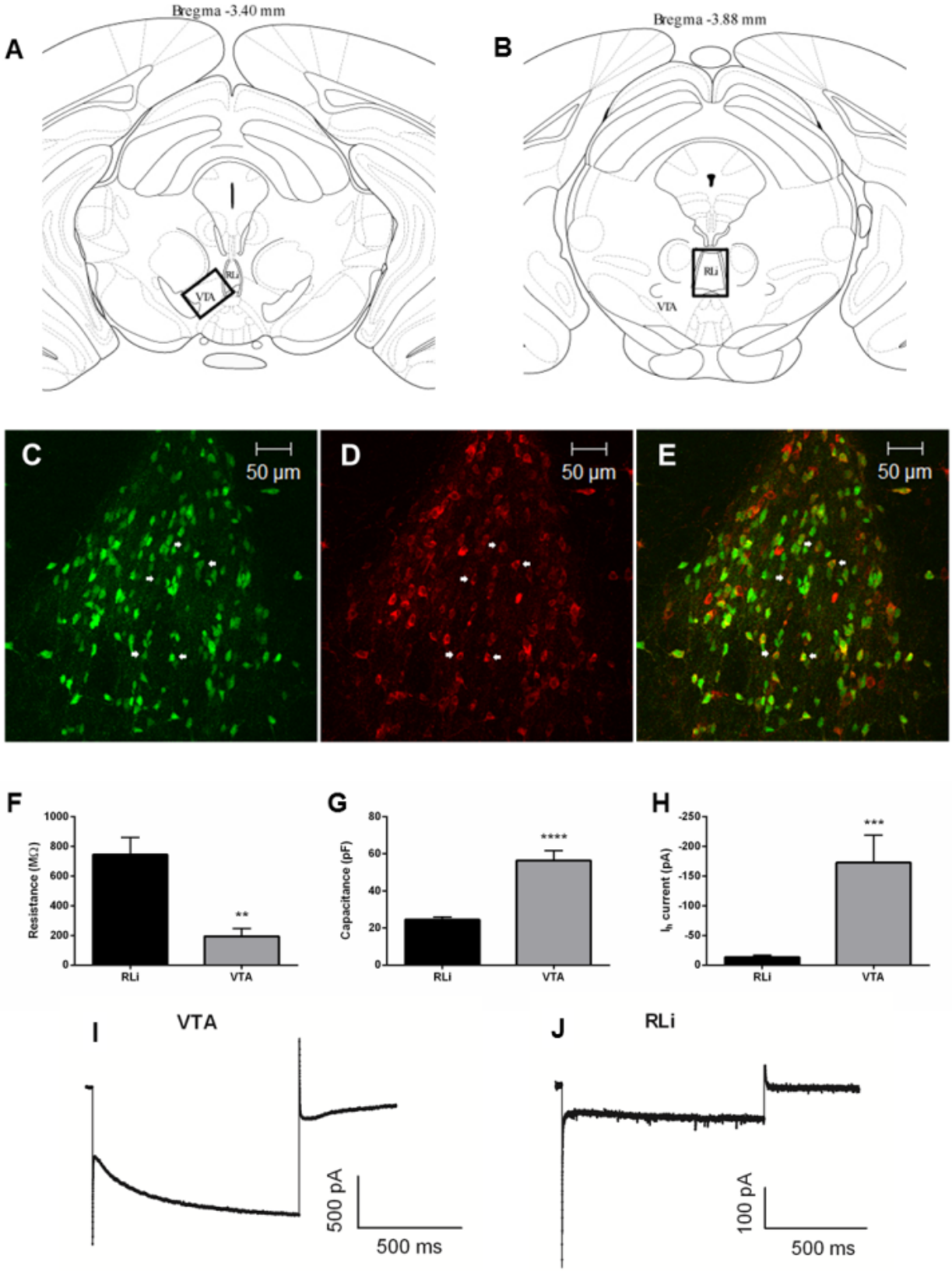
A
Bregma -3.40 mm
RLi
VTA
B
Bregma -3.88 mm
RLi
VTA
C
50 µm
D
50 µm
E
50 µm
F
Resistance (MΩ)
1000
800
600
400
200
0
**
RLi
VTA
G
Capacitance (pF)
80
60
40
20
0
****
RLi
VTA
H
I_h current (pA)
-250
-200
-150
-100
-50
0
***
RLi
VTA
I
VTA
500 pA
500 ms
J
RLi
100 pA
500 ms

Norepinephrine enhances spontaneous excitatory transmission on TH-eGFP positive neurons in the RLi via activation of α_1 adrenergic receptors

The RLi projects to regions heavily involved in stress responding and receives a large noradrenergic projection (Mejias-Aponte et al., 2009). Thus, we tested the hypothesis that norepinephrine modulates RLi dopamine neurons. We first examined the effects of norepinephrine on basal excitability and found no effect on holding current (107 ± 8% of baseline, $p > 0.05$, $n = 8$) or membrane resistance (106 ± 6% of baseline, $p > 0.05$, $n = 8$). Because norepinephrine has been shown to regulate excitatory drive in other brain regions, we measured sEPSCs on TH-eGFP neurons located in the RLi (average basal frequency, 2.4 ± 0.3 Hz; average basal amplitude, 20 ± 1 pA, $n = 28$) (Figure 8*A*). We bath applied norepinephrine (50 μM) for 10 minutes while spontaneous glutamatergic transmission was monitored using whole cell patch-clamp recordings in acutely prepared brain slices. We found that this norepinephrine application resulted in an increase in the frequency of sEPSCs (473 ± 93% of basal frequency, $F(1.3, 9.2) = 13.9$, $p < 0.01$, $n = 8$) (Figure 8*B*). Additionally, there was a modest, but significant effect on sEPSC amplitude (128 ± 11% of basal amplitude, $F(14, 98) = 2.2$, $p < 0.05$, $n = 8$) (Figure 8*C*). This increase in amplitude was present only during the last 5 minutes of norepinephrine application. There was no effect of norepinephrine on sEPSC rise time (93 ± 7% of baseline, $p > 0.05$, $n = 8$) or decay time (97 ± 4% of baseline, $p > 0.05$, $n = 8$).

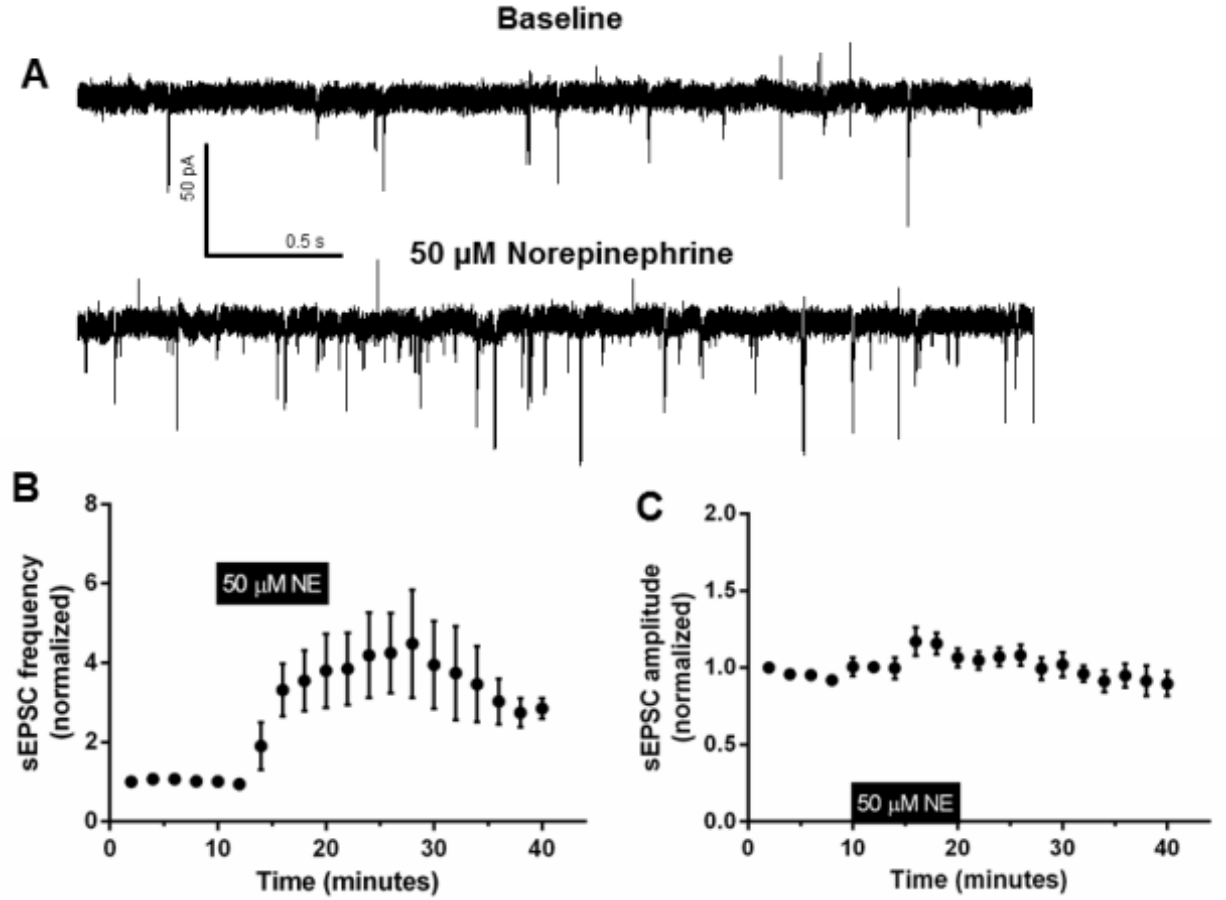

Figure 8: Norepinephrine increases spontaneous glutamatergic transmission onto RLi dopamine neurons.
(A) Representative sEPSC recordings in the RLi demonstrating the ability of norepinephrine (NE) to enhance glutamatergic transmission. (B) A 10 min application of 50 µM norepinephrine increases sEPSC frequency onto RLi dopamine neurons. (C) A 10 min application of 50 µM norepinephrine modestly increases sEPSC amplitude onto RLi dopamine neurons only during the last 5 minutes of drug application.

Since norepinephrine can act on multiple adrenergic receptors (ARs), we next tested whether α_1-, α_2-, and/or β-ARs were responsible for the actions of norepinephrine on glutamatergic transmission in RLi TH-eGFP neurons. We found that application of the α_1-AR agonist methoxamine (100 μM) increased sEPSC frequency (581 ± 169% of basal frequency, $F(1.3, 10) = 9.1$, $p < 0.01$, $n = 9$) (Figure 9*A*) but not amplitude (117 ± 10% of basal amplitude, $F(1.5, 12) = 2.0$, $p = 0.18$, $n = 9$) (Figure 9*B*) in TH-eGFP positive neurons in the RLi. Preapplication of the α_1-AR antagonist prazosin (10 μM) prevented norepinephrine induced increases in sEPSC frequency and amplitude. In fact, application of norepinephrine in the presence of prazosin led to a decrease in sEPSC frequency (60 ± 6% of basal frequency, $F(2.8, 11) = 13$, $p < 0.001$, $n = 5$) and a modest decrease in sEPSC amplitude (91 ± 2% of basal amplitude, $F(17, 68) = 2.4$, $p < 0.01$, $n = 5$) (Figure 9*C,D*). To further investigate these decreases in sEPSC frequency and amplitude, we applied the α_2-AR agonist UK-14,304. A 10 minute application of UK-14,304 (1 μM) led to a significant decrease in sEPSC frequency (60 ± 9% of basal frequency, $F(2.5, 12) = 6.8$, $p < 0.01$, $n = 6$) with a trend toward a decrease in sEPSC amplitude (89 ± 5% of basal amplitude, $F(2.3, 12) = 3.0$, $p = 0.08$, $n = 6$) (Figure 10*A,B*). Since activation of β-ARs can lead to increases in sEPSC frequency in other brain regions such as the BNST, we applied the β-AR agonist isoproterenol (3 μM) for 10 minutes and found that this application of isoproterenol did not lead to changes in sEPSC frequency (104 ± 16% of basal frequency, $F(2.4, 17) = 0.35$, $p > 0.05$, $n = 8$) or amplitude (96 ± 5% of basal amplitude, $F(1.9, 13) = 1.2$, $p > 0.05$, $n = 8$) (Figure 10*C,D*). These data indicate that norepinephrine enhances the spontaneous glutamatergic transmission in RLi TH-eGFP neurons via activation of α_1-ARs.

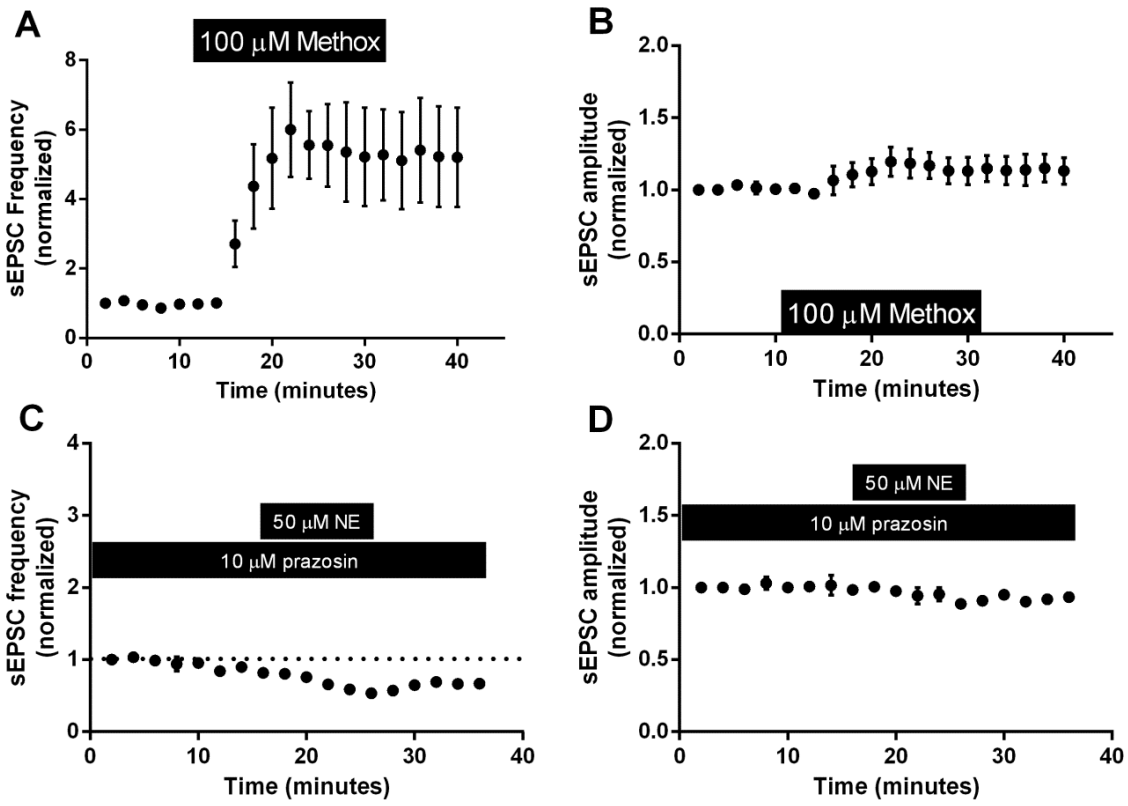

Figure 9: Activation of α_1-ARs increases sEPSC frequency onto RLi dopamine neurons.
(A) A 20 min application of 100 μM methoxamine (methox) increases sEPSC frequency onto RLi dopamine neurons. (B) A 20 min application of 100 μM methoxamine has no effect on sEPSC amplitude onto RLi dopamine neurons. (C) In the presence of the α_1-AR antagonist prazosin (10 μM), a 10 min application of 50 μM norepinephrine decreases the frequency of sEPSCs onto RLi dopamine neurons. (D) In the presence of the α_1-AR antagonist prazosin (10 μM), a 10 min application of 50 μM norepinephrine modestly decreases the amplitude of sEPSCs onto RLi dopamine neurons.

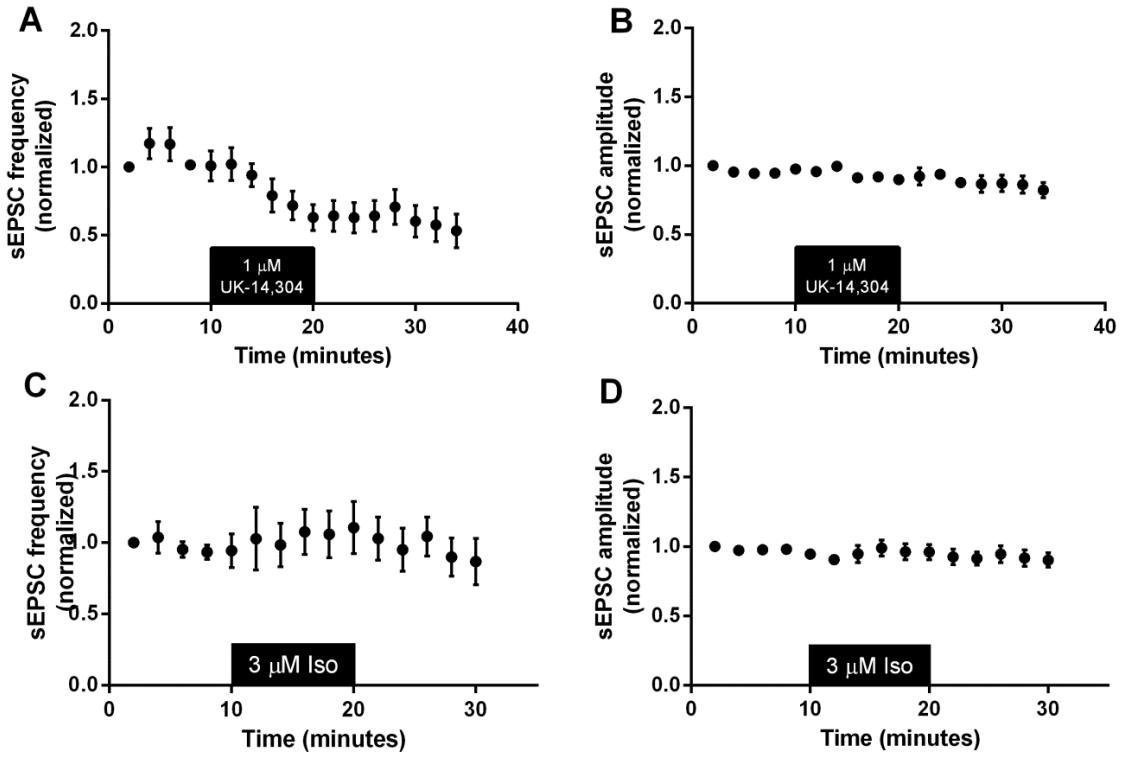

Figure 10: α_2-AR activation depresses glutamatergic transmission and β-AR activation has no effect on glutamatergic transmission onto RLi dopamine neurons.
(A) A 10 min application of 1 μM UK-14,304 decreases sEPSC frequency onto RLi dopamine neurons. (B) A 10 min application of 1 μM UK-14,304 causes a trend toward a decrease in sEPSC amplitude onto RLi dopamine neurons. (C) A 10 min application of 3 μM isoproterenol (Iso) has no effect on sEPSC frequency or (D) sEPSC amplitude onto RLi dopamine neurons.

Noradrenergic enhancement of excitatory transmission on TH-eGFP positive RLi neurons is transient

To further investigate the time course of norepinephrine's enhancement of excitatory transmission in RLi TH-eGFP neurons, we bath applied prazosin (10 μM) to slices 10 minutes after a 10 minute application of norepinephrine was completed. The prazosin was able to reverse the increase in frequency of sEPSCs caused by norepinephrine (Figure 11*A,C*) ($F(1.0, 5.2) = 8.9$, $p < 0.05$, $n = 6$). It also reduced the modest increase in amplitude of sEPSCs caused by norepinephrine (Figure 11*B,D*) ($F(1.6, 8.1) = 13$, $p < 0.01$, $n = 6$). These results indicate that the increase in glutamatergic transmission in RLi TH-eGFP neurons is not due to long term potentiation of excitatory inputs but rather from transient effects of α_1-AR activation.

α_1-AR activation increases excitatory transmission in an activity-independent manner

To further investigate the mechanism of action of norepinephrine's effects on RLi TH-eGFP neurons, we examined the ability of methoxamine to modulate activity-independent miniature EPSCs (mEPSCs). mEPSCs were isolated by the addition of the sodium channel blocker TTX (1μM) to the bath solution (average basal frequency, 1.8 ± 0.8 Hz; average basal amplitude 15 ± 1 pA, n = 7). We found that methoxamine enhanced mEPSC frequency (535 ± 128% of basal frequency, $p < 0.05$, $n = 7$) (Figure 12*A-C)*, but had no effect on mEPSC amplitude (112 ± 6% of basal amplitude, n = 7) (Figure 12*D*) in RLi TH-eGFP neurons. These results indicate that the α_1-AR induced enhancement of glutamatergic transmission in RLi TH-eGFP neurons occurs via an activity-independent mechanism and provide evidence that norepinephrine's site of action on RLi TH-eGFP neurons is presynaptic.

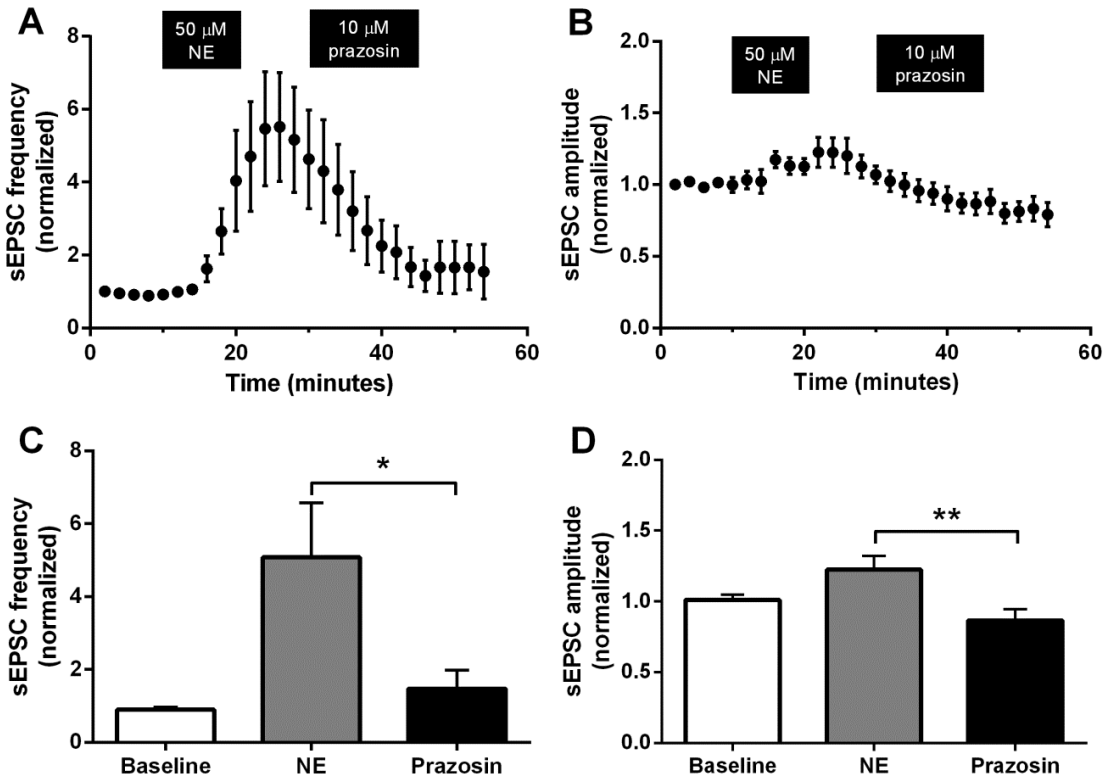

Figure 11: Norepinephrine's actions on sEPSCs are transient.
(A,C) The norepinephrine induced increase in sEPSC frequency does not persist when followed by a 15 min application of 10 μM prazosin (* denotes $p < 0.05$). (B,D) The norepinephrine induced increase in sEPSC amplitude does not persist when followed by a 15 min application of 10 μM prazosin (** denotes $p < 0.01$).

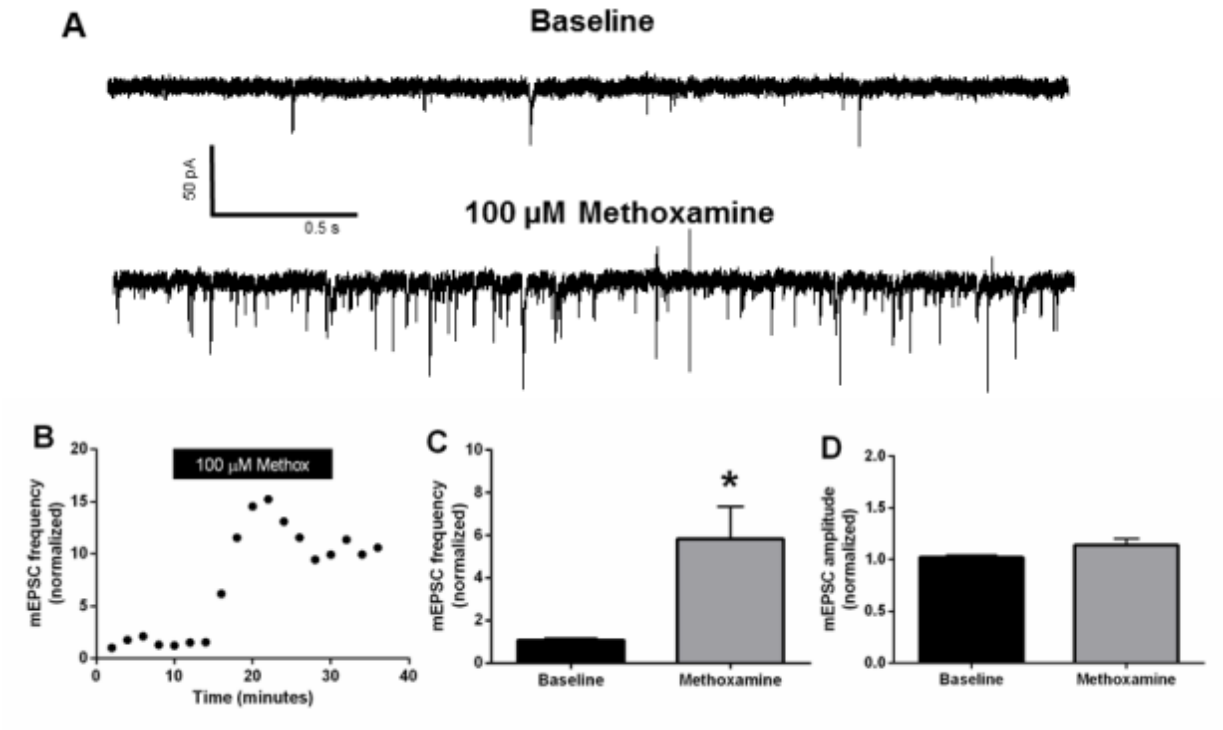

Figure 12: Methoxamine increases mEPSC frequency but not amplitude. (A) Representative mEPSC recordings in the RLi demonstrating the ability of methoxamine to enhance glutamatergic transmission. (B) A representative experiment showing the effect of 100 µM methoxamine on mEPSC frequency onto RLi dopamine neurons. (C) A 20 min application of 100 µM methoxamine increases mEPSC frequency onto RLi dopamine neurons (* denotes $p < 0.05$). (D) A 20 min application of 100 µM methoxamine has no effect on mEPSC amplitude onto RLi dopamine neurons.

Discussion

Because of the small size of the RLi coupled with the lack of I_h in RLi dopamine neurons, a reporter method is necessary to identify these neurons for electrophysiological analysis. Thus we analyzed the properties of these neurons in a TH-eGFP line previously utilized for analysis of dopamine neurons (Li et al., 2013a). In an initial characterization of the basic membrane properties of eGFP positive neurons in the RLi of these transgenic mice, we found several significant differences as compared to eGFP positive lateral parabrachial pigmented nucleus VTA neurons. The dopamine neurons in the RLi had a significantly greater membrane resistance when compared to the dopamine neurons in the parabracial pigmented nucleus of the VTA. Additionally, we found that the capacitance was significantly smaller in the RLi neurons. Finally, we found little to no I_h current in the RLi dopamine neurons. Other groups have also found a lack of I_h current in dopamine neurons with anatomical locations near the midline (Lammel et al., 2011; Li et al., 2013a). Functionally, these properties are expected to affect differences in excitability and may influence plasticity of synaptic transmission. Our findings suggest fundamental differences in the basic membrane and excitability properties between the afferent dopaminergic projections to the BNST from the VTA and RLi. These findings raise the possibility that these neurons may exhibit different firing patterns *in vivo* and thus be regulated differently by exposure to stressors or drugs of abuse.

Norepinephrine acts as a powerful modulator of excitatory neurotransmission in many brain areas. We found that the most pronounced effect of norepinephrine on RLi dopamine neuron physiology was an increase in the frequency of sEPSCs. Since

activation of β-ARs increases excitatory transmission in the hippocampus, CeA, and BNST, we attempted to mimic the effects of norepinephrine with the β-AR agonist isoproterenol (Egli et al., 2005; Gereau and Conn, 1994; Nobis et al., 2011). However, isoproterenol had no effect on sEPSC frequency or amplitude.

In the BNST, activation of α_1-ARs elicits long term depression of evoked glutamatergic transmission, but an increase in sEPSCs. Similarly, activation of α_1-ARs leads to an enhancement of glutamatergic transmission onto VTA dopamine neurons (McElligott and Winder, 2008; McElligott et al., 2010; Velasquez-Martinez et al., 2012). In the presence of the α_1-AR antagonist prazosin, we found that norepinephrine did not increase excitatory transmission. In fact, when α_1-ARs were blocked, norepinephrine decreased sEPSC frequency and amplitude. Since the α_2-AR agonist UK-14,304 led to a depression of sEPSC frequency and a trend toward a decrease in sEPSC amplitude, this decrease in excitatory transmission is likely due to the activation of α_2-ARs. Similarly, activation of α_2-ARs decreases excitatory transmission in the BNST and onto VTA dopamine neurons (Egli et al., 2005; Jimenez-Rivera et al., 2012; Shields et al., 2009). It is possible that this decrease in glutamatergic transmission is also due to the blockade of tonically active α_1-ARs (Grenhoff and Svensson, 1993). However, the timing of the effect coincides with norepinephrine application which supports α_2-AR activation mediating this decrease in excitatory transmission. It is important to note that the overall effect of norepinephrine on RLi dopamine neurons is an increase in excitatory transmission and the small α_2-AR mediated decrease in sEPSC frequency is surpassed by the large α_1-AR mediated increase in sEPSC frequency.

Since the effect of norepinephrine on sEPSC frequency was blocked by the α_1-AR antagonist, we attempted to mimic it with the α_1-AR agonist methoxamine. Indeed, methoxamine mimicked the effects of norepinephrine on RLi sEPSC frequency. This finding is a similar to that seen in VTA dopamine neurons (Velasquez-Martinez et al., 2012). In the RLi, the frequency of mEPSCs increases with the activation of α_1-ARs. The increase in mEPSC frequency indicates that α_1-ARs may act presynaptically to increase excitatory transmission on RLi dopamine neurons and that their actions are independent of presynaptic action potentials. While activation of α_1-ARs in VTA dopamine cells does not modulate mEPSCs, activation of α_1-ARs in other brain regions, such as the hypothalamus, does lead to an increase in mEPSC frequency (Gordon and Bains, 2003). The VTA dopamine neurons were identified via a large I_h current (> 200 pA) and are located more laterally, while the RLi dopamine neurons have very small, almost negligible, I_h current and are located along the midline. Therefore, these are entirely different populations of dopamine neurons which may differ in their response to inputs and outputs to projection targets. Both the lateral VTA and the RLi receive noradrenergic inputs from the locus coeruleus (LC) and the norepinephrine brainstem centers, A1, A2 and A5 (Mejias-Aponte et al., 2009). However, the lateral VTA has a higher percentage of its norepinephrine input arising from the LC, while the RLi has a higher percentage of its norepinephrine input arising from the brainstem centers. This might lead to differences in how these two groups of dopamine neurons respond to stimuli, such as stress, that lead to the release of norepinephrine in target regions.

This study indicates a potential mechanism through which norepinephrine could recruit the activity of RLi dopamine neurons. Since activation of glutamatergic afferents

mediates the firing of dopamine neurons, we would expect this α_1-AR mediated enhancement in excitatory transmission to increase the firing of dopamine neurons and release of dopamine in target regions. Stressors have been shown to increase dopamine concentration in many target regions (Abercrombie et al., 1989; Deutch et al., 1991; Kalivas and Duffy, 1995; Morrow et al., 2000; Sutoo and Akiyama, 2002). Stress causes norepinephrine release, which our data suggests would lead to an increase in excitatory drive on RLi dopamine neurons via α_1-AR activation. One possibility is that this drives dopamine release in target regions such as the BNST, where it may participate in reinforcement related behaviors as well as anxiety responses. Thus norepinephrine induced enhancement of excitatory drive on RLi dopamine neurons is a potential mechanism through which RLi dopamine neurons may be involved in the stress response.

Adapted with permission from:

Williams MA, Li C, Kash TL, Matthews RT, Winder DG. 2014. Excitatory drive onto dopaminergic neurons in the rostral linear nucleus is enhanced by norepinephrine in an alpha1 adrenergic receptor-dependent manner. *Neuropharmacology* 86:116-24

CHAPTER IV

Discussion and Future Directions

In this dissertation, I have described my studies on noradrenergic modulation of RLi DA neurons, an understudied group of DA cells. I found that NE leads to an α_1-AR mediated increase in excitatory transmission that appears to have a presynaptic site of action. There was also an α_2-AR mediated decrease in excitatory transmission, but the overall effect of NE was an increase in excitatory transmission. The overall effect of NE on excitatory transmission varies by brain region. For example, in the BNST the overall effect of NE due to the activation of α_1- and α_2-ARs is a decrease in excitatory transmission. Activation of α_1-ARs in the BNST leads to LTD, while the activation of α_2-ARs leads to an input specific, transient depression of excitatory transmission (Egli et al., 2005; Flavin et al., 2014; McElligott and Winder, 2008; McElligott et al., 2010; Shields et al., 2009). These varying effects of NE could be due to a variety of factors including differential *in vivo* recruitment of NE inputs, differential regulation of glutamate inputs, length of agonist application, specific subtypes of ARs involved, and synaptic site of action of the receptor.

An interesting characteristic of RLi DA neurons is that they lack I_h and have a higher membrane resistance than lateral VTA DA neurons (Williams et al., 2014). These postsynaptic characteristics are likely to lead to less filtering of synaptic inputs (Magee, 2000). Therefore, even though both VTA and RLi DA neurons undergo modulation of excitatory transmission by NE, RLi DA neurons may be more likely to undergo changes in firing due to NE modulation of excitatory transmission. In addition, midline DA

neurons may have a lower expression of DAT and D_2Rs so they are likely to have a sustained pattern of DA release compared to lateral VTA DA neurons (Lammel et al., 2008). Therefore, endogenous release of NE into the VTA and RLi may have differing effects on downstream target regions with the potential for larger changes in RLi DA release.

RLi dopamine neurons may respond to aversive stimuli

As discussed in Chapter I, the majority of DA neurons respond to rewarding stimuli, however, there is a small subset of DA neurons that respond to aversive stimuli. In fact, activation of the lateral habenula input to medial VTA DA neurons that project to PFC causes conditioned place aversion (CPA) behavior in animals (Lammel et al., 2012). The DA neurons that respond to aversive stimuli are located in the medial aspects of the VTA, lack I_h, and primarily project to the PFC (Brischoux et al., 2009; Lammel et al., 2011; Lammel et al., 2012). RLi DA neurons also lack I_h and project to the PFC (Deutch et al., 1991; Williams et al., 2014). In addition, RLi DA neurons receive NE input from a variety of NE cell groups and project to areas of the extended amygdala, such as the CeA and BNST, that play roles in anxiety related behaviors (Hasue and Shammah-Lagnado, 2002; Mejias-Aponte et al., 2009). Based on these similarities and the circuitry of RLi DA neurons, it seems likely that the RLi DA neurons respond to aversive stimuli. DA's involvement in motivated behavior is often thought to underlie hedonic responses, appetitive motivation and reinforcement based learning. However, DA signaling is important in aversive aspects of learning and motivation as well, such as the need to escape a harmful or stressful environment (Salamone and

Correa, 2012). This might be one reason why a subset of DA neurons respond to aversive rather than rewarding stimuli.

Norepinephrine may recruit RLi dopamine neurons during a variety of behaviors

The α_1-AR mediated increase in excitatory transmission onto RLi DA neurons may recruit this population of DA neurons during times of stress. The NE input to the RLi comes from the LC, A1, A2, and A5 areas (Mejias-Aponte et al., 2009). Endogenous NE from any one of these individual NE sources or NE from a variety of sources may underlie the α_1-AR mediated increase in excitatory transmission onto RLi DA neurons. Stressors such as restraint and foot shock, as well as physiological stressors such as cardiovascular, osmotic, and immune challenges activate cells in the LC, A1 and A2 (Abercrombie and Jacobs, 1987; Morilak et al., 1987; Sawchenko et al., 2000). In Chapter I, I also discussed a variety of evidence indicating that DA neurons are recruited during stress, including changes in DA metabolism and release and alterations in the firing of DA neurons following a stressor. Therefore, one hypothesis is that NE released from the LC, A1 and/or A2 during stress acts on α_1-ARs in the RLi to increase excitatory transmission onto RLi DA neurons and recruit them (Figure 13). This increase in excitatory transmission would presumably lead to increases in the firing of RLi DA neurons and increase DA in downstream regions such as the PFC and BNST. The BNST plays important roles in stress and anxiety responses, as well as stress-induced reinstatement of drug-seeking (Briand et al., 2010; Davis et al., 2010; Erb, 2010; Koob, 2009). In addition, DA inhibits the firing of LC neurons via activation of α_2-ARs (El Mansari et al., 2010), and in contrast, stimulation of the VTA dopaminergic

projection to the LC results in activation of the LC (Deutch et al., 1986), so the increase in DA following stress could then feedback to modulate further LC activity. It is possible that the recruitment of RLi DA neurons by NE during stress or the dysregulation of this system may contribute to stress-induced reinstatement of drug-seeking or the development of anxiety disorders.

Some of the NE areas that innervate the RLi are involved in homeostatic regulation. For example, A1 neurons control the release of vasopressin, A2 neurons are involved in regulation of food intake, and A5 neurons regulate the respiratory rhythm generator of the rostral ventrolateral medulla (Blessing and Willoughby, 1985; Hilaire et al., 2004; Rinaman, 2003). During disturbances in these homeostatic processes, it may be possible that NE acts through α_1-ARs to recruit RLi DA neurons. The RLi DA neurons may underlie the motivational drive required to initiate a behavioral action that will help restore homeostasis.

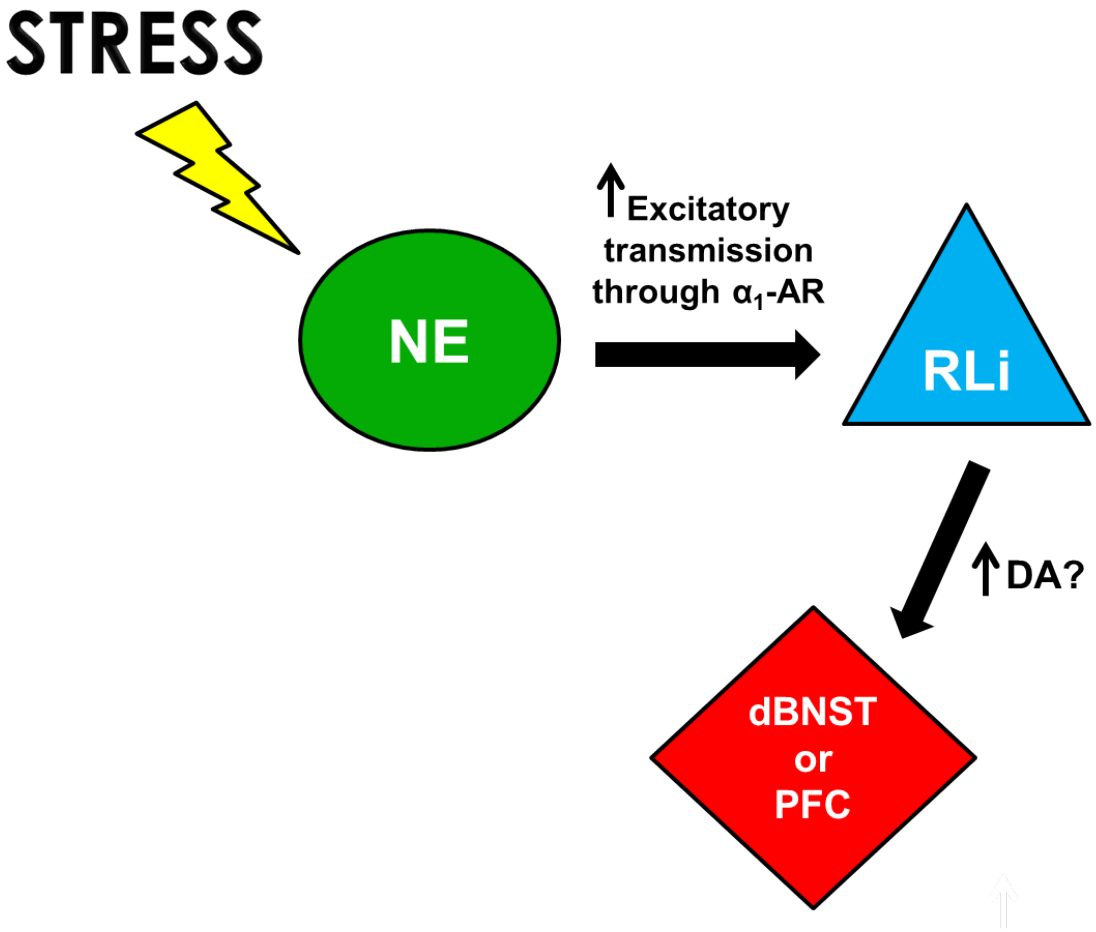

Figure 13: Model depicting the potential actions of stress on RLi circuitry. Stress initiates a release of NE from the LC or A1 and A2 regions. NE increases excitatory transmission onto RLi DA neurons which likely increases DA in target regions of the RLi such as the dBNST or PFC. In the dBNST, increased extracellular dopamine leads to increased excitatory transmission and could initiate stress-induced reinstatement of drug-seeking behavior. In the PFC, high increases in DA lead to impaired working memory. (Briand et al., 2010; Kash et al., 2008; Williams et al., 2014)

NE from the LC is involved in attention related behaviors. Tonic LC firing favors exploration of new or changing environments while phasic LC mode is associated with focused attention (Clayton et al., 2004). DA has been called a “teaching” signal in reinforcement learning that predicts when rewards are likely to occur (Montague et al., 1996; Montague et al., 2004). These ideas led to a theory for NE-DA interactions during learning and motivated behaviors developed by Aston-Jones and Cohen. LC tonic firing encourages exploration and when a new reward is discovered the DA teaching signal strengthens the behaviors that led to the reward. Then the LC goes into phasic mode to focus attention on the new reward, and when the reward is gone or no longer needed the LC switches back into tonic mode to encourage exploration (Aston-Jones and Cohen, 2005). It is possible that LC NE and RLi DA interact in this way. Alternatively, LC NE and VTA DA might coordinate during reinforcement learning associated with rewards, while LC NE and RLi DA might underlie reinforcement learning that occurs due to exposure to aversive stimuli.

The NE modulation of RLi DA neurons could play a role in many behaviors. There is still much work to be done to understand the importance of the actions of RLi DA neurons. An important area of future research is to determine what behaviors RLi DA neurons mediate and, more specifically, to determine the role of the α_1-AR mediated facilitation of excitatory transmission onto RLi DA neurons in behavior.

α_1-AR mediated enhancement of excitatory transmission onto vPAG dopamine neurons may promote wakefulness

In addition to the actions of α_1-AR on RLi DA neurons, I found that the activation of α_1-ARs enhances excitatory transmission onto vPAG DA neurons as well (Figure 21

in Appendix C). The vPAG DA neurons have been shown to promote wakefulness (Lu et al., 2006). Interestingly, prazosin, the α_1-AR antagonist, has proven efficacious in treating nightmares and sleep disturbances in people with PTSD (Mohsenin and Mohsenin, 2014; Raskind et al., 2007; Taylor et al., 2008). It is possible that prazosin is acting at α_1-ARs in the vPAG to dampen excitatory transmission onto the vPAG wake promoting DA neurons, which would induce sleep. Modafinil is a medication that is used to treat excessive sleepiness that arises from narcolepsy and other sleep disorders. The mechanism of action of modafinil in promoting wakefulness has yet to be elucidated. Using DBH knockout mice, which lack NE and have hypersensitive DA signaling, the Weinshenker lab determined that modafinil's effects in promoting wakefulness involve both NE and DA, as well as the activation of α_1-ARs (Mitchell et al., 2008). This led to the hypothesis that modafinil acts to block NET in the vPAG which will increase NE and lead to an enhancement of excitatory transmission onto vPAG DA neurons through the activation of α_1-ARs (Mitchell et al., 2008). In addition, modafinil may act to block DAT which will lead to increased DA in projection regions of the vPAG DA neurons. Simultaneously, modafinil's blockade of NET will lead to NE induced inhibition of sleep-promoting neurons in the hypothalamus. The work I have shown in this dissertation regarding α_1-AR mediated increases in excitatory transmission onto vPAG DA neurons supports this mechanism of action for modafinil.

Activation of RLi dopamine neurons may have behavioral consequences

One of the most important questions underlying the study of RLi DA neurons is the question of behavioral relevance. If RLi DA neurons appear to act similarly to

classically studied VTA DA neurons, then their further characterization may be unnecessary. Therefore, it is necessary to identify behavioral actions of RLi DA neurons. It seems likely that RLi DA neurons are part of the unique subset of DA neurons that respond to aversive stimuli or that RLi DA neurons contribute to anxiety related behaviors. The future directions outlined in this section investigate the role of RLi DA neurons in behavior.

The activation of RLi dopamine neurons may lead to anxiety like behavior

Evidence indicates that RLi DA neurons are recruited during stress, and I have shown that activation of α_1-ARs causes an increase in excitatory transmission that would likely lead to an increase in firing of RLi DA neurons (Deutch et al., 1991; Williams et al., 2014). In addition, prazosin can reduce the severity of PTSD symptoms (Green, 2014). In terms of treating PTSD, prazosin could have many sites of action, but it is possible that it is acting at dampening excitatory transmission onto RLi DA neurons. To look at the role of RLi DA neurons in stress related responses such as anxiety, *in vivo* optogenetics could be used. To specifically target RLi DA neurons, a DIO channelrhodopsin (ChR2) virus could be injected into the RLi of TH-cre mice and an optrode implanted into the RLi. Activation of ChR2 by the blue light activates the RLi DA neurons similarly to the α_1-AR mediated increase in glutamatergic transmission. Basic anxiety tests such as EPM or open field could be used to test for anxiety. If activation of the RLi DA neurons induces anxiety, activation of ChR2 may lead to less time spent in the open arms of EPM and less center time in open field. Another behavior test that the lab uses to measure stress induced anxiety is novelty induced hypophagia (NIH). In this

test, animals are trained to consume a palatable substance such as a vanilla shake. In the home cage, a familiar environment, the mouse quickly approaches the vanilla shake, but in a novel cage, there is a conflict between the desire of the vanilla shake and the novel environment. If the RLi DA neurons play a role in anxiety, activation of ChR2 in the RLi during testing days may increase the latency to eat the palatable substance in the novel cage. If the results of these experiments do indicate that RLi DA neurons play a role in anxiety behavior, halorhodopsin could be used to inhibit RLi DA neurons. The prediction is that inhibition of these cells causes a decrease in anxiety related behaviors. Appendix B describes preliminary efforts utilizing optogenetics to investigate the actions of RLi DA neurons.

RLi dopamine neurons may play a role in stress-induced reinstatement of drug-seeking behavior

The RLi DA neurons project to the BNST, a region critical for stress-induced reinstatement of drug-seeking behavior (Briand et al., 2010). In particular, NE signaling in the BNST, particularly through α_1- and β-ARs, initiates stress-induced reinstatement (Leri et al., 2002; Mantsch et al., 2010; Vranjkovic et al., 2014). In addition, a systemic injection of prazosin, the α_1-AR antagonist, blocks stress induced reinstatement of alcohol seeking (Le et al., 2011). In this study, prazosin may act within the BNST, but it may also have converging actions elsewhere, such as the RLi. One hypothesis is that RLi DA neurons may act to recruit the BNST during stress-induced reinstatement. Stress engages NE centers which may lead to α_1-AR mediated increases in excitatory transmission onto RLi DA neurons and presumably an increase in DA release in downstream regions. In the BNST, DA has been shown to have many actions which

include increases in sEPSCs and decreases in inhibitory transmission (Kash et al., 2008; Krawczyk et al., 2011a). Therefore, an increase in RLi DA release in the BNST is likely to lead to an increase in BNST activity which may lead to drug-seeking behavior. The role RLi DA neurons play in reinstatement of drug-seeking behavior can be tested through the use of *in vivo* optogenetics. A DIO ChR2 virus could be injected into the RLi of TH-cre mice and an optrode implanted in the RLi. If RLi DA neurons mediate stress-induced reinstatement, activation of RLi DA neurons may initiate reinstatement of cocaine conditioned place preference (CPP) following extinction, a behavioral paradigm that the lab has experience with (Conrad et al., 2013). If there is no effect on stress-induced reinstatement of cocaine CPP, stress-induced reinstatement of alcohol self-administration could be investigated, since prazosin has been shown to block this behavior in rats and other midline DA neuron groups are involved in the reinforcing effects of alcohol (Le et al., 2011; Li et al., 2013a). Interestingly, prazosin has also demonstrated effectiveness in reducing drinking in clinical trials of alcohol dependence (Muller et al., 2014; Simpson et al., 2009).

In addition, the actions of ablation of RLi DA neurons on stress-induced reinstatement could be investigated using a diphtheria toxin ablation strategy. In this method, an AAV-FLEX-DTR virus is injected into the RLi of TH-cre mice which incorporates the human diphtheria toxin receptor into RLi DA neurons. Then i.p. injections are used to systemically deliver diphtheria toxin which only kills cells that express the receptor, i.e. the RLi DA neurons. If the hypothesis is correct, ablation of RLi DA neurons blocks stress-induced reinstatement of cocaine CPP. It is possible that ablation of RLi DA neurons may interfere with the establishment of CPP. If this is the

case, the diphtheria toxin injections could be done after CPP has been established. These experiments indicate whether the RLi DA neurons are essential for stress-induced reinstatement.

The activation of RLi dopamine neurons may impair working memory

The RLi DA neurons that are activated by stress project to the PFC (Deutch et al., 1991). The PFC is known to mediate working memory through persistent firing of cortical pyramidal neurons (Goldman-Rakic, 1995). Stress impairs working memory through high levels of D1 receptor activation that reduce PFC neuronal firing (Vijayraghavan et al., 2007). Recently it was determined that stress induced D1 receptor mediated increases in cAMP lead to the opening of hyperpolarization-activated cyclic nucleotide-gated (HCN) channels which increases I_h and inhibits cell firing (Gamo et al., 2015). DA is known to have an inverted U-shaped effect in the PFC where moderate levels of DA are beneficial but high levels of DA are detrimental and impair PFC function (Vijayraghavan et al., 2007). Therefore, in times of stress DA increases in the PFC may lead to impaired working memory. This stress induced DA release may be from RLi DA neurons. One hypothesis is that activation of RLi DA neurons may impair PFC mediated working memory. To test this hypothesis, *in vivo* optogenetics studies such as those outlined above could be used in combination with a delayed alternation spatial working memory task in a T-maze. Activation of RLi DA neurons may impair working memory in this task. Patients with schizophrenia have an upregulation of D1 receptor expression in the PFC and show impaired working memory that is exacerbated with stress (Abi-Dargham et al., 2012). Investigations into the actions of RLi DA neurons and working

memory may lead to novel treatment mechanisms for schizophrenia and other psychiatric disorders.

RLi DA neurons project to both the BNST and the PFC, brain regions involved in stress, anxiety and reward related behaviors. One interesting question is the issue of collateralization and whether the same RLi DA neuron projects to both of these brain regions. There is evidence for collateralization of some groups of DA neurons, while others don't show much collateralization. For example, some nigrostriatal DA neurons send collaterals to the thalamus (Freeman et al., 2001), while there is minimal collateral branching of VTA DA projections to the primary motor cortex, NAc and PFC (Hosp et al., 2015). Whether or not the RLi DA projections to the PFC and BNST arise from the same neurons or different subsets of RLi DA neurons, stress may increase DA in both of these regions. The PFC sends glutamatergic projections to the BNST (Massi et al., 2008). This triad sets up an interesting circuit that could play important roles in many stress related behaviors and pathologies (Figure 14).

RLi dopamine neurons may mediate conditioned place aversion behavior

As discussed above RLi DA neurons share characteristics with the subset of DA neurons that respond to aversive stimuli. Therefore, it might be possible that activation of RLi DA neurons mediates conditioned place aversion behavior. This hypothesis can be tested using *in vivo* optogenetics in a TH-cre mouse line as outlined above. During the conditioning session, ChR2 is activated on one side of a two chamber apparatus. If activation of RLi DA neurons induces CPA, on the testing day the mouse may prefer the chamber where it did not experience the light activation.

If the RLi plays a role in any of the above behaviors, further characterization of RLi DA neurons might reveal mechanisms that could contribute to the development of novel treatments for schizophrenia, anxiety disorders or addiction. Recruitment of RLi DA neurons during these behaviors may be due to increases in excitatory drive. Since my studies indicate that activation of α_1- and α_2-ARs modulate excitatory transmission onto RLi DA neurons, further characterization and manipulation of these systems could uncover treatments for these pathological conditions.

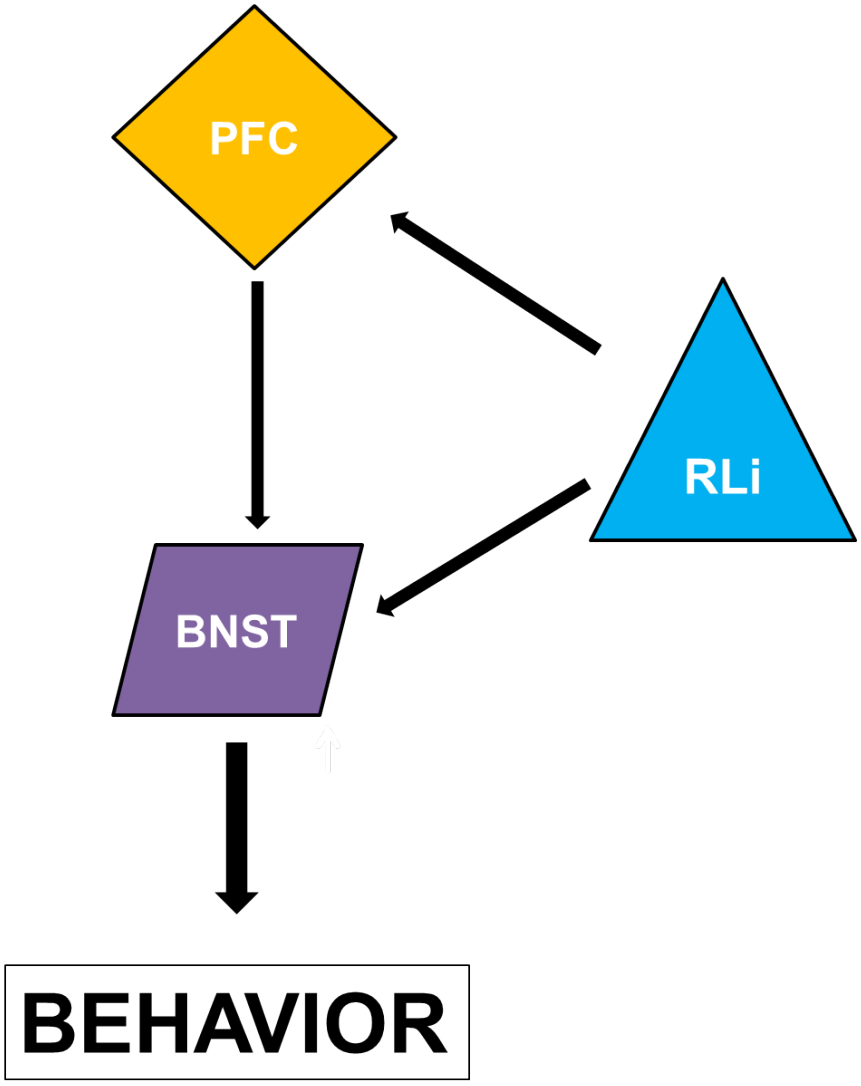

Figure 14: Model depicting the circuit triad of the RLi, PFC and BNST. The RLi DA neurons project to both the BNST and the PFC. It is possible that the same DA neurons project to both of these regions or that subsets project to each region. Stress may increase RLi DA in the BNST and PFC. The PFC sends glutamatergic afferents to the BNST. This triad could play important roles in many behaviors such as working memory and stress-induced reinstatement of drug-seeking.

Stress may increase glutamatergic transmission onto RLi dopamine neurons in an α_1-AR dependent manner

An important question to address is to determine the role of the α_1-AR mediated facilitation of excitatory transmission onto RLi DA neurons in behavior. The literature indicates that after administration of an acute stressor DA concentration and metabolism increase in DA projection regions such as the NAc, mPFC, and CeA (Coco et al., 1992; Deutch et al., 1991; Kalivas and Duffy, 1995; Morrow et al., 1997; Morrow et al., 2000; Sutoo and Akiyama, 2002). However, after chronic stressors the concentration and metabolism of DA decreases in the NAc (Imperato et al., 1993; Mangiavacchi et al., 2001). Glutamate afferents mediate the firing of DA neurons, particularly burst firing (Harnett et al., 2009; Overton and Clark, 1992; Seutin et al., 1993). Therefore, changes in excitatory transmission may change the rate of DA neuron firing and subsequently the release of DA in target regions. In Chapter III, I have shown that activation of α_1-ARs increases excitatory transmission in RLi DA neurons. Since NE centers are engaged during stress and there are noradrenergic projections to the RLi, I hypothesize that acute restraint stress increases glutamatergic transmission in much the same way as the application of NE and methoxamine. In order to test this hypothesis, electrophysiology experiments could be done in animals following restraint stress. The stressor mimics the actions of methoxamine, and after acute restraint stress, there may be an α_1-AR dependent increase in frequency of sEPSCs on RLi DA neurons compared to control animals. This increase in sEPSCs could be blocked by a systemic injection of prazosin prior to administration of the stressor or reversed by applying prazosin to the slice. If there is no increase in sEPSC frequency following restraint stress, another stressor such as foot shock or exposure to predator odor could

be used, or it might indicate that this mechanism is not involved in the stress response. NE has also been shown to be involved in attention related behaviors and perhaps this might be the reason for the NE modulation of RLi DA neurons (Aston-Jones et al., 2000; Aston-Jones and Cohen, 2005; Bouret and Sara, 2004). Another explanation is that the effect occurs following stress but is transient and cannot be identified through electrophysiology recordings; Figure 11 does indicate that the α_1-AR mediated increase in excitatory transmission may be transient. In recordings following chronic restraint stress, one might expect to see no change or decreases in glutamatergic transmission on RLi DA neurons since there are decreases in DA levels after chronic stressors.

These experiments may indicate whether the α_1-AR mediated increase in excitatory transmission onto RLi occurs as part of the stress response. If this action occurs following a stressor, further investigations into the mechanisms of the α_1-AR mediated increase in excitatory transmission may give clues towards the development of treatments for pathological conditions that arise due to stress, such as anxiety disorders, depression, or PTSD.

Activation of α_1-ARs may underlie stress induced immediate early gene expression in RLi dopamine neurons

An increase in *c-fos* expression following exposure to a stressor indicates that RLi DA neurons are recruited during stress (Deutch et al., 1991). Identification of the neurotransmitter system underlying the stress-induced *c-fos* expression allows for further insights into the actions of RLi DA neurons in the stress response. One hypothesis is that RLi DA neurons are recruited by NE through activation of α_1-ARs during stress. In order to investigate this hypothesis, we attempted to block stress-

induced increases in Zif268, an immediate early gene also known as Egr-1, in RLi DA neurons with a systemic injection of prazosin, an α_1-AR antagonist, prior to administration of the stressor. Our initial attempts at this blockade were inconclusive (see Figure 17 in Appendix A). Therefore, it might be worthwhile to repeat these experiments by changing some of the experimental parameters. For example, although we used a dose of prazosin (2 mg/kg) within the range of those used in the literature perhaps a different dose of prazosin or a different α_1-AR antagonist altogether, such as terazosin or HEAT (2-[[beta-(-4-hydroxyphenyl)ethyl]aminomethyl]-1-tetralone) might yield better results (Greenwell et al., 2009; Le et al., 2011). We have also made preliminary investigations into the timeline of stress induced Zif268 expression and find that prolonging the time from the start of the stressor before perfusion of the mouse may maximize Zif268 expression (see Figure 18 in Appendix A). This gives a larger window to see a reduction with the antagonist. After the preliminary time-course experiments, the Zif268 antibody stopped working and we could not get adequate staining above background with new lots of antibody. Recently, the lab has begun fluorescent *c-fos* immunohistochemistry. Therefore, future experiments in this area could use *c-fos* immunohistochemistry. One caveat with these future studies is that the systemic injection of the α_1-AR antagonist won't delineate whether activation of α_1-ARs in the RLi or another brain region or even peripheral α_1-ARs underlie the stress-induced Zif268 expression in RLi DA neurons. Therefore, the best approach is to inject the α_1-AR antagonist directly into the RLi through a cannula prior to administration of the stressor.

It is possible that a different neurotransmitter system is involved in the recruitment of RLi DA neurons during stress. A prime candidate might be CRF. CRF

concentration is known to increase during stress, and CRF has been shown to increase excitatory transmission onto dopamine neurons of the VTA and may also have actions within the RLi (Bonci and Borgland, 2009; Valentino et al., 1993). If prazosin fails to block stress induced increases in Zif268 expression, perhaps CRFR antagonists might be a good step to try next. Determining the neurotransmitter system underlying the recruitment of RLi DA neurons during stress opens the door for many future investigations into behaviorally relevant actions of RLi DA neurons. It could possibly uncover a novel mechanism involved in the stress response that could lead to more effective treatments for anxiety disorders or PTSD.

Summary

The heterogeneity of DA neurons has been a topic of active research in the last few years. It has become apparent that different molecular expression profiles, anatomical connectivity, and physiological properties likely lead to a functional heterogeneity among subsets of midbrain DA neurons. In this dissertation I report sub-regions of DA neurons that project to the dorsal BNST of a TH-eGFP mouse. The largest numbers of dBNST projecting DA neurons were found in the VTA, RLi and caudal portion of the DR and adjacent vPAG. The results of these studies were used to guide electrophysiological studies of understudied RLi DA neurons. I found that RLi DA neurons lack I_h and have a higher membrane resistance than lateral VTA DA neurons (Williams et al., 2014). These are shared characteristics among other midline DA neurons such as those of the vPAG and PFC projecting medial VTA DA neurons and influence how a neuron responds to synaptic input (Lammel et al., 2011; Li et al.,

2013a). Since there is a substantial NE input to the RLi DA neurons and they project to the BNST and PFC, regions heavily involved in stress and anxiety circuitry, I examined the effects of NE on excitatory transmission of RLi DA neurons (Mejias-Aponte et al., 2009). I found that NE increased excitatory transmission onto RLi DA neurons via activation of α_1-ARs. In addition, activation of α_2-ARs leads to a mild decrease in excitatory transmission (Williams et al., 2014). NE may recruit RLi DA neurons during a variety of behaviors such as stress or disturbances in homeostasis (Deutch et al., 1991). Due to their projections to the BNST and PFC, RLi DA neurons may also play a role in stress-induced reinstatement of drug-seeking or working memory, which is impaired in psychiatric disorders such as schizophrenia. In addition, the vPAG DA neurons play a role in the sleep-wake cycle and treatments of sleep related disorders may act on this system (Lu et al., 2006; Mitchell et al., 2008). In fact, prazosin, an α_1-AR antagonist, is currently used to reduce severity of symptoms and treat sleep disturbances associated with PTSD (Mohsenin and Mohsenin, 2014; Raskind et al., 2007; Taylor et al., 2008). If the RLi DA neurons are indeed involved in stress, anxiety, and addiction related behaviors, their further characterization may lead to effective novel treatment mechanisms for PTSD, anxiety disorders, and drug addiction.

APPENDIX A

Stress induced Zif268 expression in dopamine neurons

As mentioned in Chapter IV, we confirmed that stress increases immediate early gene expression in RLi DA neurons of mice. After a 60 min session of restraint stress there is an increase in the percentage of Zif268 positive, TH positive cells in the RLi and lateral VTA of adult mice following restraint stress (Figure 15). This stress-induced Zif268 increase does not occur in dorsal raphe DA neurons, which is why RLi DA neurons were the focus of the electrophysiology studies. Since 3-4 week old mice were required to visualize viable cells in the RLi for electrophysiology studies, we confirmed that stress induced increases in Zif268 expression in RLi DA neurons also occur in adolescent mice (Figure 16).

Since I found that the activation of α_1-ARs increases excitatory transmission onto RLi DA neurons, we hypothesized that this increase in excitatory transmission was responsible for recruiting RLi DA neurons during stress. In order to test this hypothesis we attempted to block the stress induced Zif268 expression in RLi DA neurons through systemic injection of prazosin, the α_1-AR antagonist, 30 minutes prior to the start of the stressor. This initial attempt was inconclusive (Figure 17). In all of the above experiments, animals were perfused immediately upon cessation of restraint, 60 minutes from the start of the stressor. We hypothesized that increasing the time from the start of the stressor to perfusion might give larger increases in protein expression. This would give a larger window to block Zif268 expression with prazosin. Indeed, waiting 45 minutes after the cessation of the stressor to perfuse the animal does give

larger increases in Zif268 expression (Figure 18). After the preliminary time-course experiments, the Zif268 antibody (Santa Cruz sc-110 lot L3107) stopped working and we could not get adequate staining above background with a new lot (Santa Cruz sc-100 lot B2513) of antibody so we did not pursue this further. Potential future directions related to these data are outlined in Chapter IV.

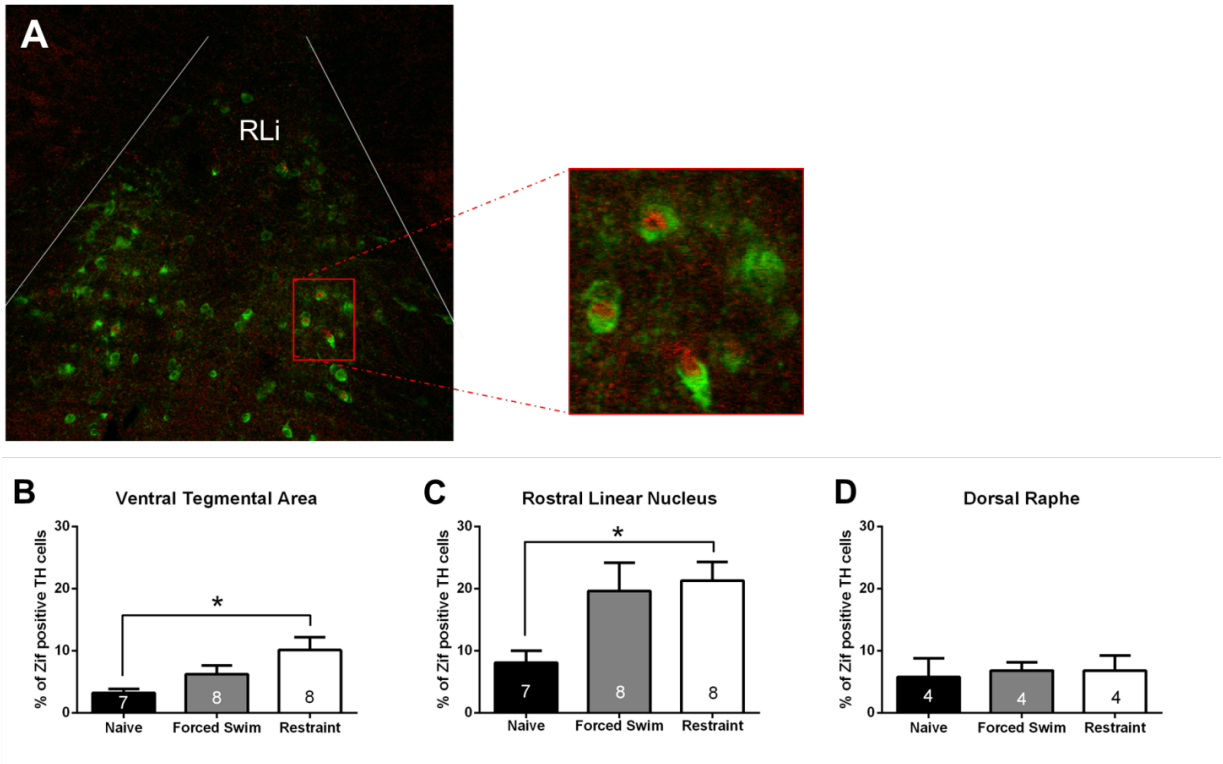

Figure 15: Restraint stress increases Zif268 expression in TH+ neurons of the VTA and RLi, but not the DR in adult mice.
(A) Image taken at 20x on a confocal microscope of a coronal section of the RLi showing TH (green) and Zif268 (red) immunohistochemistry. This mouse was perfused immediately after a 60 min session of restraint stress. Inset: close up of colocalized zif268 and TH positive cells. (B) Cell counts of the percent of TH cells that are zif268 positive in the VTA in naïve mice, mice perfused immediately after a 60 min restraint session, and mice perfused 60 min after the start of 6 min forced swim stress ($F(2,20)=4.99$, $p=0.018$), (C) RLi ($F(2,20)=4.14$, $p=0.031$), and (D) dorsal raphe ($F(2,9)=0.066$, $p=0.94$. A one way ANOVA was used followed by Tukey's multiple comparisons test when $p<0.05$. * indicates $p<0.05$ and the n for each group is listed on the graph.

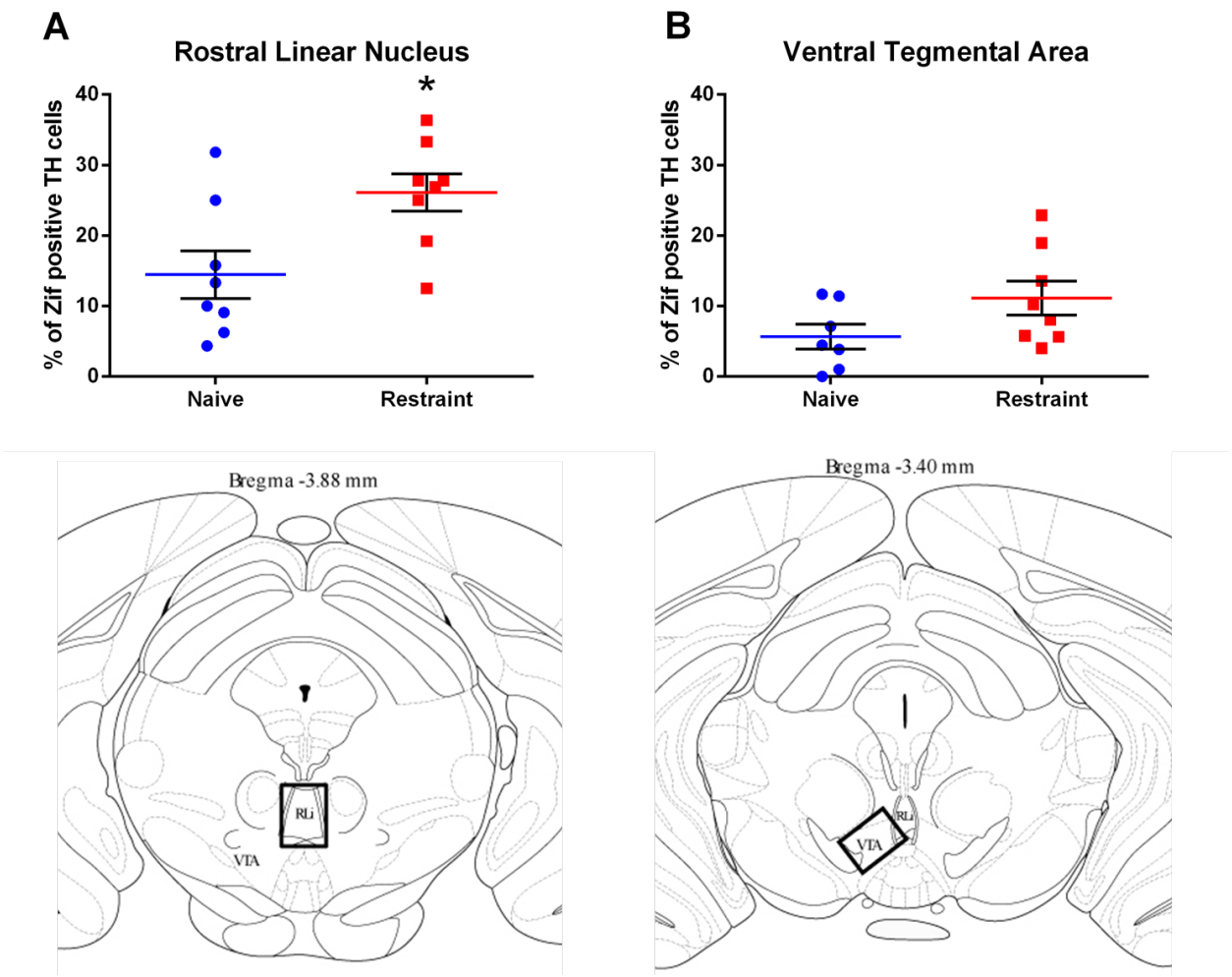

Figure 16: Restraint stress increases Zif268 expression in TH+ neurons of the RLi, but not the VTA in adolescent mice.
(A) Cell counts of the percent of TH cells that are zif268 positive in naïve mice and mice that undergo 60 min restraint stress session in the RLi ($t(14)=2.72$, $p=0.017$), and (B) VTA ($t(13)=1.80$, $p=0.096$). Below each graph is a brain atlas diagram from Paxinos and Watson and the black box indicates the region used for cell counting. A student's t-test was used to determine statistical significance. *indicates $p<0.05$ and the n for each group is listed on the bar

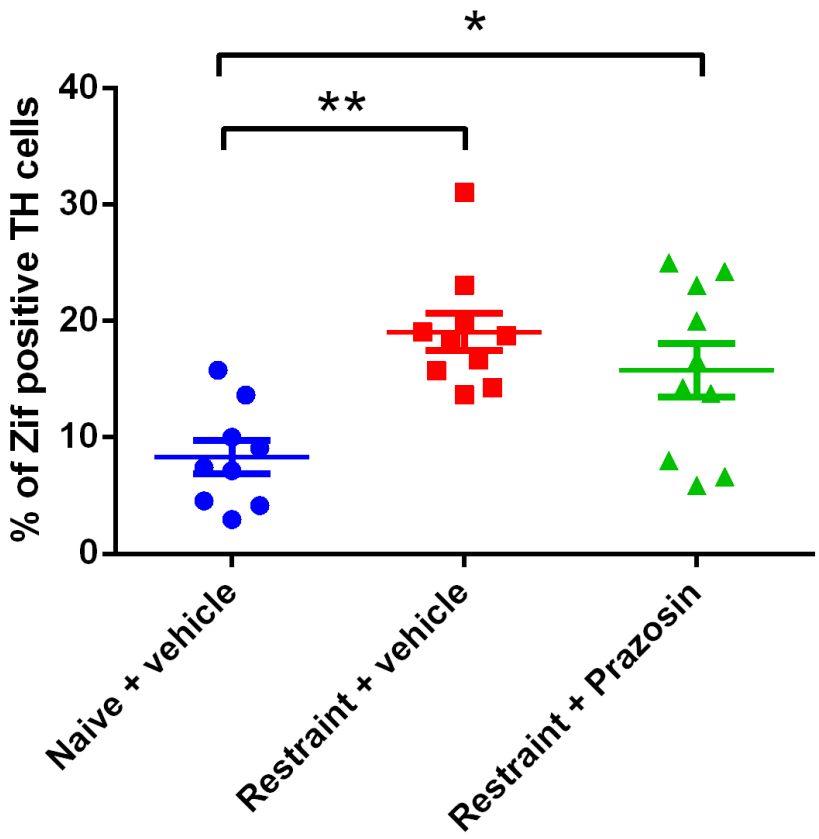

Figure 17: Prazosin (2 mg/kg) does not block stress-induced Zif268 expression in the RLi.
Cell counts of the percent of TH cells that are zif268 positive in the RLi ($F(2,26)=8.610$, $p=0.001$). A one way ANOVA was used followed by Tukey's multiple comparisons test. * indicates $p<0.05$, and ** indicates $p<0.01$.

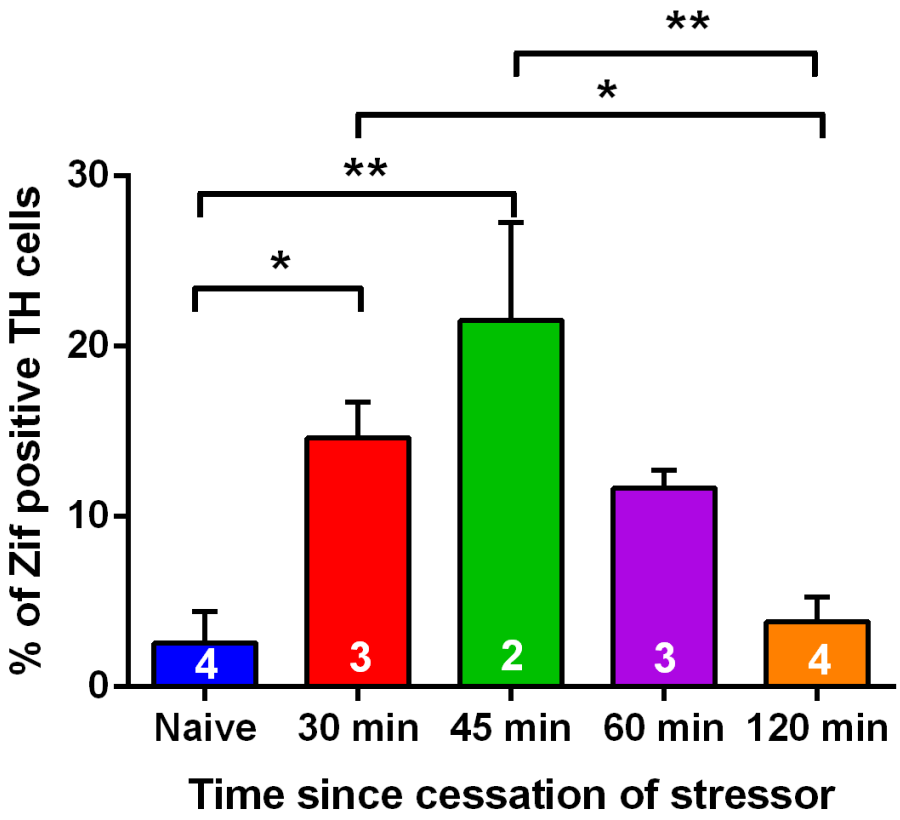

Figure 18: Time course of stress-induced Zif268 expression in the RLi. Cell counts of the percent of TH cells that are zif268 positive in the RLi following a 60 minute restraint stress session ($F(4,11)=11.8$, $p=0.0006$). A one way ANOVA was used followed by Tukey's multiple comparisons test. * indicates $p<0.05$, ** indicates $p<0.01$, and the n for each group is listed on the bar graph.

APPENDIX B

Using optogenetics to investigate the actions of RLi dopamine release in the BNST

Since I faced technical difficulties with electrophysiology recordings in RLi DA neurons in animals over 4 weeks old, we decided to investigate the downstream actions of RLi DA in the BNST. This section contains some preliminary studies from an optogenetics pilot project. An AAV-DIO-ChR2-YFP virus (300nl) was injected into the RLi (AP = -3.98; ML = 0; DV = -3.98) of TH-cre mice. Expression of ChR2 was present in the RLi and fibers can be seen in the dBNST (Figure 19). There was strong ChR2 expression in the RLi, and there was some spread of the virus into the interfascicular, medial PBP, and paranigral nuclei in some animals. The images in figure 19 were taken from slices that were fixed and immunostained following electrophysiology recordings so the antibody penetration is rather weak. These images indicate that there is ChR2 expression in the RLi and dBNST, but the fidelity of the viral expression cannot be determined. It appears that there is expression of ChR2 in some TH+ neurons, but it is difficult to determine how much ectopic expression of ChR2 is present. If these optogenetics experiments were to continue, better images and accurate cell counts are needed to address the issue of fidelity (Lammel et al., 2015; Stuber et al., 2015).

The next step is to elicit DA release from the terminals of RLi DA neurons in the dBNST. Different light stimulation protocols were attempted while recording sEPSCs from dBNST neurons. dBNST cells were recorded in areas of high YFP-ChR2 expression as visualized by fluorescence on the electrophysiology rig. Prior studies in the lab indicate that DA increases sEPSC frequency in the BNST so it is possible that

the right light stimulation protocol could increase sEPSC frequency onto dBNST neurons (Kash et al., 2008). At first, we started with lower stimulation frequencies (varied from 2-10Hz, 5-15 pulses, 5ms/pulse) because we were worried about depleting DA quickly and there was the possibility of glutamate corelease from RLi DA neurons. Also, these stimulation frequencies cover the range of non-burst firing seen in VTA DA neurons (Paladini and Roeper, 2014). No light evoked EPSCs were witnessed in any of the stimulation protocols and we did not see much change in sEPSC frequency or amplitude (data not shown). We expected that we would see light evoked EPSCs since there is evidence of glutamate corelease in midline DA neurons (Hnasko et al., 2010; Stuber et al., 2010), therefore it is likely that the stimulation did not elicit DA release. Therefore, the stimulation frequencies were increased with varying results (10-20Hz, 5-15 pulses, 5ms/pulse). In some cells, the same stimulation frequency was repeated a few times while in others the frequency of stimulation was increased every six minutes to see if one proved more successful than others. A few examples of these cells are shown in Figure 20. There are a few possible explanations for the variety of responses seen in Figure 20D. The BNST is composed of many different cell types so the different types of responses could be due to recordings from different types of BNST neurons (Hammack et al., 2007). In addition, the different stimulation protocols and the variability of ChR2 expression near any given cell may give different levels of DA release. We also can't confirm that we are in fact getting DA release with any of the stimulation protocols. Therefore, if optogenetics experiments investigating the role of RLi DA input to the BNST were to continue, slice amperometry is necessary to determine the correct stimulation protocol to elicit DA release in the BNST.

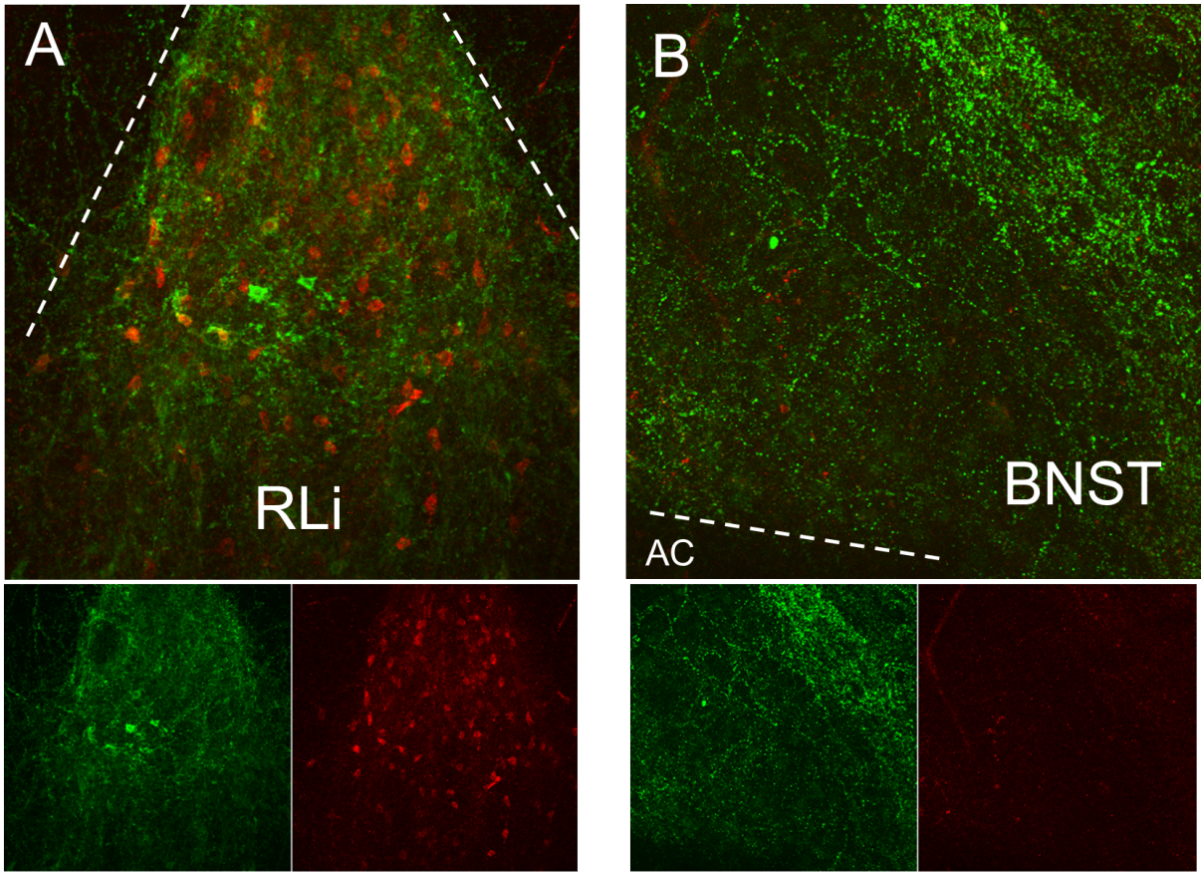

Figure 19: Optogenetic targeting of the RLi dopamine input to the BNST. (A) Confocal image at 20X showing colocalization of ChR2 (green) (300 µL injection of AAV-DIO-ChR2-eYFP) with TH (red) in the RLi of a TH-cre mouse. (B) Confocal image at 40X showing colocalization of ChR2 (green) with TH (red) in the BNST.

Figure 20: Optogenetic stimulation of the RLi dopamine input to the BNST. (A) Graph of the sEPSC frequency and amplitude of a BNST neuron from a TH-cre mouse that was injected with ChR2 in the RLi. This cell had a decrease in sEPSC frequency after stimulation with blue light. Each blue arrow represents a stimulation protocol corresponding to the legend to the right of the graph. Change in size of the arrow indicates an increase in the stimulation frequency or number of pulses. (B) Example of a cell with an increase in sEPSC frequency after stimulation with blue light. (C) Example of a cell with an increase in sEPSC amplitude following stimulation with blue light. (D) Pie chart indicating the varied responses in sEPSCs of BNST neurons after stimulation with blue light.

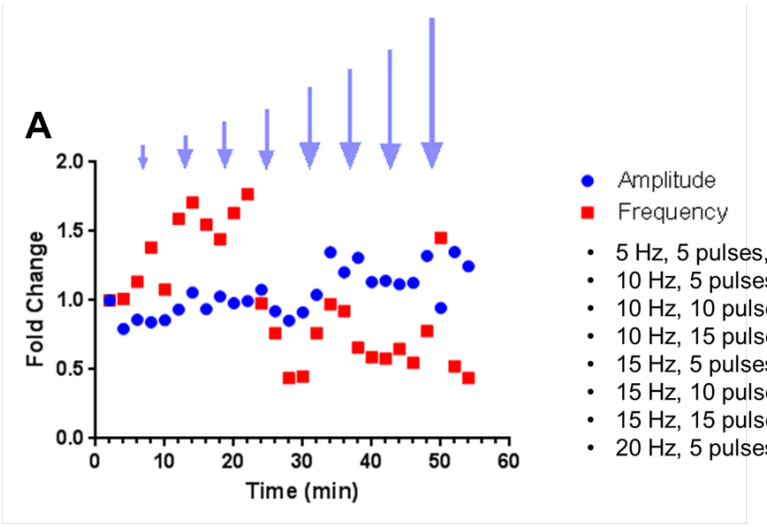
A
Fold Change
Time (min)
Amplitude
Frequency
5 Hz, 5 pulses, 5ms/pulse
10 Hz, 5 pulses, 5ms/pulse
10 Hz, 10 pulses, 5ms/pulse
10 Hz, 15 pulses, 5ms/pulse
15 Hz, 5 pulses, 5 ms/pulse
15 Hz, 10 pulses, 5 ms/pulse
15 Hz, 15 pulses, 5 ms/pulse
20 Hz, 5 pulses, 5 ms/pulse

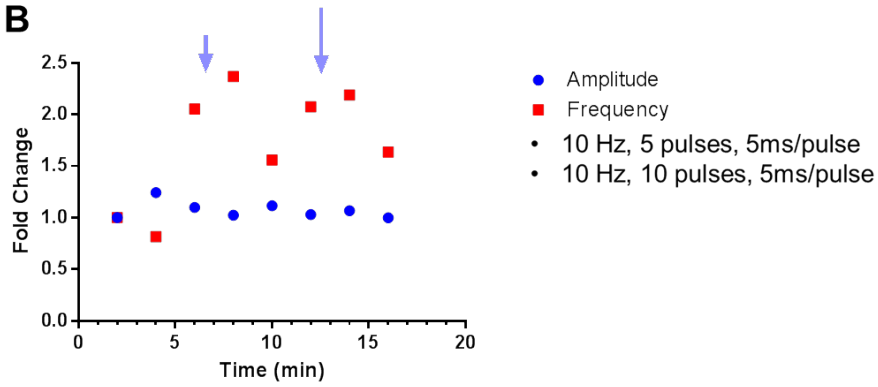
B
Fold Change
Time (min)
Amplitude
Frequency
10 Hz, 5 pulses, 5ms/pulse
10 Hz, 10 pulses, 5ms/pulse

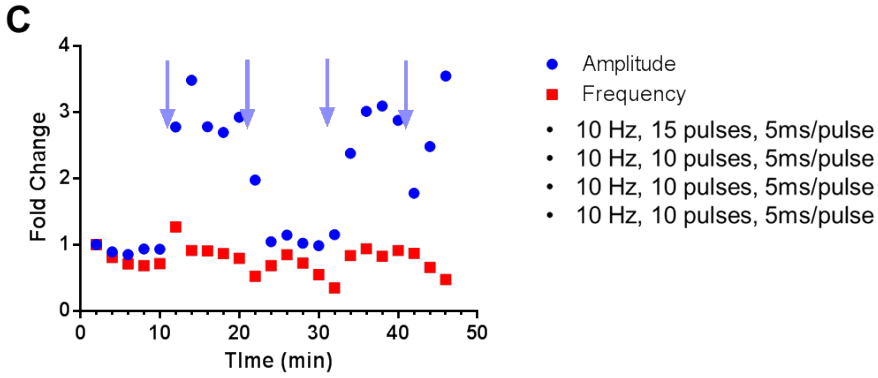
C
Fold Change
TIme (min)
Amplitude
Frequency
10 Hz, 15 pulses, 5ms/pulse
10 Hz, 10 pulses, 5ms/pulse
10 Hz, 10 pulses, 5ms/pulse
10 Hz, 10 pulses, 5ms/pulse

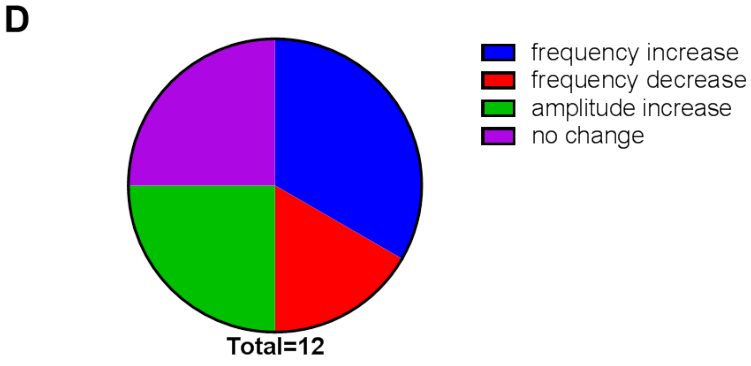
D
frequency increase
frequency decrease
amplitude increase
no change
Total=12

APPENDIX C

Activation of α_1-ARs increases sEPSC frequency onto vPAG dopamine neurons

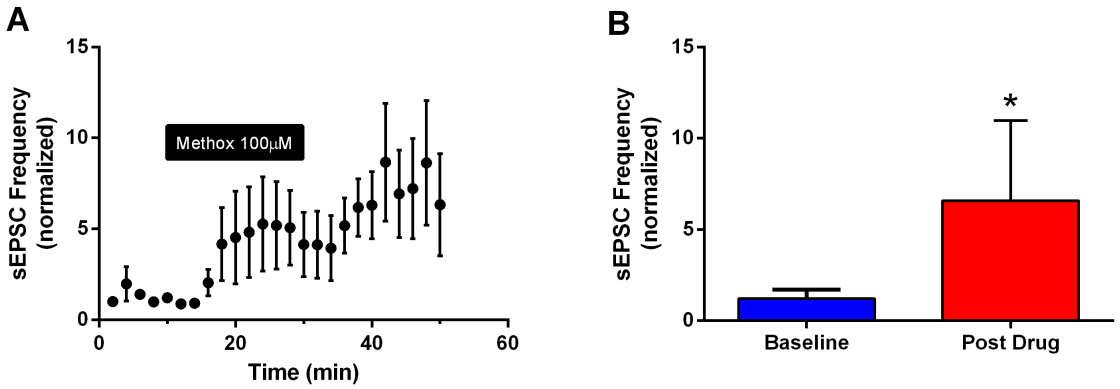

Figure 21: Methoxamine increases sEPSC frequency but not amplitude onto vPAG dopamine neurons.
(A,B) A 20 min application of 100 μM methoxamine increases mEPSC frequency onto vPAG dopamine neurons ($t(4)=2.87$, $p=0.046$), but has no change on amplitude (data not shown). A paired student's t-test was used to determine statistical significance,* denotes $p < 0.05$, $n=5$.

REFERENCES

Abercrombie, E.D., Jacobs, B.L., 1987. Single-unit response of noradrenergic neurons in the locus coeruleus of freely moving cats. II. Adaptation to chronically presented stressful stimuli. J Neurosci. 7**,** 2844-8.

Abercrombie, E.D., Keller, R.W., Jr., Zigmond, M.J., 1988. Characterization of hippocampal norepinephrine release as measured by microdialysis perfusion: pharmacological and behavioral studies. Neuroscience. 27**,** 897-904.

Abercrombie, E.D., Keefe, K.A., DiFrischia, D.S., Zigmond, M.J., 1989. Differential effect of stress on in vivo dopamine release in striatum, nucleus accumbens, and medial frontal cortex. J Neurochem. 52**,** 1655-8.

Abi-Dargham, A., et al., 2012. Increased prefrontal cortical D(1) receptors in drug naive patients with schizophrenia: a PET study with [(1)(1)C]NNC112. J Psychopharmacol. 26**,** 794-805.

Alheid, G.F., Beltramino, C.A., De Olmos, J.S., Forbes, M.S., Swanson, D.J., Heimer, L., 1998. The neuronal organization of the supracapsular part of the stria terminalis in the rat: the dorsal component of the extended amygdala. Neuroscience. 84**,** 967-96.

Alreja, M., Liu, W., 1996. Noradrenaline induces IPSCs in rat medial septal/diagonal band neurons: involvement of septohippocampal GABAergic neurons. J Physiol. 494 (Pt 1)**,** 201-15.

Anstrom, K.K., Woodward, D.J., 2005. Restraint increases dopaminergic burst firing in awake rats. Neuropsychopharmacology. 30**,** 1832-40.

Anstrom, K.K., Miczek, K.A., Budygin, E.A., 2009. Increased phasic dopamine signaling in the mesolimbic pathway during social defeat in rats. Neuroscience. 161**,** 3-12.

Aston-Jones, G., Rajkowski, J., Cohen, J., 2000. Locus coeruleus and regulation of behavioral flexibility and attention. Prog Brain Res. 126**,** 165-82.

Aston-Jones, G., Cohen, J.D., 2005. An integrative theory of locus coeruleus-norepinephrine function: adaptive gain and optimal performance. Annu Rev Neurosci. 28**,** 403-50.

Aubert, M., Guiramand, J., Croce, A., Roch, G., Szafarczyk, A., Vignes, M., 2001. An endogenous adrenoceptor ligand potentiates excitatory synaptic transmission in cultured hippocampal neurons. Cereb Cortex. 11**,** 878-87.

Bannon, M.J., Michaud, R.L., Roth, R.H., 1981. Mesocortical dopamine neurons. Lack of autoreceptors modulating dopamine synthesis. Mol Pharmacol. 19**,** 270-5.

Barrot, M., 2014. The ventral tegmentum and dopamine: A new wave of diversity. Neuroscience. 282C, 243-247.

Beckstead, R.M., Domesick, V.B., Nauta, W.J., 1979. Efferent connections of the substantia nigra and ventral tegmental area in the rat. Brain Res. 175, 191-217.

Bergles, D.E., Doze, V.A., Madison, D.V., Smith, S.J., 1996. Excitatory actions of norepinephrine on multiple classes of hippocampal CA1 interneurons. J Neurosci. 16, 572-85.

Bjorklund, A., Dunnett, S.B., 2007. Dopamine neuron systems in the brain: an update. Trends Neurosci. 30, 194-202.

Blessing, W.W., Willoughby, J.O., 1985. Inhibiting the rabbit caudal ventrolateral medulla prevents baroreceptor-initiated secretion of vasopressin. J Physiol. 367, 253-65.

Bonci, A., Borgland, S., 2009. Role of orexin/hypocretin and CRF in the formation of drug-dependent synaptic plasticity in the mesolimbic system. Neuropharmacology. 56 Suppl 1, 107-11.

Borgland, S.L., Malenka, R.C., Bonci, A., 2004. Acute and chronic cocaine-induced potentiation of synaptic strength in the ventral tegmental area: electrophysiological and behavioral correlates in individual rats. J Neurosci. 24, 7482-90.

Bouret, S., Sara, S.J., 2004. Reward expectation, orientation of attention and locus coeruleus-medial frontal cortex interplay during learning. Eur J Neurosci. 20, 791-802.

Braga, M.F., Aroniadou-Anderjaska, V., Manion, S.T., Hough, C.J., Li, H., 2004. Stress impairs alpha(1A) adrenoceptor-mediated noradrenergic facilitation of GABAergic transmission in the basolateral amygdala. Neuropsychopharmacology. 29, 45-58.

Briand, L.A., Vassoler, F.M., Pierce, R.C., Valentino, R.J., Blendy, J.A., 2010. Ventral tegmental afferents in stress-induced reinstatement: the role of cAMP response element-binding protein. J Neurosci. 30, 16149-59.

Brischoux, F., Chakraborty, S., Brierley, D.I., Ungless, M.A., 2009. Phasic excitation of dopamine neurons in ventral VTA by noxious stimuli. Proc Natl Acad Sci U S A. 106, 4894-9.

Bromberg-Martin, E.S., Matsumoto, M., Hikosaka, O., 2010. Dopamine in motivational control: rewarding, aversive, and alerting. Neuron. 68, 815-34.

Bylund, D.B., Eikenberg, D.C., Hieble, J.P., Langer, S.Z., Lefkowitz, R.J., Minneman, K.P., Molinoff, P.B., Ruffolo, R.R., Jr., Trendelenburg, U., 1994. International Union of Pharmacology nomenclature of adrenoceptors. Pharmacol Rev. 46, 121-36.

Cecchi, M., Khoshbouei, H., Javors, M., Morilak, D.A., 2002a. Modulatory effects of norepinephrine in the lateral bed nucleus of the stria terminalis on behavioral and neuroendocrine responses to acute stress. Neuroscience. 112**,** 13-21.

Cecchi, M., Khoshbouei, H., Morilak, D.A., 2002b. Modulatory effects of norepinephrine, acting on alpha 1 receptors in the central nucleus of the amygdala, on behavioral and neuroendocrine responses to acute immobilization stress. Neuropharmacology. 43**,** 1139-47.

Chiodo, L.A., Bannon, M.J., Grace, A.A., Roth, R.H., Bunney, B.S., 1984. Evidence for the absence of impulse-regulating somatodendritic and synthesis-modulating nerve terminal autoreceptors on subpopulations of mesocortical dopamine neurons. Neuroscience. 12**,** 1-16.

Clayton, E.C., Rajkowski, J., Cohen, J.D., Aston-Jones, G., 2004. Phasic activation of monkey locus ceruleus neurons by simple decisions in a forced-choice task. J Neurosci. 24**,** 9914-20.

Coco, M.L., Kuhn, C.M., Ely, T.D., Kilts, C.D., 1992. Selective activation of mesoamygdaloid dopamine neurons by conditioned stress: attenuation by diazepam. Brain Res. 590**,** 39-47.

Conrad, K.L., Louderback, K.M., Milano, E.J., Winder, D.G., 2013. Assessment of the impact of pattern of cocaine dosing schedule during conditioning and reconditioning on magnitude of cocaine CPP, extinction, and reinstatement. Psychopharmacology (Berl). 227**,** 109-16.

Cooper, D.C., 2002. The significance of action potential bursting in the brain reward circuit. Neurochem Int. 41**,** 333-40.

Dahlström, A., Fuxe, K., 1964. Evidence for the existence of monoamine-containing neurons in the central nervous system, Vol., Uppsala,.

Davis, M., Walker, D.L., Miles, L., Grillon, C., 2010. Phasic vs sustained fear in rats and humans: role of the extended amygdala in fear vs anxiety. Neuropsychopharmacology. 35**,** 105-35.

Day, H.E., Campeau, S., Watson, S.J., Jr., Akil, H., 1997. Distribution of alpha 1a-, alpha 1b- and alpha 1d-adrenergic receptor mRNA in the rat brain and spinal cord. J Chem Neuroanat. 13**,** 115-39.

Deister, C.A., Teagarden, M.A., Wilson, C.J., Paladini, C.A., 2009. An intrinsic neuronal oscillator underlies dopaminergic neuron bursting. J Neurosci. 29**,** 15888-97.

Del-Fava, F., Hasue, R.H., Ferreira, J.G., Shammah-Lagnado, S.J., 2007. Efferent connections of the rostral linear nucleus of the ventral tegmental area in the rat. Neuroscience. 145**,** 1059-76.

Deutch, A.Y., Goldstein, M., Roth, R.H., 1986. Activation of the locus coeruleus induced by selective stimulation of the ventral tegmental area. Brain Res. 363, 307-14.

Deutch, A.Y., Roth, R.H., 1990. The determinants of stress-induced activation of the prefrontal cortical dopamine system. Prog Brain Res. 85, 367-402; discussion 402-3.

Deutch, A.Y., Lee, M.C., Gillham, M.H., Cameron, D.A., Goldstein, M., Iadarola, M.J., 1991. Stress selectively increases fos protein in dopamine neurons innervating the prefrontal cortex. Cereb Cortex. 1, 273-92.

Dong, H., Petrovich, G.D., Swanson, L.W., 2000. Organization of projections from the juxtacapsular nucleus of the BST: a PHAL study in the rat. Brain Res. 859, 1-14.

Dong, H.W., Petrovich, G.D., Watts, A.G., Swanson, L.W., 2001. Basic organization of projections from the oval and fusiform nuclei of the bed nuclei of the stria terminalis in adult rat brain. J Comp Neurol. 436, 430-55.

Dong, H.W., Swanson, L.W., 2003. Projections from the rhomboid nucleus of the bed nuclei of the stria terminalis: implications for cerebral hemisphere regulation of ingestive behaviors. J Comp Neurol. 463, 434-72.

Dong, Y., Fu, Y.M., Sun, J.L., Zhu, Y.H., Sun, F.Y., Zheng, P., 2005. Neurosteroid enhances glutamate release in rat prelimbic cortex via activation of alpha1-adrenergic and sigma1 receptors. Cell Mol Life Sci. 62, 1003-14.

Dumont, E.C., Williams, J.T., 2004. Noradrenaline triggers GABAA inhibition of bed nucleus of the stria terminalis neurons projecting to the ventral tegmental area. J Neurosci. 24, 8198-204.

Egli, R.E., Kash, T.L., Choo, K., Savchenko, V., Matthews, R.T., Blakely, R.D., Winder, D.G., 2005. Norepinephrine modulates glutamatergic transmission in the bed nucleus of the stria terminalis. Neuropsychopharmacology. 30, 657-68.

El Mansari, M., Guiard, B.P., Chernoloz, O., Ghanbari, R., Katz, N., Blier, P., 2010. Relevance of norepinephrine-dopamine interactions in the treatment of major depressive disorder. CNS Neurosci Ther. 16, e1-17.

Erb, S., 2010. Evaluation of the relationship between anxiety during withdrawal and stress-induced reinstatement of cocaine seeking. Prog Neuropsychopharmacol Biol Psychiatry. 34, 798-807.

Falck, B., Hillarp, N.-Å., Thieme, G., Torp, A., 1962. Fluorescence of catechol amines and related compounds condensed with formaldehyde. Journal of Histochemistry and Cytochemistry. 10, 348-354.

Fallon, J.H., Moore, R.Y., 1978. Catecholamine innervation of the basal forebrain. IV. Topography of the dopamine projection to the basal forebrain and neostriatum. J Comp Neurol. 180, 545-80.

Fields, H.L., Hjelmstad, G.O., Margolis, E.B., Nicola, S.M., 2007. Ventral tegmental area neurons in learned appetitive behavior and positive reinforcement. Annu Rev Neurosci. 30, 289-316.

Flavin, S.A., Winder, D.G., 2013. Noradrenergic control of the bed nucleus of the stria terminalis in stress and reward. Neuropharmacology. 70, 324-30.

Flavin, S.A., Matthews, R.T., Wang, Q., Muly, E.C., Winder, D.G., 2014. alpha(2A)-adrenergic receptors filter parabrachial inputs to the bed nucleus of the stria terminalis. J Neurosci. 34, 9319-31.

Flores, J.A., Galan-Rodriguez, B., Ramiro-Fuentes, S., Fernandez-Espejo, E., 2006. Role for dopamine neurons of the rostral linear nucleus and periaqueductal gray in the rewarding and sensitizing properties of heroin. Neuropsychopharmacology. 31, 1475-88.

Francesconi, W., et al., 2009. Protracted withdrawal from alcohol and drugs of abuse impairs long-term potentiation of intrinsic excitability in the juxtacapsular bed nucleus of the stria terminalis. J Neurosci. 29, 5389-401.

Freeman, A., Ciliax, B., Bakay, R., Daley, J., Miller, R.D., Keating, G., Levey, A., Rye, D., 2001. Nigrostriatal collaterals to thalamus degenerate in parkinsonian animal models. Ann Neurol. 50, 321-9.

Galloway, M.P., Wolf, M.E., Roth, R.H., 1986. Regulation of dopamine synthesis in the medial prefrontal cortex is mediated by release modulating autoreceptors: studies in vivo. J Pharmacol Exp Ther. 236, 689-98.

Gamo, N.J., et al., 2015. Stress Impairs Prefrontal Cortical Function via D1 Dopamine Receptor Interactions with Hyperpolarization-Activated Cyclic Nucleotide-Gated Channels. Biol Psychiatry.

Garris, P.A., Wightman, R.M., 1994. Different kinetics govern dopaminergic transmission in the amygdala, prefrontal cortex, and striatum: an in vivo voltammetric study. J Neurosci. 14, 442-50.

Geisler, S., Zahm, D.S., 2005. Afferents of the ventral tegmental area in the rat-anatomical substratum for integrative functions. J Comp Neurol. 490, 270-94.

Gereau, R.W.t., Conn, P.J., 1994. Presynaptic enhancement of excitatory synaptic transmission by beta-adrenergic receptor activation. J Neurophysiol. 72, 1438-42.

Goldman-Rakic, P.S., 1995. Cellular basis of working memory. Neuron. 14, 477-85.

Gonon, F.G., 1988. Nonlinear relationship between impulse flow and dopamine released by rat midbrain dopaminergic neurons as studied by in vivo electrochemistry. Neuroscience. 24, 19-28.

Gordon, G.R., Bains, J.S., 2003. Priming of excitatory synapses by alpha1 adrenoceptor-mediated inhibition of group III metabotropic glutamate receptors. J Neurosci. 23, 6223-31.

Gordon, G.R., Bains, J.S., 2005. Noradrenaline triggers multivesicular release at glutamatergic synapses in the hypothalamus. J Neurosci. 25, 11385-95.

Grace, A.A., Bunney, B.S., 1980. Nigral dopamine neurons: intracellular recording and identification with L-dopa injection and histofluorescence. Science. 210, 654-6.

Grace, A.A., Bunney, B.S., 1983. Intracellular and extracellular electrophysiology of nigral dopaminergic neurons--1. Identification and characterization. Neuroscience. 10, 301-15.

Grace, A.A., Onn, S.P., 1989. Morphology and electrophysiological properties of immunocytochemically identified rat dopamine neurons recorded in vitro. J Neurosci. 9, 3463-81.

Grace, A.A., 1991. Regulation of spontaneous activity and oscillatory spike firing in rat midbrain dopamine neurons recorded in vitro. Synapse. 7, 221-34.

Grace, A.A., Floresco, S.B., Goto, Y., Lodge, D.J., 2007. Regulation of firing of dopaminergic neurons and control of goal-directed behaviors. Trends Neurosci. 30, 220-7.

Green, B., 2014. Prazosin in the treatment of PTSD. J Psychiatr Pract. 20, 253-9.

Greene, J.G., Dingledine, R., Greenamyre, J.T., 2005. Gene expression profiling of rat midbrain dopamine neurons: implications for selective vulnerability in parkinsonism. Neurobiol Dis. 18, 19-31.

Greenwell, T.N., Walker, B.M., Cottone, P., Zorrilla, E.P., Koob, G.F., 2009. The alpha1 adrenergic receptor antagonist prazosin reduces heroin self-administration in rats with extended access to heroin administration. Pharmacol Biochem Behav. 91, 295-302.

Grenhoff, J., Svensson, T.H., 1988. Clonidine regularizes substantia nigra dopamine cell firing. Life Sci. 42, 2003-9.

Grenhoff, J., Svensson, T.H., 1989. Clonidine modulates dopamine cell firing in rat ventral tegmental area. Eur J Pharmacol. 165, 11-8.

Grenhoff, J., Nisell, M., Ferre, S., Aston-Jones, G., Svensson, T.H., 1993. Noradrenergic modulation of midbrain dopamine cell firing elicited by stimulation of the locus coeruleus in the rat. J Neural Transm Gen Sect. 93, 11-25.

Grenhoff, J., Svensson, T.H., 1993. Prazosin modulates the firing pattern of dopamine neurons in rat ventral tegmental area. Eur J Pharmacol. 233, 79-84.

Guiard, B.P., El Mansari, M., Blier, P., 2008a. Cross-talk between dopaminergic and noradrenergic systems in the rat ventral tegmental area, locus ceruleus, and dorsal hippocampus. Mol Pharmacol. 74**,** 1463-75.

Guiard, B.P., El Mansari, M., Merali, Z., Blier, P., 2008b. Functional interactions between dopamine, serotonin and norepinephrine neurons: an in-vivo electrophysiological study in rats with monoaminergic lesions. Int J Neuropsychopharmacol. 11**,** 625-39.

Hammack, S.E., Mania, I., Rainnie, D.G., 2007. Differential expression of intrinsic membrane currents in defined cell types of the anterolateral bed nucleus of the stria terminalis. J Neurophysiol. 98**,** 638-56.

Harnett, M.T., Bernier, B.E., Ahn, K.C., Morikawa, H., 2009. Burst-timing-dependent plasticity of NMDA receptor-mediated transmission in midbrain dopamine neurons. Neuron. 62**,** 826-38.

Hasue, R.H., Shammah-Lagnado, S.J., 2002. Origin of the dopaminergic innervation of the central extended amygdala and accumbens shell: a combined retrograde tracing and immunohistochemical study in the rat. J Comp Neurol. 454**,** 15-33.

Hein, L., 2006. Adrenoceptors and signal transduction in neurons. Cell Tissue Res. 326**,** 541-51.

Hensler, J.G., Artigas, F., Bortolozzi, A., Daws, L.C., De Deurwaerdere, P., Milan, L., Navailles, S., Koek, W., 2013. Catecholamine/Serotonin interactions: systems thinking for brain function and disease. Adv Pharmacol. 68**,** 167-97.

Herold, S., Hecker, C., Deitmer, J.W., Brockhaus, J., 2005. alpha1-Adrenergic modulation of synaptic input to Purkinje neurons in rat cerebellar brain slices. J Neurosci Res. 82**,** 571-9.

Hilaire, G., Viemari, J.C., Coulon, P., Simonneau, M., Bevengut, M., 2004. Modulation of the respiratory rhythm generator by the pontine noradrenergic A5 and A6 groups in rodents. Respir Physiol Neurobiol. 143**,** 187-97.

Hillman, K.L., Lei, S., Doze, V.A., Porter, J.E., 2009. Alpha-1A adrenergic receptor activation increases inhibitory tone in CA1 hippocampus. Epilepsy Res. 84**,** 97-109.

Hnasko, T.S., Chuhma, N., Zhang, H., Goh, G.Y., Sulzer, D., Palmiter, R.D., Rayport, S., Edwards, R.H., 2010. Vesicular glutamate transport promotes dopamine storage and glutamate corelease in vivo. Neuron. 65**,** 643-56.

Hnasko, T.S., Hjelmstad, G.O., Fields, H.L., Edwards, R.H., 2012. Ventral tegmental area glutamate neurons: electrophysiological properties and projections. J Neurosci. 32**,** 15076-85.

Hokfelt, T., Mårtensson, R., Bjorklund, A., Kleinau, S., Goldstein, M., 1984. Distributional maps of tyrosine-hydroxylase-immunoreactive neurons in the rat brain. In: Classical transmitters in the CNS. Vol., A. Bjorklund, T. Hokfelt, ed.^eds. Elsevier, Amsterdam, pp. 277–379.

Honkaniemi, J., 1992. Colocalization of peptide- and tyrosine hydroxylase-like immunoreactivities with Fos-immunoreactive neurons in rat central amygdaloid nucleus after immobilization stress. Brain Res. 598**,** 107-13.

Honkaniemi, J., Fuxe, K., Rechard, L., Koistinaho, J., Isola, J., Gustafsson, J.A., Okret, S., Pelto-Huikko, M., 1992. Colocalization of Fos- and Glucocorticoid Receptor-Like Immunoreactivities in the Rat Amygdaloid Complex After Immobilization Stress. J Neuroendocrinol. 4**,** 547-555.

Hopf, F.W., Martin, M., Chen, B.T., Bowers, M.S., Mohamedi, M.M., Bonci, A., 2007. Withdrawal from intermittent ethanol exposure increases probability of burst firing in VTA neurons in vitro. J Neurophysiol. 98**,** 2297-310.

Hosp, J.A., Nolan, H.E., Luft, A.R., 2015. Topography and collateralization of dopaminergic projections to primary motor cortex in rats. Exp Brain Res. 233**,** 1365-75.

Ikemoto, S., Bonci, A., 2014. Neurocircuitry of drug reward. Neuropharmacology. 76 Pt B**,** 329-41.

Imperato, A., Cabib, S., Puglisi-Allegra, S., 1993. Repeated stressful experiences differently affect the time-dependent responses of the mesolimbic dopamine system to the stressor. Brain Res. 601**,** 333-6.

Inyushin, M.U., Arencibia-Albite, F., Vazquez-Torres, R., Velez-Hernandez, M.E., Jimenez-Rivera, C.A., 2010. Alpha-2 noradrenergic receptor activation inhibits the hyperpolarization-activated cation current (Ih) in neurons of the ventral tegmental area. Neuroscience. 167**,** 287-97.

Jimenez-Rivera, C.A., Feliu-Mojer, M., Vazquez-Torres, R., 2006. Alpha-noradrenergic receptors modulate the development and expression of cocaine sensitization. Ann N Y Acad Sci. 1074**,** 390-402.

Jimenez-Rivera, C.A., Figueroa, J., Vazquez-Torres, R., Velez-Hernandez, M.E., Schwarz, D., Velasquez-Martinez, M.C., Arencibia-Albite, F., 2012. Presynaptic inhibition of glutamate transmission by alpha2 receptors in the VTA. Eur J Neurosci. 35**,** 1406-15.

Jones, B.E., Moore, R.Y., 1977. Ascending projections of the locus coeruleus in the rat. II. Autoradiographic study. Brain Res. 127**,** 25-53.

Jones, L.S., Gauger, L.L., Davis, J.N., 1985. Anatomy of brain alpha 1-adrenergic receptors: in vitro autoradiography with [125I]-heat. J Comp Neurol. 231**,** 190-208.

Ju, G., Swanson, L.W., 1989. Studies on the cellular architecture of the bed nuclei of the stria terminalis in the rat: I. Cytoarchitecture. J Comp Neurol. 280**,** 587-602.

Kalivas, P.W., Duffy, P., 1995. Selective activation of dopamine transmission in the shell of the nucleus accumbens by stress. Brain Res. 675**,** 325-8.

Kandel, E.R., 2013. Principles of neural science, Vol., McGraw-Hill, New York.

Kash, T.L., Nobis, W.P., Matthews, R.T., Winder, D.G., 2008. Dopamine enhances fast excitatory synaptic transmission in the extended amygdala by a CRF-R1-dependent process. J Neurosci. 28**,** 13856-65.

Katz, P.S., Edwards, D.H., 1999. Metamodulation: the control and modulation of neuromodulation. In: Beyond neurotransmission: neuromodulation and its importance for information processing. Vol., P.S. Katz, ed.^eds. Oxford University Press, Oxford, UK, pp. 349–381.

Kauer, J.A., Malenka, R.C., 2007. Synaptic plasticity and addiction. Nat Rev Neurosci. 8**,** 844-58.

Kawaguchi, Y., Shindou, T., 1998. Noradrenergic excitation and inhibition of GABAergic cell types in rat frontal cortex. J Neurosci. 18**,** 6963-76.

Kirkwood, A., Rozas, C., Kirkwood, J., Perez, F., Bear, M.F., 1999. Modulation of long-term synaptic depression in visual cortex by acetylcholine and norepinephrine. J Neurosci. 19**,** 1599-609.

Kobayashi, M., Kojima, M., Koyanagi, Y., Adachi, K., Imamura, K., Koshikawa, N., 2009. Presynaptic and postsynaptic modulation of glutamatergic synaptic transmission by activation of alpha(1)- and beta-adrenoceptors in layer V pyramidal neurons of rat cerebral cortex. Synapse. 63**,** 269-81.

Koob, G.F., 2009. Brain stress systems in the amygdala and addiction. Brain Res. 1293**,** 61-75.

Korf, J., Aghajanian, G.K., Roth, R.H., 1973. Increased turnover of norepinephrine in the rat cerebral cortex during stress: role of the locus coeruleus. Neuropharmacology. 12**,** 933-8.

Krawczyk, M., Georges, F., Sharma, R., Mason, X., Berthet, A., Bezard, E., Dumont, E.C., 2011a. Double-dissociation of the catecholaminergic modulation of synaptic transmission in the oval bed nucleus of the stria terminalis. J Neurophysiol. 105**,** 145-53.

Krawczyk, M., Sharma, R., Mason, X., Debacker, J., Jones, A.A., Dumont, E.C., 2011b. A switch in the neuromodulatory effects of dopamine in the oval bed nucleus of the stria terminalis associated with cocaine self-administration in rats. J Neurosci. 31**,** 8928-35.

Krawczyk, M., et al., 2013. D1 dopamine receptor-mediated LTP at GABA synapses encodes motivation to self-administer cocaine in rats. J Neurosci. 33, 11960-71.

Krawczyk, M., Debacker, J., Mason, X., Jones, A.A., Dumont, E.C., 2014. Dopamine decreases NMDA currents in the oval bed nucleus of the stria terminalis of cocaine self-administering rats. Prog Neuropsychopharmacol Biol Psychiatry. 51C, 83-88.

Lacey, M.G., Mercuri, N.B., North, R.A., 1989. Two cell types in rat substantia nigra zona compacta distinguished by membrane properties and the actions of dopamine and opioids. J Neurosci. 9, 1233-41.

Lammel, S., Hetzel, A., Hackel, O., Jones, I., Liss, B., Roeper, J., 2008. Unique properties of mesoprefrontal neurons within a dual mesocorticolimbic dopamine system. Neuron. 57, 760-73.

Lammel, S., Ion, D.I., Roeper, J., Malenka, R.C., 2011. Projection-specific modulation of dopamine neuron synapses by aversive and rewarding stimuli. Neuron. 70, 855-62.

Lammel, S., Lim, B.K., Ran, C., Huang, K.W., Betley, M.J., Tye, K.M., Deisseroth, K., Malenka, R.C., 2012. Input-specific control of reward and aversion in the ventral tegmental area. Nature. 491, 212-7.

Lammel, S., Steinberg, E.E., Foldy, C., Wall, N.R., Beier, K., Luo, L., Malenka, R.C., 2015. Diversity of transgenic mouse models for selective targeting of midbrain dopamine neurons. Neuron. 85, 429-38.

Le, A.D., Funk, D., Juzytsch, W., Coen, K., Navarre, B.M., Cifani, C., Shaham, Y., 2011. Effect of prazosin and guanfacine on stress-induced reinstatement of alcohol and food seeking in rats. Psychopharmacology (Berl). 218, 89-99.

Lee, A., Wissekerke, A.E., Rosin, D.L., Lynch, K.R., 1998. Localization of alpha2C-adrenergic receptor immunoreactivity in catecholaminergic neurons in the rat central nervous system. Neuroscience. 84, 1085-96.

Lei, S., Deng, P.Y., Porter, J.E., Shin, H.S., 2007. Adrenergic facilitation of GABAergic transmission in rat entorhinal cortex. J Neurophysiol. 98, 2868-77.

Lein, E.S., et al., 2007. Genome-wide atlas of gene expression in the adult mouse brain. Nature. 445, 168-76.

Lepor, H., Kazzazi, A., Djavan, B., 2012. alpha-Blockers for benign prostatic hyperplasia: the new era. Curr Opin Urol. 22, 7-15.

Leri, F., Flores, J., Rodaros, D., Stewart, J., 2002. Blockade of stress-induced but not cocaine-induced reinstatement by infusion of noradrenergic antagonists into the bed nucleus of the stria terminalis or the central nucleus of the amygdala. J Neurosci. 22, 5713-8.

Li, C., McCall, N.M., Lopez, A.J., Kash, T.L., 2013a. Alcohol effects on synaptic transmission in periaqueductal gray dopamine neurons. Alcohol. 47, 279-87.

Li, S., Shi, Y., Kirouac, G.J., 2014. The hypothalamus and periaqueductal gray are the sources of dopamine fibers in the paraventricular nucleus of the thalamus in the rat. Front Neuroanat. 8, 136.

Li, X., Qi, J., Yamaguchi, T., Wang, H.L., Morales, M., 2013b. Heterogeneous composition of dopamine neurons of the rat A10 region: molecular evidence for diverse signaling properties. Brain Struct Funct. 218, 1159-76.

Liprando, L.A., Miner, L.H., Blakely, R.D., Lewis, D.A., Sesack, S.R., 2004. Ultrastructural interactions between terminals expressing the norepinephrine transporter and dopamine neurons in the rat and monkey ventral tegmental area. Synapse. 52, 233-44.

Lobb, C.J., Wilson, C.J., Paladini, C.A., 2010. A dynamic role for GABA receptors on the firing pattern of midbrain dopaminergic neurons. J Neurophysiol. 104, 403-13.

Lu, J., Jhou, T.C., Saper, C.B., 2006. Identification of wake-active dopaminergic neurons in the ventral periaqueductal gray matter. J Neurosci. 26, 193-202.

Magee, J.C., 2000. Dendritic integration of excitatory synaptic input. Nat Rev Neurosci. 1, 181-90.

Mangiavacchi, S., Masi, F., Scheggi, S., Leggio, B., De Montis, M.G., Gambarana, C., 2001. Long-term behavioral and neurochemical effects of chronic stress exposure in rats. J Neurochem. 79, 1113-21.

Mantsch, J.R., Weyer, A., Vranjkovic, O., Beyer, C.E., Baker, D.A., Caretta, H., 2010. Involvement of noradrenergic neurotransmission in the stress- but not cocaine-induced reinstatement of extinguished cocaine-induced conditioned place preference in mice: role for beta-2 adrenergic receptors. Neuropsychopharmacology. 35, 2165-78.

Mantz, J., Thierry, A.M., Glowinski, J., 1989. Effect of noxious tail pinch on the discharge rate of mesocortical and mesolimbic dopamine neurons: selective activation of the mesocortical system. Brain Res. 476, 377-81.

Marek, G.J., Aghajanian, G.K., 1996. Alpha 1B-adrenoceptor-mediated excitation of piriform cortical interneurons. Eur J Pharmacol. 305, 95-100.

Marek, G.J., Aghajanian, G.K., 1999. 5-HT2A receptor or alpha1-adrenoceptor activation induces excitatory postsynaptic currents in layer V pyramidal cells of the medial prefrontal cortex. Eur J Pharmacol. 367, 197-206.

Margolis, E.B., Lock, H., Hjelmstad, G.O., Fields, H.L., 2006. The ventral tegmental area revisited: is there an electrophysiological marker for dopaminergic neurons? J Physiol. 577, 907-24.

Margolis, E.B., Mitchell, J.M., Ishikawa, J., Hjelmstad, G.O., Fields, H.L., 2008. Midbrain dopamine neurons: projection target determines action potential duration and dopamine D(2) receptor inhibition. J Neurosci. 28**,** 8908-13.

Massi, L., Elezgarai, I., Puente, N., Reguero, L., Grandes, P., Manzoni, O.J., Georges, F., 2008. Cannabinoid receptors in the bed nucleus of the stria terminalis control cortical excitation of midbrain dopamine cells in vivo. J Neurosci. 28**,** 10496-508.

Matsui, A., Williams, J.T., 2011. Opioid-sensitive GABA inputs from rostromedial tegmental nucleus synapse onto midbrain dopamine neurons. J Neurosci. 31**,** 17729-35.

Matsumoto, M., Hikosaka, O., 2009. Two types of dopamine neuron distinctly convey positive and negative motivational signals. Nature. 459**,** 837-41.

McElligott, Z.A., Winder, D.G., 2008. Alpha1-adrenergic receptor-induced heterosynaptic long-term depression in the bed nucleus of the stria terminalis is disrupted in mouse models of affective disorders. Neuropsychopharmacology. 33**,** 2313-23.

McElligott, Z.A., Klug, J.R., Nobis, W.P., Patel, S., Grueter, B.A., Kash, T.L., Winder, D.G., 2010. Distinct forms of Gq-receptor-dependent plasticity of excitatory transmission in the BNST are differentially affected by stress. Proc Natl Acad Sci U S A. 107**,** 2271-6.

Mejias-Aponte, C.A., Drouin, C., Aston-Jones, G., 2009. Adrenergic and noradrenergic innervation of the midbrain ventral tegmental area and retrorubral field: prominent inputs from medullary homeostatic centers. J Neurosci. 29**,** 3613-26.

Meloni, E.G., Gerety, L.P., Knoll, A.T., Cohen, B.M., Carlezon, W.A., Jr., 2006. Behavioral and anatomical interactions between dopamine and corticotropin-releasing factor in the rat. J Neurosci. 26**,** 3855-63.

Meye, F.J., Adan, R.A., 2014. Feelings about food: the ventral tegmental area in food reward and emotional eating. Trends Pharmacol Sci. 35**,** 31-40.

Missale, C., Nash, S.R., Robinson, S.W., Jaber, M., Caron, M.G., 1998. Dopamine receptors: from structure to function. Physiol Rev. 78**,** 189-225.

Mitchell, H.A., Bogenpohl, J.W., Liles, L.C., Epstein, M.P., Bozyczko-Coyne, D., Williams, M., Weinshenker, D., 2008. Behavioral responses of dopamine beta-hydroxylase knockout mice to modafinil suggest a dual noradrenergic-dopaminergic mechanism of action. Pharmacol Biochem Behav. 91**,** 217-22.

Mohsenin, S., Mohsenin, V., 2014. Diagnosis and management of sleep disorders in posttraumatic stress disorder:a review of the literature. Prim Care Companion CNS Disord. 16.

Montague, P.R., Dayan, P., Sejnowski, T.J., 1996. A framework for mesencephalic dopamine systems based on predictive Hebbian learning. J Neurosci. 16**,** 1936-47.

Montague, P.R., McClure, S.M., Baldwin, P.R., Phillips, P.E., Budygin, E.A., Stuber, G.D., Kilpatrick, M.R., Wightman, R.M., 2004. Dynamic gain control of dopamine delivery in freely moving animals. J Neurosci. 24**,** 1754-9.

Moore, H., Rose, H.J., Grace, A.A., 2001. Chronic cold stress reduces the spontaneous activity of ventral tegmental dopamine neurons. Neuropsychopharmacology. 24**,** 410-9.

Morikawa, H., Paladini, C.A., 2011. Dynamic regulation of midbrain dopamine neuron activity: intrinsic, synaptic, and plasticity mechanisms. Neuroscience. 198**,** 95-111.

Morilak, D.A., Fornal, C.A., Jacobs, B.L., 1987. Effects of physiological manipulations on locus coeruleus neuronal activity in freely moving cats. II. Cardiovascular challenge. Brain Res. 422**,** 24-31.

Morrow, B.A., Lee, E.J., Taylor, J.R., Elsworth, J.D., Nye, H.E., Roth, R.H., 1997. (S)-(-)-HA-966, a gamma-hydroxybutyrate-like agent, prevents enhanced mesocorticolimbic dopamine metabolism and behavioral correlates of restraint stress, conditioned fear and cocaine sensitization. J Pharmacol Exp Ther. 283**,** 712-21.

Morrow, B.A., Roth, R.H., Elsworth, J.D., 2000. TMT, a predator odor, elevates mesoprefrontal dopamine metabolic activity and disrupts short-term working memory in the rat. Brain Res Bull. 52**,** 519-23.

Muller, C.A., Geisel, O., Banas, R., Heinz, A., 2014. Current pharmacological treatment approaches for alcohol dependence. Expert Opin Pharmacother. 15**,** 471-81.

Nestler, E.J., Carlezon, W.A., Jr., 2006. The mesolimbic dopamine reward circuit in depression. Biol Psychiatry. 59**,** 1151-9.

Nikulina, E.M., Johnston, C.E., Wang, J., Hammer, R.P., Jr., 2014. Neurotrophins in the ventral tegmental area: Role in social stress, mood disorders and drug abuse. Neuroscience. 282C**,** 122-138.

Nobis, W.P., Kash, T.L., Silberman, Y., Winder, D.G., 2011. beta-Adrenergic receptors enhance excitatory transmission in the bed nucleus of the stria terminalis through a corticotrophin-releasing factor receptor-dependent and cocaine-regulated mechanism. Biol Psychiatry. 69**,** 1083-90.

Oades, R.D., Halliday, G.M., 1987. Ventral tegmental (A10) system: neurobiology. 1. Anatomy and connectivity. Brain Res. 434**,** 117-65.

Overton, P., Clark, D., 1992. Iontophoretically administered drugs acting at the N-methyl-D-aspartate receptor modulate burst firing in A9 dopamine neurons in the rat. Synapse. 10**,** 131-40.

Paladini, C.A., Iribe, Y., Tepper, J.M., 1999. GABAA receptor stimulation blocks NMDA-induced bursting of dopaminergic neurons in vitro by decreasing input resistance. Brain Res. 832, 145-51.

Paladini, C.A., Tepper, J.M., 1999. GABA(A) and GABA(B) antagonists differentially affect the firing pattern of substantia nigra dopaminergic neurons in vivo. Synapse. 32, 165-76.

Paladini, C.A., Williams, J.T., 2004. Noradrenergic inhibition of midbrain dopamine neurons. J Neurosci. 24, 4568-75.

Paladini, C.A., Roeper, J., 2014. Generating bursts (and pauses) in the dopamine midbrain neurons. Neuroscience. 282C, 109-121.

Phillipson, O.T., 1979a. The cytoarchitecture of the interfascicular nucleus and ventral tegmental area of Tsai in the rat. J Comp Neurol. 187, 85-98.

Phillipson, O.T., 1979b. Afferent projections to the ventral tegmental area of Tsai and interfascicular nucleus: a horseradish peroxidase study in the rat. J Comp Neurol. 187, 117-43.

Piascik, M.T., Perez, D.M., 2001. Alpha1-adrenergic receptors: new insights and directions. J Pharmacol Exp Ther. 298, 403-10.

Purves, D., 2012. Neuroscience, Vol., Sinauer Associates, Sunderland, Mass.

Rainbow, T.C., Parsons, B., Wolfe, B.B., 1984. Quantitative autoradiography of beta 1- and beta 2-adrenergic receptors in rat brain. Proc Natl Acad Sci U S A. 81, 1585-9.

Raskind, M.A., et al., 2007. A parallel group placebo controlled study of prazosin for trauma nightmares and sleep disturbance in combat veterans with post-traumatic stress disorder. Biol Psychiatry. 61, 928-34.

Redmond, A.J., Morrow, B.A., Elsworth, J.D., Roth, R.H., 2002. Selective activation of the A10, but not A9, dopamine neurons in the rat by the predator odor, 2,5-dihydro-2,4,5-trimethylthiazoline. Neurosci Lett. 328, 209-12.

Rinaman, L., 2003. Hindbrain noradrenergic lesions attenuate anorexia and alter central cFos expression in rats after gastric viscerosensory stimulation. J Neurosci. 23, 10084-92.

Saal, D., Dong, Y., Bonci, A., Malenka, R.C., 2003. Drugs of abuse and stress trigger a common synaptic adaptation in dopamine neurons. Neuron. 37, 577-82.

Salamone, J.D., Correa, M., 2012. The mysterious motivational functions of mesolimbic dopamine. Neuron. 76, 470-85.

Sareen, J., Chartier, M., Paulus, M.P., Stein, M.B., 2006. Illicit drug use and anxiety disorders: findings from two community surveys. Psychiatry Res. 142, 11-7.

Sawchenko, P.E., Li, H.Y., Ericsson, A., 2000. Circuits and mechanisms governing hypothalamic responses to stress: a tale of two paradigms. Prog Brain Res. 122, 61-78.

Scheiderer, C.L., Dobrunz, L.E., McMahon, L.L., 2004. Novel form of long-term synaptic depression in rat hippocampus induced by activation of alpha 1 adrenergic receptors. J Neurophysiol. 91, 1071-7.

Scheiderer, C.L., Smith, C.C., McCutchen, E., McCoy, P.A., Thacker, E.E., Kolasa, K., Dobrunz, L.E., McMahon, L.L., 2008. Coactivation of M(1) muscarinic and alpha1 adrenergic receptors stimulates extracellular signal-regulated protein kinase and induces long-term depression at CA3-CA1 synapses in rat hippocampus. J Neurosci. 28, 5350-8.

Schultz, W., Apicella, P., Ljungberg, T., 1993. Responses of monkey dopamine neurons to reward and conditioned stimuli during successive steps of learning a delayed response task. J Neurosci. 13, 900-13.

Schultz, W., 2010. Multiple functions of dopamine neurons. F1000 Biol Rep. 2.

Sesack, S.R., Hawrylak, V.A., Matus, C., Guido, M.A., Levey, A.I., 1998. Dopamine axon varicosities in the prelimbic division of the rat prefrontal cortex exhibit sparse immunoreactivity for the dopamine transporter. J Neurosci. 18, 2697-708.

Seutin, V., Johnson, S.W., North, R.A., 1993. Apamin increases NMDA-induced burst-firing of rat mesencephalic dopamine neurons. Brain Res. 630, 341-4.

Sharma, A., Couture, J., 2014. A review of the pathophysiology, etiology, and treatment of attention-deficit hyperactivity disorder (ADHD). Ann Pharmacother. 48, 209-25.

Shields, A.D., Wang, Q., Winder, D.G., 2009. alpha2A-adrenergic receptors heterosynaptically regulate glutamatergic transmission in the bed nucleus of the stria terminalis. Neuroscience. 163, 339-51.

Silberman, Y., Winder, D.G., 2013. Corticotropin releasing factor and catecholamines enhance glutamatergic neurotransmission in the lateral subdivision of the central amygdala. Neuropharmacology. 70, 316-23.

Simon, H., Le Moal, M., Stinus, L., Calas, A., 1979. Anatomical relationships between the ventral mesencephalic tegmentum--a 10 region and the locus coeruleus as demonstrated by anterograde and retrograde tracing techniques. J Neural Transm. 44, 77-86.

Simpson, T.L., Saxon, A.J., Meredith, C.W., Malte, C.A., McBride, B., Ferguson, L.C., Gross, C.A., Hart, K.L., Raskind, M., 2009. A pilot trial of the alpha-1 adrenergic antagonist, prazosin, for alcohol dependence. Alcohol Clin Exp Res. 33, 255-63.

Sinha, R., Shaham, Y., Heilig, M., 2011. Translational and reverse translational research on the role of stress in drug craving and relapse. Psychopharmacology (Berl). 218, 69-82.

Smagin, G.N., Swiergiel, A.H., Dunn, A.J., 1995. Corticotropin-releasing factor administered into the locus coeruleus, but not the parabrachial nucleus, stimulates norepinephrine release in the prefrontal cortex. Brain Res Bull. 36, 71-6.

Stuber, G.D., Klanker, M., de Ridder, B., Bowers, M.S., Joosten, R.N., Feenstra, M.G., Bonci, A., 2008. Reward-predictive cues enhance excitatory synaptic strength onto midbrain dopamine neurons. Science. 321, 1690-2.

Stuber, G.D., Hnasko, T.S., Britt, J.P., Edwards, R.H., Bonci, A., 2010. Dopaminergic terminals in the nucleus accumbens but not the dorsal striatum corelease glutamate. J Neurosci. 30, 8229-33.

Stuber, G.D., Stamatakis, A.M., Kantak, P.A., 2015. Considerations when using cre-driver rodent lines for studying ventral tegmental area circuitry. Neuron. 85, 439-45.

Sutoo, D., Akiyama, K., 2002. Neurochemical changes in mice following physical or psychological stress exposures. Behav Brain Res. 134, 347-54.

Swanson, L.W., 1982. The projections of the ventral tegmental area and adjacent regions: a combined fluorescent retrograde tracer and immunofluorescence study in the rat. Brain Res Bull. 9, 321-53.

Taylor, F.B., Martin, P., Thompson, C., Williams, J., Mellman, T.A., Gross, C., Peskind, E.R., Raskind, M.A., 2008. Prazosin effects on objective sleep measures and clinical symptoms in civilian trauma posttraumatic stress disorder: a placebo-controlled study. Biol Psychiatry. 63, 629-32.

Thomas, M.J., Beurrier, C., Bonci, A., Malenka, R.C., 2001. Long-term depression in the nucleus accumbens: a neural correlate of behavioral sensitization to cocaine. Nat Neurosci. 4, 1217-23.

Tobler, P.N., Fiorillo, C.D., Schultz, W., 2005. Adaptive coding of reward value by dopamine neurons. Science. 307, 1642-5.

Ungless, M.A., Singh, V., Crowder, T.L., Yaka, R., Ron, D., Bonci, A., 2003. Corticotropin-releasing factor requires CRF binding protein to potentiate NMDA receptors via CRF receptor 2 in dopamine neurons. Neuron. 39, 401-7.

Ungless, M.A., Magill, P.J., Bolam, J.P., 2004. Uniform inhibition of dopamine neurons in the ventral tegmental area by aversive stimuli. Science. 303, 2040-2.

Valentino, R.J., Foote, S.L., Page, M.E., 1993. The locus coeruleus as a site for integrating corticotropin-releasing factor and noradrenergic mediation of stress responses. Ann N Y Acad Sci. 697, 173-88.

Velasquez-Martinez, M.C., Vazquez-Torres, R., Jimenez-Rivera, C.A., 2012. Activation of alpha1-adrenoceptors enhances glutamate release onto ventral tegmental area dopamine cells. Neuroscience. 216, 18-30.

Velasquez-Martinez, M.C., Vazquez-Torres, R., Rojas, L.V., Sanabria, P., Jimenez-Rivera, C.A., 2015. Alpha-1 adrenoreceptors modulate GABA release onto ventral tegmental area dopamine neurons. Neuropharmacology. 88, 110-21.

Vijayraghavan, S., Wang, M., Birnbaum, S.G., Williams, G.V., Arnsten, A.F., 2007. Inverted-U dopamine D1 receptor actions on prefrontal neurons engaged in working memory. Nat Neurosci. 10, 376-84.

Vranjkovic, O., Gasser, P.J., Gerndt, C.H., Baker, D.A., Mantsch, J.R., 2014. Stress-induced cocaine seeking requires a beta-2 adrenergic receptor-regulated pathway from the ventral bed nucleus of the stria terminalis that regulates CRF actions in the ventral tegmental area. J Neurosci. 34, 12504-14.

Walker, D.L., Davis, M., 2008. Role of the extended amygdala in short-duration versus sustained fear: a tribute to Dr. Lennart Heimer. Brain Struct Funct. 213, 29-42.

Walsh, J.J., Han, M.H., 2014. The heterogeneity of ventral tegmental area neurons: Projection functions in a mood-related context. Neuroscience. 282C, 101-108.

Williams, M.A., Li, C., Kash, T.L., Matthews, R.T., Winder, D.G., 2014. Excitatory drive onto dopaminergic neurons in the rostral linear nucleus is enhanced by norepinephrine in an alpha1 adrenergic receptor-dependent manner. Neuropharmacology. 86, 116-24.

Yamaguchi, T., Wang, H.L., Li, X., Ng, T.H., Morales, M., 2011. Mesocorticolimbic glutamatergic pathway. J Neurosci. 31, 8476-90.

Zahm, D.S., Grosu, S., Williams, E.A., Qin, S., Berod, A., 2001. Neurons of origin of the neurotensinergic plexus enmeshing the ventral tegmental area in rat: retrograde labeling and in situ hybridization combined. Neuroscience. 104, 841-51.